

UNCLASSIFIED

AD NUMBER

AD839526

LIMITATION CHANGES

TO:

Approved for public release; distribution is unlimited.

FROM:

Distribution authorized to U.S. Gov't. agencies and their contractors; Critical Technology; AUG 1968. Other requests shall be referred to Naval Weapons Center, China Lake, CA 93555. This document contains export-controlled technical data.

AUTHORITY

USNWC ltr dtd 24 Mar 1972

THIS PAGE IS UNCLASSIFIED

AD839526

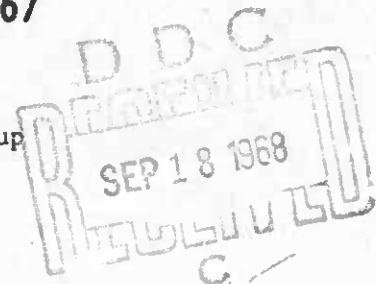
# METAL PARTICLE COMBUSTION PROGRESS REPORT

## 1 JULY 1965-1 MAY 1967

by

Metal Combustion Study Group

Edited by J. L. Prentice

Research Department

**ABSTRACT.** This report includes (1) a summary of experimental studies at this Center on the xenon flash-initiated combustion of single particles of aluminum, boron, titanium and zirconium in air, oxygen, carbon dioxide and various oxygen-argon mixtures at pressures from 1-4.5 atmospheres, and a summary of aluminum and boron particle combustion in various gas burner flames, (2) development and application of an analytical droplet burning model to describe boron particle combustion, and (3) a discussion of metal particle fragmentation mechanisms including definition of some necessary conditions for fragmentation as well as a description of the most probable mechanism. The report concludes with a brief summary section describing the status of the metal combustion problem.

Significant new data on the agglomeration phenomenon and other preignition processes are presented. Extensive use of the scanning electron microscope (SEM) was made in studying both preignition phenomena and metal specimens quenched during various phases of burning. Results indicate that quasi-steady combustion behavior is directly related to the thermophysical properties of the metals and their oxides. Disposition of the combustion products in the reaction zone exerts the controlling influence on the mode of termination of combustion. Droplet burning models treating the case of spherical symmetry (hydrocarbon droplet analogy) are shown to be deficient, particularly for aluminum combustion, where early large scale deviation from such symmetry occurs.



**NAVAL WEAPONS CENTER**  
CHINA LAKE, CALIFORNIA \* AUGUST 1968

93555

**DISTRIBUTION STATEMENT**

THIS DOCUMENT IS SUBJECT TO SPECIAL EXPORT CONTROLS AND EACH TRANSMITTAL TO FOREIGN GOVERNMENTS OR FOREIGN NATIONALS MAY BE MADE ONLY WITH PRIOR APPROVAL OF THE NAVAL WEAPONS CENTER.

# NAVAL WEAPONS CENTER AN ACTIVITY OF THE NAVAL MATERIAL COMMAND

M. R. Etheridge, Capt., USN ..... Commander  
Thomas S. Amle, Ph.D. .... Technical Director

---

## FOREWORD

This is the second report by the Metal Combustion Study Group on a program related to the combustion of metals in solid rocket propellants. The report covers the period from 1 July 1965 to 1 May 1967. The program has been carried out jointly by the Aerothermochemistry Division and the Chemical Kinetics Branch of the Research Department under the direction of Mr. E. W. Price, Head, Aerothermochemistry Division, and is sponsored by the National Aeronautics and Space Administration under Work Order No. 6032. Members of the contributing team were C. M. Drew, A. S. Gordon, R. H. Knipe, K. J. Kraeutle, J. L. Prentice, and E. W. Price.

This report is transmitted for information only. It does not represent the official view or final judgement of the Naval Weapons Center.

Released by  
J. E. CRUMP, Head (Acting)  
Aerothermochemistry Division  
3 June 1968

Under authority of  
HUGH W. HUNTER, Head  
Research Department

NWC Technical Publication 4435

Published by.....Research Department  
Collation.....cover, 61 leaves, DD Form 1473, abstract cards  
First printing.....230 unnumbered copies  
Security classification.....UNCLASSIFIED

ACCESSION for	
CFSTI	WHITE SECTION <input type="checkbox"/>
DOC	BUFF SECTION <input checked="" type="checkbox"/>
UNANNOUNCED	<input type="checkbox"/>
JUSTIFICATION	
BY	
DISTRIBUTION-AVAILABILITY CODE	
DIST.	AVAIL. AND IN SPECIAL
2	

## CONTENTS

1.	Introduction . . . . .	1
1.1.	Use of Metals in Solid Propellants . . . . .	1
1.2.	Approach of the Present Project. . . . .	2
1.3.	General Character of Metal Combustion. . . . .	3
2.	Experimental Methods . . . . .	5
2.1.	Gas Burner Studies . . . . .	5
2.2.	Xenon Flash Ignition Method. . . . .	7
2.2.1.	Combustion Chamber . . . . .	8
2.2.2.	Flash Lamp and Power Supply. . . . .	8
2.2.3.	Data Acquisition . . . . .	11
2.3.	Investigation of the Preignition Behavior of Aluminum by DTA . . . . .	12
2.4.	Investigation of Preignition Behavior in the Hot-Stage Microscope . . . . .	13
2.5.	Particle Quenching . . . . .	14
2.5.1.	The Sampling Problem and the History of a Burning Droplet . . . . .	14
2.5.2.	Interpretation of Quench Samples . . . . .	16
2.6.	Scanning Electron Microscope Technique Applied to Quenched Samples. . . . .	16
2.6.1.	Operating Principle of the SEM . . . . .	17
2.6.2.	Scanning Electron Microscope Technique . . . . .	18
3.	Preignition Processes. . . . .	19
3.1.	Condition of Aluminum Particles Before Testing . . . . .	19
3.2.	Effect of Heating in Air . . . . .	21
3.3.	Rapid Heating of Aluminum Particles in a Burner Flame. . . . .	29
3.4.	Interpretation of Results. . . . .	31
4.	Ignition of Metals . . . . .	32
4.1.	Definition of Ignition . . . . .	32
4.2.	Factors Governing Character of Ignition. . . . .	33
4.3.	Observations of Ignition . . . . .	34
5.	Quasi-Steady Combustion. . . . .	37
5.1.	Screening Studies. . . . .	37
5.2.	Aluminum Combustion. . . . .	39
5.2.1.	Surface Oxide. . . . .	45
5.3.	Boron Combustion . . . . .	48
5.4.	Summary. . . . .	53

6.	Terminal Stages of Combustion. . . . .	56
6.1.	Aluminum . . . . .	59
6.1.1.	Flash-Ignited Aluminum Particles Burning in Oxygen-Argon Mixtures . . . . .	60
6.1.2.	Flash-Ignited Aluminum Particles Burning in Air . . . . .	60
6.1.3.	Flash-Ignited Aluminum Particles Burning in Oxygen-Argon-Nitrogen Mixtures. . . . .	69
6.1.4.	Flash-Ignited Aluminum Particles Burning in Carbon Dioxide. . . . .	73
6.1.5.	Flash-Ignited Aluminum Particles Burning in Pure Oxygen . . . . .	73
6.1.6.	Aluminum Particle Combustion in Carbon Monoxide-Oxygen Flames. . . . .	73
6.1.7.	Summary. . . . .	75
6.2.	Titanium . . . . .	76
6.2.1.	Flash-Ignited Titanium Particles Burning in Air . . . . .	77
6.2.2.	Flash-Ignited Titanium Particles Burning in Oxygen-Argon Mixtures . . . . .	79
6.2.3.	Flash-Ignited Titanium Particles Burning in Carbon Dioxide. . . . .	79
6.2.4.	Flash-Ignited Titanium Particles Burning in Pure Oxygen . . . . .	79
6.3.	Zirconium. . . . .	80
6.3.1.	Flash-Ignited Zirconium Particles Burning in Air . . . . .	80
6.3.2.	Flash-Ignited Zirconium Particles Burning in Oxygen-Argon Mixtures . . . . .	83
6.3.3.	Flash-Ignited Zirconium Particles Burning in Carbon Dioxide. . . . .	85
6.3.4.	Flash-Ignited Zirconium Particles Burning in Pure Oxygen . . . . .	85
6.4.	Boron. . . . .	85
6.4.1.	Flash-Ignited Boron Particles Burning in Air . . . . .	86
6.4.2.	Flash-Ignited Boron Particles Burning in Oxygen-Argon Mixtures . . . . .	88
6.4.3.	Flash-Ignited Boron Particles Burning in Carbon Dioxide. . . . .	90
6.4.4.	Flash-Ignited Boron Particles Burning in Pure Oxygen . . . . .	90
6.5.	Discussion of Droplet Fragmentation Processes and Mechanisms . . . . .	90
6.5.1.	Rupture of a Metal Vapor-Inflated Oxide Shell. .	92
6.5.2.	Superheating . . . . .	93
6.5.3.	Gas-Driven Fragmentations. . . . .	94

7.	Status of the Metal Combustion Problem . . . . .	101
7.1.	Preignition-Agglomeration . . . . .	101
7.2.	Ignition . . . . .	102
7.3.	Quasi-Steady Combustion . . . . .	102
7.4.	Terminal Stage of Combustion . . . . .	103
7.5.	Thermodynamics-High Temperature Chemistry . . . . .	103
7.6.	Combustion Modeling . . . . .	104
7.7.	Suggestions for Future Work . . . . .	104
Appendix: A Computational Model for the Study of Boron Particle Combustion at Low Environmental Temperatures . . . . .		106
References . . . . .		112

ACKNOWLEDGMENT

The authors wish to acknowledge with appreciation the efforts of Mrs. Celia Brophy in performing the literature searches which were a necessary adjunct to this investigation and her assistance with portions of the flash heating studies of single metal particles. The services of Mrs. Hazel Parish in performing scanning electron microscope analyses of metal combustion specimens is also acknowledged.

## 1. INTRODUCTION

This report summarizes work conducted on the study of combustion of metal particles during the period 1 July 1965 to 1 May 1967, and is a continuation of work reported previously in several journal articles, Appendix A and in Ref. 1. The interest in metal particle combustion stems from increasing use of powdered metals as fuels, particularly in solid rocket propellants.

### 1.1. USE OF METALS IN SOLID PROPELLANTS

Since about 1955, powdered metals have been used in increasing amounts as fuel ingredients in rocket propellants. Serious consideration has been given to beryllium, boron, zirconium, and magnesium, in addition to the widespread use of aluminum. In principle, the virtues of metals are their density (compared to other propellant ingredients) and the high flame temperatures resulting from combustion. For practical reasons, the metal is used in propellant formulations that are rather fuel-rich, and combustion takes place in combustors whose volume is kept as small as possible. These conditions are not conducive to complete combustion, and the value of a metal as a fuel ingredient is thus often limited appreciably by the degree to which complete combustion is approached.

Unlike other propellant ingredients, metals do not decompose to vapors upon heating, and direct vaporization does not occur until relatively high temperatures are reached. As a result, the molecular-scale mixing of the metal with oxidizer necessary for reaction does not occur readily, and metal combustion does not proceed as readily as other steps in the propellant combustion. This in turn leads to two combustion problems. First, the combustion of particles may not proceed to completion during the residence of the particle in the combustor. This problem may be attacked by reducing the size of the metal particles to reduce their burning time. However, this usually does not increase the combustion efficiency greatly because of the second problem, agglomeration of metal particles on the burning surface of the propellant. This second problem results from the reluctance of metals to vaporize at the burning surface temperature of 600°C or so. Thus, fine particles of a few microns diameter typically accumulate to droplets of 30 - 200 microns before appreciable combustion has occurred, and the combustion time is subsequently long because of the large droplet size.

The details of metal combustion in propellants are highly dependent on the properties of the metal and its oxide, and until recently have been poorly understood. Considerable progress in understanding has resulted from studies of the mechanism of combustion of single metal particles in gaseous environments. From such studies, it is becoming increasingly practical to explain the combustion behavior of metals in propellant flames, and to forecast or resolve combustion problems. The importance of this and future progress can be appreciated in the context of some current metal combustion problems. One example is the continued difficulties with attainment of "theoretical" specific impulse from propellants with optimized mixture ratios, especially in low pressure "space" motors. A second example is the observation that the dynamics of the metal combustion processes are conducive to oscillatory combustion in some types of rocket motors. A third example is the difficulty of achieving acceptable burning characteristics of propellants having very high metal contents, propellants designed for use in "air augmented" rockets.

Beyond the objective of understanding how metals burn in propellants, there exists the largely undeveloped technology of improving combustion--not only in propellants, but in pyrotechnic flares, torches, etc. The growth of understanding provides the logical basis needed to guide development of coated particles that won't agglomerate, or will ignite at low temperatures, or will burn more rapidly. Understanding may guide development of alloys that burn better, or may aid in optimizing the combination of metal and oxidizing species. In view of the variety of metals, alloys, coatings, and oxidizers potentially available, and in view of the prohibitive cost of obtaining and testing all these combinations as propellants, advances in understanding seem to be an important aspect of progress.

## 1.2. APPROACH OF THE PRESENT PROJECT

The original work on this project was oriented around the then-available technique of combustion of metal particles in gas burner flames, with observations made by high speed photography, and by quench-plate sampling of burning particles. Because the combustion of single particles was found to be quite complicated, study of the behavior of clouds of particles was deferred. More recently, a xenon flash ignition apparatus was developed for single particle studies which permitted close control of all relevant combustion variables, the gas burner technique was upgraded, and supporting theoretical studies were undertaken of spherical combustion models as well as a re-examination of the bond energies of metal oxides. In these efforts it was proposed that the qualitative aspects of combustion of various metal particles in atmospheres of interest in propellant flames could be determined and explained. In later stages of the project it was proposed that the results be applied to propellant-burning situations where agglomeration, particle ignition, and combustion of clouds of particles posed further, more difficult problems.

Because of the complicated nature of the combustion process, the studies were undertaken by a team of scientists with mutually complimentary backgrounds including experience in chemical kinetics, heat transfer, fluid dynamics, combustion modeling, propellant combustion and experimental skills such as photography and microscopy. Members of the Metal Combustion Study Group have conducted individual researches, and have met regularly as a seminar team to achieve the interdisciplinary learning so essential to objective pursuit of this kind of problem.

An earlier report (Ref. 1), summarizing progress up to 30 June 1965, was concerned primarily with combustion of aluminum particles. This work has continued, and the combustion of aluminum in oxidizers based on oxygen is now largely understood. In addition, recent studies have concerned several other metals, new experimental methods, and behavior of accumulations of metal particles. Attention is turning increasingly to mechanisms of ignition, agglomeration, and how to control multiple particle behavior in general.

### 1.3. GENERAL CHARACTER OF METAL COMBUSTION

The combustion of metal particles is distinctive in two respects, compared to other propellant ingredients. The metal is not easily gassified, and its oxide tends to accumulate in condensed form on the particle surface and impede diffusion of oxidizer to the metal. These attributes are related to the melting and boiling points of the metal and its oxides, the wetting characteristics of the liquid oxide on the metal, and the structural character of the oxide coating. In view of the contrasting combinations of these properties (Table 1.1) for different metals, it is not surprising that the ignition and combustion behavior of these metals differ markedly. Thus, some metals such as aluminum ignite only reluctantly because the particle surface is covered to very high temperature by a protective oxide coating. Once this coating is melted, the oxide withdraws from much of the metal surface due to the high surface tension of  $Al_2O_3$ , and vigorous combustion occurs. Magnesium forms an oxide layer, but it is permeable and permits continued oxidation even at relatively low temperatures. Zirconium oxide and oxygen are both soluble in zirconium, so no protective layer is formed. Both magnesium and zirconium are easy to ignite. Boron forms an oxide which melts at fairly low temperature, permitting continued oxidation at a moderate rate by diffusion in the liquid; when the temperature becomes high enough to vaporize the oxide, the combustion rate increases commensurate with the more favorable diffusion situation. Of the samples noted, only boron produces a stoichiometric oxide which is gaseous at a temperature significantly below the steady-state flame temperature.

Because of the variety of properties of metals and oxides involved, it is difficult to generalize at this point about the combustion behavior of interest. However, a variety of phenomena occur that have been studied in the present project. These phenomena concern primarily

TABLE 1.1. Melting and Boiling Temperatures of Selected Metals and Metal Oxides<sup>a</sup>

Metal	Melting Point (°K)	Boiling Point (°K)	Metal Oxide	Melting Point (°K)	Boiling Point (°K)
Al	932	2736	Al <sub>2</sub> O <sub>3</sub>	2313	3800
B	2450	3931	B <sub>2</sub> O <sub>3</sub>	723	2316
Be	1556	2757	BeO	2820	[4060]
Ti	1950	3550	TiO <sub>2</sub>	2128	unknown
Zr	2128	4747	ZrO <sub>2</sub>	3100	> 5000

<sup>a</sup> For the sake of consistency all values are taken from the latest JANAF thermochemical tables.

post-ignition behavior because the experimental techniques used until quite recently were not selected for ignition studies. During combustion, transitions in burning rate are seen which are related to such effects as the onset of vaporization of the surface oxide (e.g., boron). When the boiling point of the oxide is very high, such transitions in burning behavior may be due instead to disruption of the oxide coating which sometimes results in blowing of oxide bubbles or spinning behavior (e.g., aluminum). If the disruption is sufficiently violent, as might occur with a solidifying oxide coating, the particle may fragment into several smaller burning particles (aluminum, zirconium). These and other deviations from steady burning with spherical symmetry have been studied in some detail because they seem to be the rule rather than the exception, and reveal much about the mechanism of combustion.

In summarizing the present work it was decided to divide the report into sections that were amenable to emphasis of combustion mechanisms. For background, the experimental methods are summarized in Section 2, including primarily new developments not reported in Ref. 1. Section 3 concerned behavior of metals prior to onset of self-sustaining reactions. Section 4 discusses the concept of ignition as it pertains to metals. Section 5 summarizes the observations of relatively steady combustion behavior between the attainment of ignition and the occurrence of burn-out or fragmentation. Section 6 describes observations of the terminal phase of combustion--either burnout or fragmentation. In each section, an interpretation of results is presented that summarizes the knowledge relevant to the section. Section 7 is a brief summary of the status of the metal combustion problem.

## 2. EXPERIMENTAL METHODS

A significant portion of the effort on this program has been devoted to methods of study of metal combustion, and these developments have continued during the present reporting period. In the following, a brief description is given of the improvements in the gas burner and flash ignition experiment and the particle quench technique. In addition, descriptions are given of experiments newly applied to the program. These experiments include differential thermal analysis, hot-stage microscopy, and scanning electron microscopy.

### 2.1. GAS BURNER STUDIES

The gas burner apparatus was developed originally because it provided a convenient means of igniting particles in an environment similar to that in a rocket motor. Use of different fuel gases and mixture ratios has permitted modification of the temperature and chemistry of the environment, and ignition has been possible with several metals of interest, including aluminum, 70/30 aluminum/magnesium alloy, boron and beryllium. Particle combustion has been studied in all of the following flames: hydrogen-oxygen, carbon monoxide-oxygen, cyanogen-oxygen and hydrocarbon-oxygen. The  $H_2-O_2$  flame excludes carbon and nitrogen, the  $CO-O_2$  flame excludes nitrogen and minimizes the hydrogen content (a trace of hydrogen is required to stabilize the flame). The  $(CN)_2-O_2$  flame completely excludes hydrogen, and provides very high flame temperatures ( $4850^\circ K$  calcd.). These variations in flame properties were sought because of expected or known effects on combustion. Observation of combustion behavior was made primarily by high speed photography and by inference from residues on quench plates which collected particles and smoke residues from the reaction region. The burner apparatus is shown in Fig. 2.1.

Development of the burner facility has been continued during the present report period, with the objectives of greater photographic resolution and better control and range of flame environment. An enclosure for the apparatus has been provided that permits operation at pressures up to 3 atm. (absolute). This revision includes an adjustable exhaust to control pressure, and an increase in flow rates to avoid unacceptable contraction of the flame volume at higher pressures. The present system should also permit operation at subatmospheric pressure, but this has not been attempted. Operation at elevated pressure has posed some as

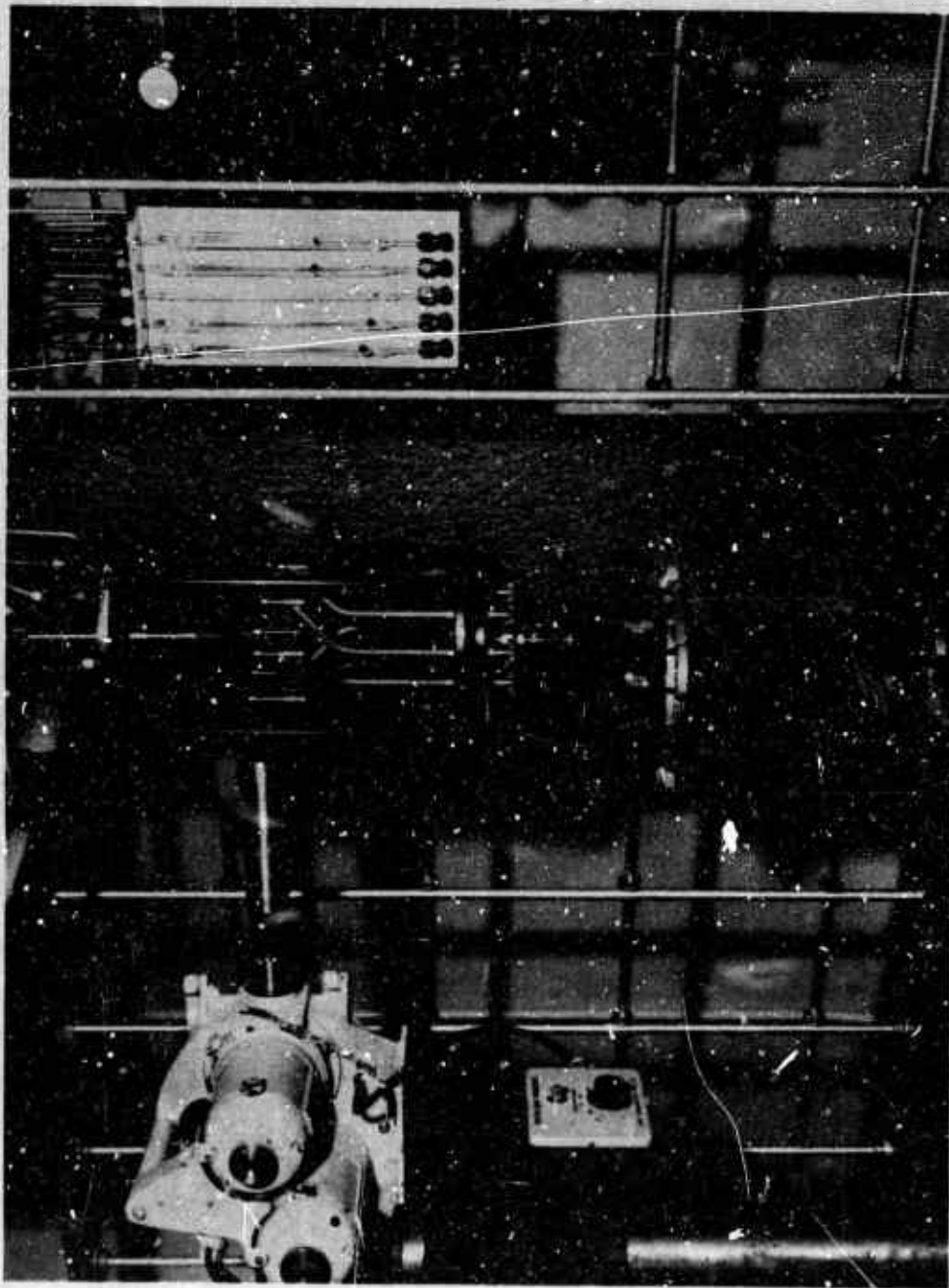


FIG. 2.1. View of the Modified Gas Burner Apparatus Showing High Speed Camera, Particle Sampling Apparatus and Glass Housing for Combustion Experiments With Counterflow of Selected Gases.

yet unresolved problems. The orifice of the particle injector tends to plug, and the viewing ports for photography become dirty quickly. Quench sampling has functioned properly.

The burner facility has also been equipped with a flow system that permits introduction of a cold gas stream oriented in opposition to the downward flow of reaction products from the burner. Arranged coaxially with the burner, this counterflow arrangement establishes a stagnation region where the two flows meet, with the burning metal particles falling through this region and entering the "cold-flow" region. This arrangement provides three new situations of interest. The combustion behavior of particles can be observed in the counterflow gas, including changes when going from flame gases to counterflow gas. The motion of the burning particle is reduced by the flow field, permitting longer stay-time in the focal volume of the high speed camera, and hence providing coverage of a larger part of the burning history of each particle. One further feature of the counterflow arrangement is the development of relative motion between particle and its gaseous environment resulting from unequal deceleration of particle and gas as the stagnation region is approached. This leads to separation of the reaction products of the particle from the vicinity of the particle, which in turn helps to resolve the structure of the reaction zone.

The burner facility has been equipped with a Hycam 400 foot model rotating prism camera, which provides appreciably better resolution than the previous camera, including both superior optics and shorter effective exposure time. Operation at 9000 frames per second is routinely attainable, and the camera can be adapted for 12,000 frames per second if needed.

A further extension of the facility has been the introduction of back or side illumination for use with the high speed photography. This involved provision of additional ports in the burner enclosure, equipped with quartz windows and filters to control wave length of the illumination. A xenon lamp was installed as a source of illumination, and provision was made for a light chopper which would permit motion picture viewing of the combustion field alternately with and without external illumination. These provisions permit a resolution between luminous and nonluminous material in the combustion region, and the intensity-color properties of the external illumination permit resolution of details that are not self-luminous in the presence of self-luminous material.

## 2.2. XENON FLASH IGNITION METHOD

The flash heating technique employed in this laboratory, (with modifications to permit studies at higher pressures), is an adaptation of that first reported by Nelson and Richardson (Ref. 2). The flash heating method takes advantage of the temperature rise resulting from the absorption of the intense light pulse from a capacitor discharge lamp at the surface of a solid of high specific area. The technique has

demonstrated that it is easily possible to raise the temperature of properly prepared solids several thousand degrees in a few milliseconds (Ref. 3). Metal wires, foils, and powders are easily melted or vaporized in this way. Since the source of heat is separated from the oxidizing atmosphere and has a brightness temperature typically in excess of  $10,000^{\circ}\text{K}$ , the procedure is also applicable to the ignition of even the most refractory metals in atmospheres that may be varied over a broad range of compositions and pressures.

### 2.2.1. Combustion Chamber

Combustion of the metal particles was accomplished in the Pyrex chamber shown in Fig. 2.2. The chamber is composed of a tube 23 mm o.d., of either Pyrex or quartz, surmounted by the particle release mechanism and joined at the bottom to an 85 mm o.d. pipe flange with side arm. The drop tube may be varied in length from a few centimeters to a meter or more merely by varying the length of the pipe which is fastened below the pipe flange. A commercially available Pyrex pipe (flanged on both ends) of about 91 cm length was used during most of this study. The end of the reaction chamber may be terminated in any fashion desired depending on what data acquisition schemes are employed.

The particle release mechanism presented some special problems owing to the fact that the mechanism must not only reproducibly drop squares of metal foils or spherical particles on command, but must also form a pressure tight seal for the chamber top for tests up to about 7 atms (100 psia). This design change was necessary because the former apparatus did not deliver acceptable reproducibility. It had the further disadvantages of imparting an undesirable initial acceleration to the particle and it would not permit experiments to be run at elevated pressures. Figure 2.3 shows a detailed view of the particle release mechanism. The metal specimen to be combusted is placed on the trap door while in the latched position and the unit is then screwed down tight onto the top of the reaction vessel. The O-ring in the chamber top is thus seated against the body of the particle release unit and forms the pressure seal. The unit is triggered from an electromechanical sequencer which energizes the solenoid, jerking the magnetic latch pin upward and permitting the door to fall. The door's own inertia is sufficient in this case to permit the apparatus to operate reproducibly.

Accurately sized squares of foil were prepared for use in these experiments by a technique described elsewhere (Ref. 1).

### 2.2.2. Flash Lamp and Power Supply

The helical quartz flash lamp used in this study was the Kemlite, Type 4H4-TU. This lamp has a 5-turn helix which is 3 cm i.d. by about 7.6 cm long with the electrodes bent at right angles to the axis of the helix. This new lamp design was preferable because it allowed permanent-type metal reflectors of clam shell design to be used where formerly

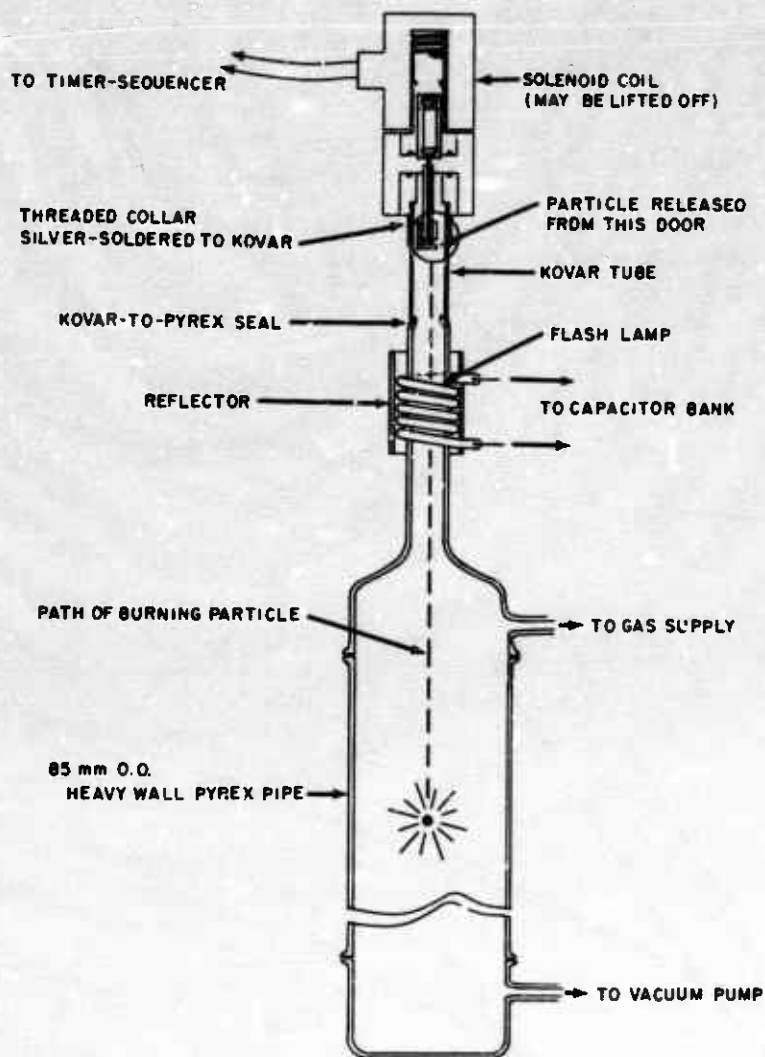


FIG. 2.2. Diagram of Xenon Flash Heating Apparatus Showing Method of Release and Trajectory of Burning Particle.

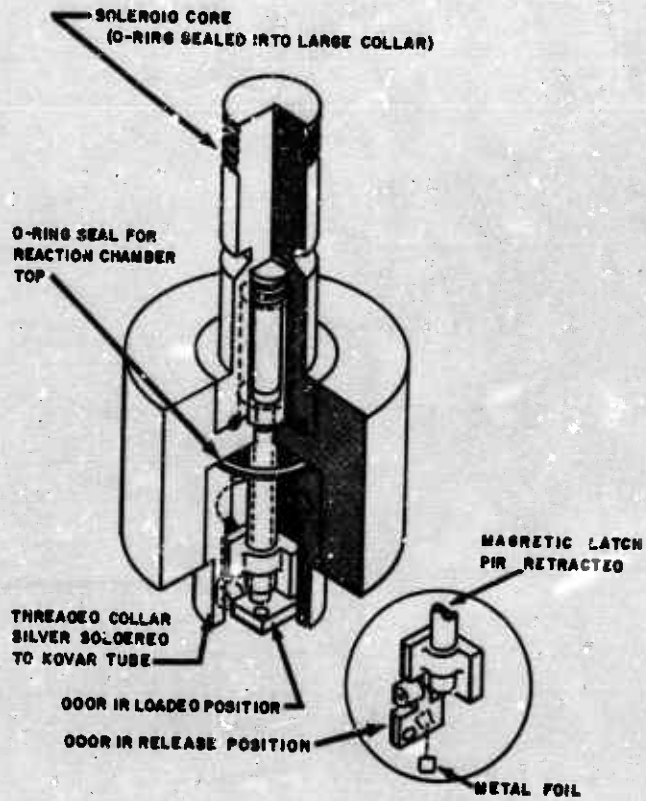


FIG. 2.3. Cutaway Drawing of Particle Release Mechanism on Flash Heating Apparatus Showing Operating Mechanism.

heavy aluminum foil was loosely wrapped around the lamp and had to be replaced after a few lamp firings. In the absence of calibration data for these lamps, the results of a study by Kuebler and Nelson (Ref. 4) on nearly identical lamps were used to estimate the radiant energy delivered by this lamp. When operated at an energy input of 6600 electrical joules for aluminum ignition the lamp is estimated to deliver about 40 thermal joules/cm<sup>2</sup> to a spot on the lamp axis.

Difficulty in igniting aluminum foils early in this investigation due to excessive surface reflectivity of the metal led to the use of additional circuit inductance to reduce the peak amplitude of the flash and lengthen its duration. In addition, a mild phosphoric acid etch of the foil surface was used. The modest pulse shaping employed gave a pulse duration of about 2 ms at half height, with the remaining exponential decay lasting about 4-7 ms. The combination of altered electrical circuit parameters and metal surface etching provided satisfactory ignitions.

The energy storage system is the Lear Siegler, Inc., Laser Stimulator, Model C-102. This particular system consists of a 4000-volt variable power supply and two 450  $\mu$ F capacitor banks, one of which is switchable in 75  $\mu$ F increments. The total energy storage capability is thus 8000 joules.

A typical experiment is initiated by triggering the particle release mechanism remotely through the sequencer, releasing the particle (foil, sphere, or granule) to free-fall through the flash lamp. When the particle is within the working area of the lamp the delay timer remotely fires the flash lamp, melting the particle into a spherical droplet and igniting it immediately. The particle continues to fall and accomplishes its combustion in the large diameter section of pipe seen in Fig. 2.2.

### 2.2.3. Data Acquisition

The burning metal droplets are photographed in free-fall by both high speed cinematography and still-plate track photography. Burning and explosion times are derived from the high speed motion pictures, while details of the luminous track during combustion as well as the particle explosions are taken from still plate track photographs.

The burning specimens may be quenched at any time during burning by inserting glass plates at various heights within the pipe and capturing the particle. In this way, by sampling at successively lower positions in the pipe, the evolution of the burning geometry may be reconstructed by photographing these quenched specimens.

Specimens for x-ray examination may be secured by collecting oxide residues from burnt-out droplets or by a sampling procedure like that described above, using a suitable liquified inert gas for quenching rather than the glass plates.

Reproducibility in these experiments is quite good, being  $\pm 2\%$  in the explosion times for titanium and zirconium. For aluminum combustion in air the reproducibility is about  $\pm 10\%$ , while that for aluminum in oxygen-argon mixtures is about  $\pm 5\%$ .

### 2.3. INVESTIGATION OF THE PREIGNITION BEHAVIOR OF ALUMINUM BY DTA

The methods of thermal analysis have been widely used to investigate organic and inorganic materials, including the salts of metals (Ref. 6). The research of pure metals and their alloys by thermal analysis is usually limited to the determination of melting points, phase transitions and phase diagrams. Differential thermal analysis (DTA) is a branch of thermal analysis which is very convenient for this type of work. There are a number of designs of DTA apparatus usable at temperatures of interest for the study of metals and refractories. A complete set of basic DTA components is available in this laboratory. Therefore, it is planned to use the equipment after necessary modifications for the study of the preignition behavior of aluminum. In the following a short outline of the method and its application will be given based on the DTA experience made in the low temperature range ( $<550^{\circ}\text{C}$ ).

The typical DTA apparatus consists of a metal block which can be heated at a preselected rate and which contains two identical cells symmetrically located with respect to the block and heating element. One cell contains inert material, the other the sample plus inert material. A differential thermocouple is installed in order to measure differences in temperature between corresponding points in the sample and reference cells. Thus, heat release or consumption associated with reactions in the solid can be detected and registered by measuring the differential temperature. So far, two sample holders have been checked out; namely, quartz and alumina tubes. Both have disadvantages: the aluminum reacts with the quartz at points of contact and, in the case of the alumina tube, the sample holder material is a product of the process to be studied, which may have an uncontrollable influence on the reaction.

Heating rates can be varied between  $4^{\circ}\text{C}/\text{min}$  and  $40^{\circ}\text{C}/\text{min}$ . This will give enough flexibility for preliminary quantitative measurements. However, because the heating of metals in a propellant occurs much faster, the goal must be to increase experimental heating rates as much as possible without exceeding the capability of the method. It is hoped to achieve heating rates of the order of  $1000^{\circ}\text{C}/\text{min}$  with a radiation furnace which will allow the heater element to be separated from corrosive gases of the sample environment.

The main purpose of the DTA experiments will be the study of the oxidation of aluminum particles on heating above the melting point in different atmospheres. This includes determination of the degree of oxidation and the amount of self-heating during the process. The first

feature can be examined by analyzing the DTA exotherms, the second by following the temperature rise of the sample as a function of time. Both directly affect the ignition of the metal.

During the present reporting period, the DTA apparatus has been applied primarily to tests on ammonium perchlorate (AP) (on another project). Preliminary tests with aluminum powder indicate promise for this method in study of preignition behavior.

#### 2.4. INVESTIGATION OF PREIGNITION BEHAVIOR IN THE HOT-STAGE MICROSCOPE

The use of an optical microscope for the study of quenched aluminum particles has been described in detail in the last progress report on aluminum combustion (Ref. 1). It increased the understanding of quenched samples of aluminum particles which were ignited and burned in various environments. The acquisition of a hot-stage permits examination of aluminum and its reaction products during the preignition period. The stage and its applications are described here.

The water-cooled microscope hot-stage is designed for a maximum temperature of 1350°C and can be used for observations in transmitted and incident light. It is heated resistively and the heating rate can be programmed and controlled by an available DTA programmer. The hot-stage has several interchangeable heating cartridges as well as a metal support for the use of different kinds of object carriers and crucibles. The sample container is sealed by a glass disc which can be rotated. If reaction products condense on the disc the obscured area may be replaced by a clean portion through a small turn. The disc seal is gas-tight. This permits observations in different gas atmospheres. The object can be oriented and aligned parallel to the surface of the stage by a centering device. The maximum heating rate obtainable with the commercial set-up is about 500°C/min.

The microscope has a built-in automatic 35 mm camera. This facilitates picture taking, especially at high temperatures where considerable brightness variations and a rapid succession of phases can occur. Thus, hot-stage and photomicroscope are a powerful tool for the detailed investigation of the history of aluminum particles during heating in non-oxidizing or oxidizing atmospheres. Of particular interest is the reaction of the oxide skin, which is present on any normal aluminum particle, upon heating and the transition of a particle through the melting point of the metal. It is well known (Ref. 7) that aluminum which is embedded in a propellant matrix tends to agglomerate during the process of propellant burning. Preliminary experiments show that agglomeration can occur above the melting point and below the ignition point of aluminum. The study of the agglomeration mechanism will be a main part of the planned hot-stage microscopy.

## 2.5. PARTICLE QUENCHING

The clearest resolution of details of metal combustion to date has been by use of the quench-plate method, wherein a plate, generally of glass, is inserted in the path of a falling, burning metal particle and the particle and residue impinge on the plate. Microscopic study of the plate is made under very favorable conditions, compared to those prevailing in real-time combustion photography, which accounts for the detail attainable. In the present report period, the quench plate method has been used extensively in the flash ignition apparatus, as well as the gas burner. No major changes in technique were made. Application of the scanning electron microscope has greatly enhanced the value of the quench-plate method. In the following, some problems of interpretation of quench samples are discussed, while the results for specific test conditions are discussed in later sections of the report.

### 2.5.1. The Sampling Problem and the History of a Burning Droplet

In the course of burning, a metal droplet usually goes through a sequence of events characteristic of the metal and atmospheric environment. By obtaining quench samples at different times in the burning history, one expects to see the evidence of the progressive character of burning. However, the reconstruction of the progression is complicated by the fact that each quench sample is from the combustion of a different particle; the burning time in the case of burner ignited specimens is not necessarily known accurately, and each particle burns a little differently, so it is sometimes difficult to reconstruct the combustion history from a collection of quench samples. This problem is usually not serious in the flash ignition experiment, because combustion behavior is quite reproducible (when the original particles are alike). Thus, a series of quench samples such as those in Fig. 2.4 gives an excellent insight into the progressive character of the combustion. Even fragmentation was sufficiently reproducible with aluminum to permit quench sampling in the neighborhood of the "fragmentation site" in the particle trajectory, and obtain something akin to expanded time resolution. The impingement quench method as applied to titanium and zirconium has not been successful due to a tendency on the part of burning droplets of these metals to splatter on impact and continue burning for a significant time. In some situations boron particles bounce upon impingement, leaving smoke patterns without the central particle.

Quenching has provided evidence of a number of details of metal combustion in the gas burner experiment that would otherwise be unknown, details such as the jetting of aluminum oxide droplets. In a few instances, quenches have been obtained in conjunction with high resolution, high speed photography, which revealed that oxide droplets found on the quench plates existed as oxide balloons during burning (Section 5.2).

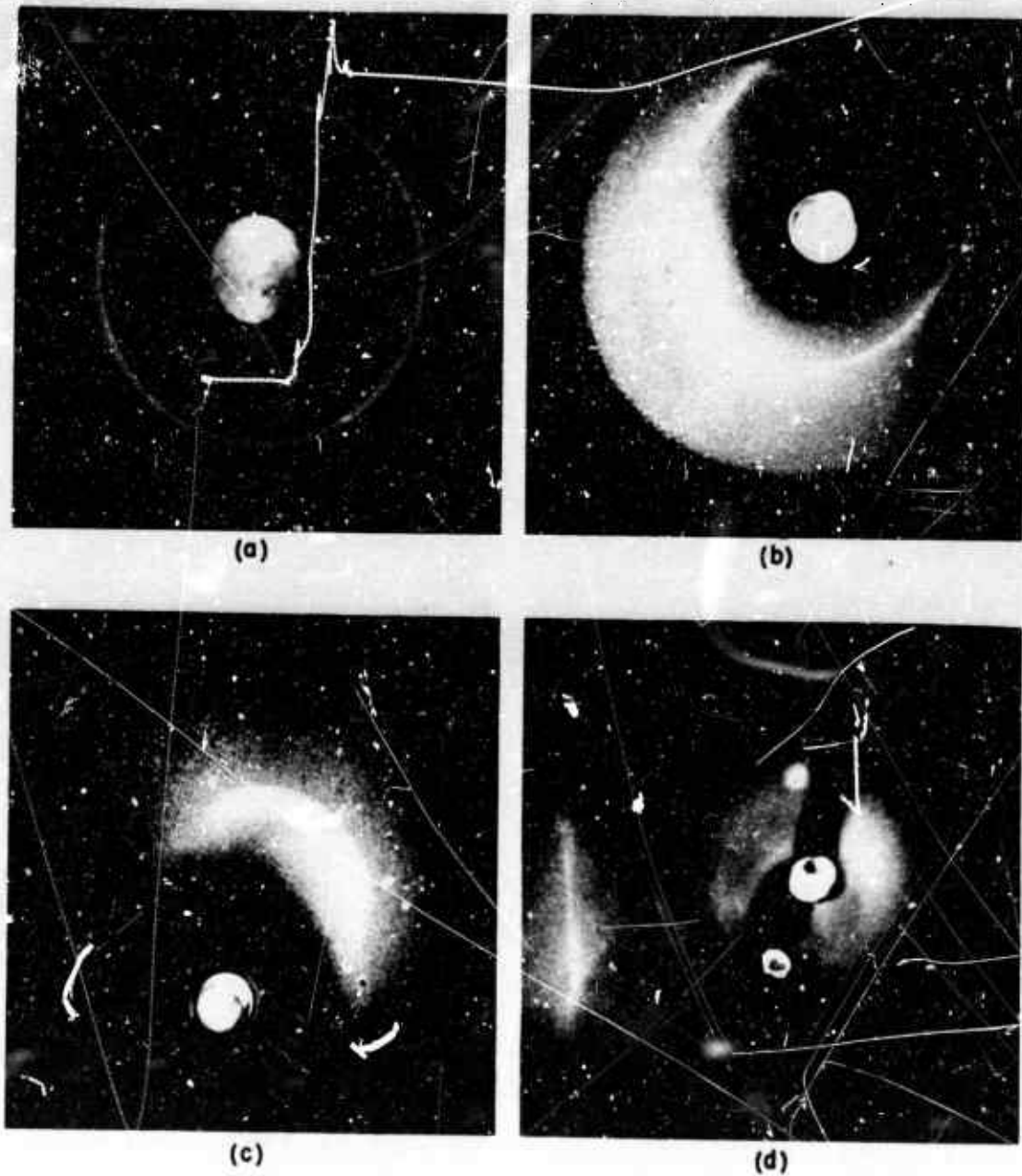


FIG. 2.4. Optical Photomicrographs ( $\times 50X$ ) of Flash Ignited Aluminum Particles Quenched While Burning in Ambient Air. Series shows evolution of burning geometry from (a) shortly after ignition to (d) incipient fragmentation of specimen quenched in oxide-down position.

Demonstration of the progressive details of particle combustion is less decisive in the gas burner experiment than in the flash ignition experiment, because combustion behavior is less reproducible. When a charge of particles is introduced into the product gases of the burner flame, particles are seen to ignite throughout the length of the flame, and quenching at a particular location may yield particles which represent all phases of the combustion history. The problems posed by these sampling difficulties in the burner experiment are, for the most part, alleviated by the flash ignition experiment and by growing mechanistic insight. However, even under the worst conditions for sampling, the quench plate method still shows dramatically the gross difference between results with different metals and gaseous environments.

### 2.5.2. Interpretation of Quench Samples

The similarity of pictures of quench samples to pictures of the actual combustion field is so striking that pictures of quenched samples are often mistaken for combustion pictures. However, detailed interpretations of quench samples usually require some consideration of behavior that occurs during the quench rather than during burning. An example noted above is the identification of aluminum oxide droplets as the residue from oxide "balloons". Another is the observation of unusually thick smoke deposits around quenched boron droplets (Fig. 2.5), deposits apparently produced by combustion after impingement. Likewise, some of the "flame structure" suggested by the smoke rings around quenched aluminum particles is very likely caused by thermal or gas flow effects, or possibly by electrostatic forces. Another suspected artifact of quenching revealed in the previous report (Ref. 1) was the oxide-free region surrounding most large ( $>20\mu$ ) aluminum oxide particles on quench plates. Finally, it is doubtful that the shape of a quenched droplet is the same as the original burning droplet, and some modification in surface detail is likely. In spite of these many pitfalls to interpretation of quench samples it will be seen in later parts of this report that the samples can be extremely revealing of combustion behavior--and especially so if the pitfalls are known.

### 2.6. SCANNING ELECTRON MICROSCOPE TECHNIQUE APPLIED TO QUENCHED SAMPLES

Previous studies of quenched samples were made with optical microscopes. The limit of resolution was typically 0.5 micron, whereas finer detail appeared to exist. Even more important, the use of high magnification is accompanied by serious limitation of the depth of focus. This is a severe limitation in analyzing samples, but even more serious in the documentation of observations by photography. Since the last report, use has been made of a new type of microscope (the scanning electron microscope, (SEM)) which gives resolution superior to the optical microscope, while preserving great depth of field. Samples were first studied on a machine time rental basis on a unit at The Westinghouse Corporation known as a "Microscan". The remarkable detail visible in the photographs



FIG. 2.5. Flash-Ignited 180 $\mu$  Boron Particle Burned in Ambient Air. Quenched on glass plate.

obtained on this unit led to studies of other applications at the Naval Weapons Center (NWC), which in turn led to purchase by NWC of a Cambridge Instrument Company Mk II Stereoscan. This instrument is being used extensively on the present program.

#### 2.6.1. Operating Principle of the SEM

The SEM illuminates the test sample by a moving electron beam, with the beam scanning the viewing region in a raster pattern. A scintillator/photomultiplier system monitors the secondary electrons emitted by the illuminated test sample. The resulting signal is displayed on an oscilloscope "screen" as intensity modulation of a spot which scans in synchronization with the scanning electron beams. The result is an image on the screen with magnification equal to the ratio of screen dimension to dimension of the region scanned. Resolution is ultimately limited to the diameter of the electron beam, which is usually under 200  $\text{\AA}$  (.02 microns) in the present work. The great depth of field results from the

fact that the beam diameter is reasonably uniform in the sample volume. The magnification is controlled by the voltages on the displacement plates for the electron beam. Details of the present instrument are available from the manufacturer, or the United States vendor.<sup>1</sup>

#### 2.6.2. Scanning Electron Microscope Technique

Application of the SEM to the present studies involves considerable care in preparation of samples and operation of the instrument. The most serious problem results from accumulation of charge on the sample during exposure, leading to electron saturation of the scintillator-photomultiplier and producing great bands of white across the photographic record. This banding on the record completely obscures significant portions of the specimen. Prior to examination by SEM, samples are coated with a thin metal film by vacuum deposition. Materials which have been used are gold, palladium, silver, chromium, and aluminum, in layers about 500 Å thick. Since this thickness is within the resolving power of the instrument, interpretation of very fine detail should be made with due consideration of possible effects of coating irregularities. A gold-palladium alloy has been used most extensively as a utilitarian coating material for all types of specimens examined by SEM in this laboratory but it is not really satisfactory for studying quenched aluminum specimens due to a distressing tendency to accumulate charge as described above. As a result, new coating materials are being investigated which will hopefully overcome this limitation. Results of efforts to date will be evident in later parts of this report.

---

<sup>1</sup> Engis Equipment Company, Morton Grove, Illinois.

### 3. PREIGNITION PROCESSES

The behavior of metal particles and groups of particles before they ignite can have considerable influence on ignition and subsequent combustion. This is so for two reasons, one because the preignition formation of surface oxides affects ignition, and the other because particles may become attached to each other in such a way as to form much larger droplets upon ignition. These factors are often more decisive in the characteristics of propellant combustion than is the combustion process itself. In view of this, increasing effort has been directed towards understanding of preignition behavior. In the present section, results are presented of studies of aluminum subjected to sub-ignition heating in air and in a gas burner flame. The scanning electron microscope was used to particularly good effect in this work.

#### 3.1. CONDITION OF ALUMINUM PARTICLES BEFORE TESTING

In the studies of preignition behavior, the results are primarily in the form of microscopic examination of samples subjected to sub-ignition heating histories. In order to interpret the observations, it is necessary to know the condition of the particles before the tests. In the case of spherical, 99.99% pure aluminum particles with diameters between 105-125 $\mu$  used in most of the tests, samples were photographed with the SEM, with the results shown in Fig. 3.1. At low magnification, the particles are seen to have coarse wrinkles, while higher magnification shows a grainy quality of the surface. The particles were originally produced in an argon plasma, and cooled in the absence of oxygen. The coarse wrinkles are very likely due to contraction of the interior of the particle during freezing, at a time when the surface was already viscous or solid.

The grainy quality of the surface is probably due to the oxidation of the surface at room temperatures after preparation of the particles. It is generally believed that a thin, impervious oxide surface is formed on aluminum that inhibits continued oxidation. However, the volume of the oxide formed from a given volume of metal is about 2.5 times the metal volume, a condition which may cause surface irregularities. These details of the oxide structure are very likely affected also by the extent of adherence of the oxide to the underlying metal, and the susceptibility of the oxide and metal to plastic flow. Since very little is known about these properties of the metal and its oxide, any interpretation at present of the surface details is speculation.

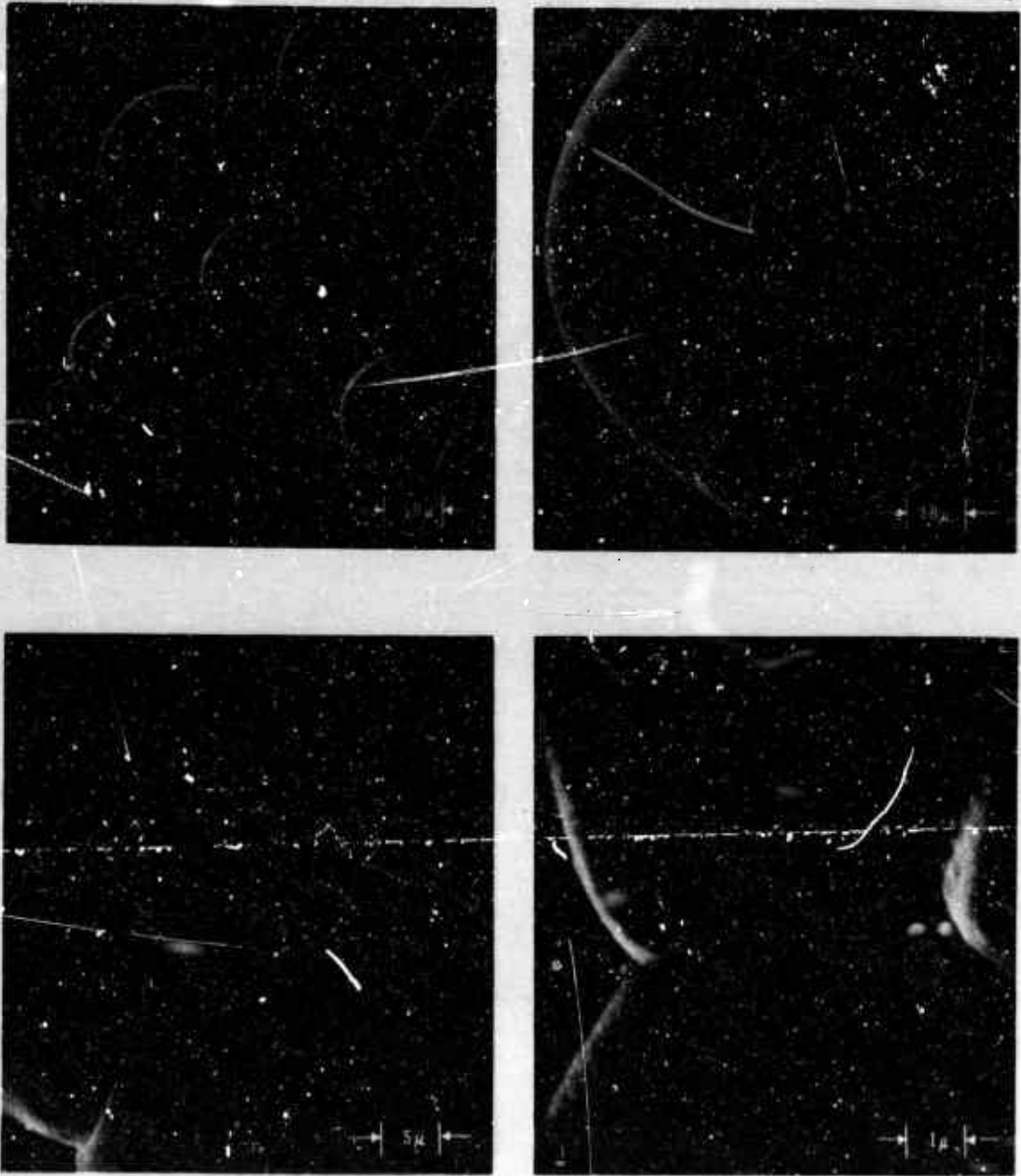


FIG. 3.1. Spherical Aluminum Particles, as Received, with Diameters Between  $105\mu$  and  $125\mu$ .

### 3.2. EFFECT OF HEATING IN AIR

A simple method of studying the preignition behavior of aluminum is to heat it without producing ignition, and observe the samples during heating and after cooling. Pending receipt of a hot-stage microscope for observation during heating, tests were made by heating samples of the aluminum described in Section 3.1, cooling them, and studying them by microscopy. The samples were heated by placing them on a 12.5 mm diameter by 1 mm thick sapphire disc in air and heating the disc from the underside with a small, sharp flame. After approximately 10 seconds at a temperature of about 1400°C, the system was allowed to cool to room temperature.

The aluminum samples as treated were examined by means of an optical microscope and the scanning electron microscope. The particles were seen to be similar in shape to the unheated particles except that some had adhered to each other, or in some instances run together. Some were rather transparent to light, and some were opaque when viewed in the optical microscope (Fig. 3.2). The transparent particles were seen upon breaking to be hollow, indicating that the aluminum had run out, leaving an oxide shell. The SEM pictures showed more clearly that there were hollow shells, presumably of aluminum oxide (Fig. 3.3). The exterior of both the hollow and solid particles exhibited a complex pattern of lines that appeared to be cracks sealed over with a new oxide.

Because of the remarkable detail visible in the SEM pictures, they are described in detail here. Two samples of the heated aluminum particles were prepared and coated with silver in order to take pictures by the scanning electron microscope. On one sample, some of the oxide spheres were intentionally broken to allow a study of their interior. The other sample was not altered. Accordingly, two series of photographs have been obtained.

The first series is represented by Fig. 3.2-3.5. Figure 3.2 is an optical microscope photograph which is used to distinguish between transparent and opaque particles. The area within the frame was photographed by SEM and is shown in Fig. 3.3. An arrow (Fig. 3.3) points to a broken oxide sphere which was selected for high magnification. There are two agglomerated metal particles showing portions of wrinkled surface and areas of the original oxide layer. Figure 3.4 shows a section of Fig. 3.3 in more detail. Opaque particles are marked with an "O", transparent or partially transparent ones with a "T". It can be seen that opaque-appearing particles can have partially collapsed oxide layers (concave areas). The oxide skin in these cases is not adherent or the shells are only partially filled with metal which obscures the cross-section in transmitted light. An arrow on one half of the broken shell points to the residue of a second shell. Apparently two original aluminum particles formed a pair by a metal and oxide bridge. During the heating the metal leaked through the cracks and holes in the oxide and

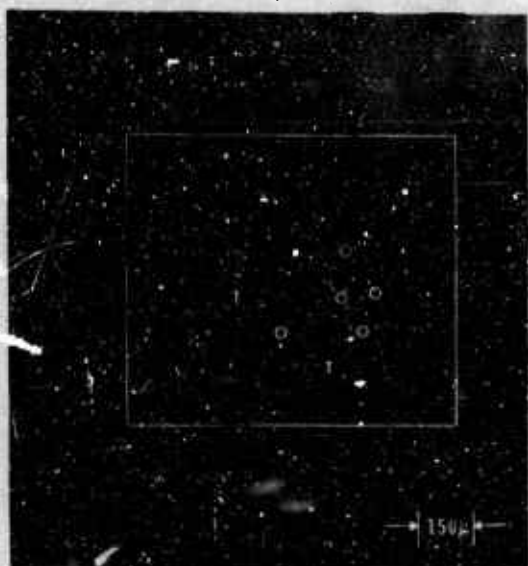


FIG. 3.2. Optical Microscope Photograph of Aluminum Particles After Heating to 1400°C and Cooling. O = opaque, T = transparent particles.

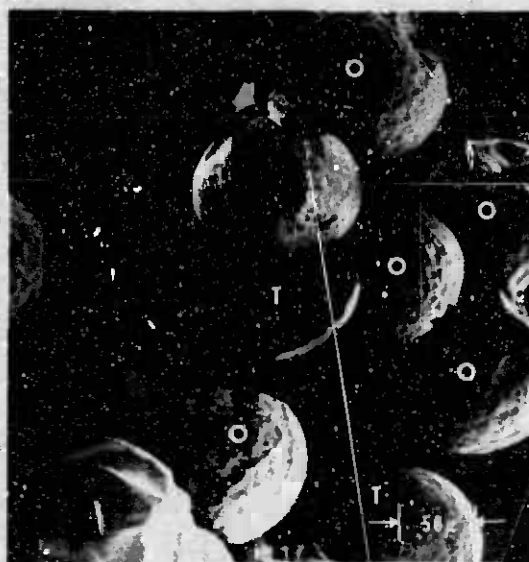


FIG. 3.3. Scanning Electron Microscope Photograph of Framed Section of Fig. 3.2. Arrow points to a broken oxide sphere.



FIG. 3.4. SEM Photograph of Section of Fig. 3.3. O denotes opaque particles, T transparent particles. Arrow points to residue of a second shell which broke away.

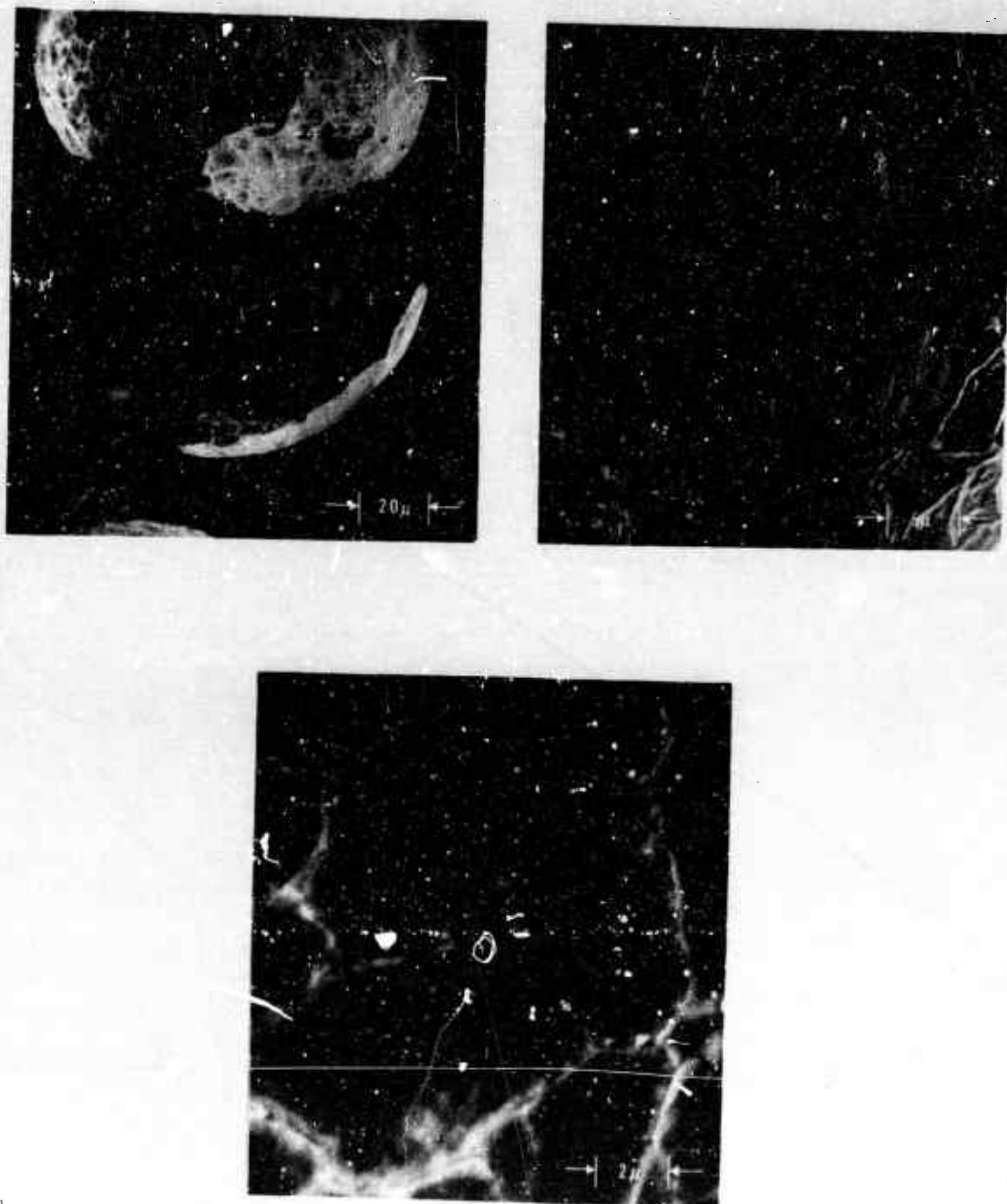


FIG. 3.5. Three Views at Different Magnifications on Inner Side of the Broken Shell Shown in Fig. 3.4.

from the empty shell, which had the shape of two connected spheres. One half of the specimen (equivalent to one sphere) was lost during the preparation of the sample and the other half (equivalent to another sphere) was broken as can be seen in Fig. 3.4. A circular area shows where the bridge connected both aluminum spheres before the liquid metal leaked through the oxide. Figure 3.5 exhibits the details of the inner side of a broken shell. A network composed of a large number of irregularly arranged cracks can be seen. This pattern of cracks is not present on the original particles (see section 3.1). The crack pattern can be more clearly observed on the outer side of an oxide shell and a representative example is shown in the second series (unbroken sample) of pictures.

Another area of the sample is shown on the optical photomicrograph of Fig. 3.6. A comparison SEM photograph is shown in Fig. 3.7. Corresponding transparent particles in Fig. 3.6 and 3.7 are marked by a "T" and opaque spheres by an "O". A group of three particles was chosen for high magnification (Fig. 3.8 and 3.9). The center particle (see arrow in Fig. 3.8) is completely transparent (hollow) and joined by two opaque neighbor particles. Figure 3.10 shows details of the outer surface of the transparent, hollow particle. One can see the same type of crack pattern observed in the interior of the broken sphere in Fig. 3.5. However, the cracks have the appearance of welding seams. The seams look like seals of the cracks which were so clearly visible in the interior of a broken sphere. Indeed, one can imagine that the enclosed metal fractured the oxide envelope on heating and that the metal, which escapes through the cracks, becomes oxidized, thus building up a seal of the cracks. The selfhealing process would work similarly at leaks different from cracks (holes, etc.). Where particles touch each other or touch the sapphire support, the liquid metal can flow without much oxidation and thus empty a sphere or agglomerate. The difference between the thermal expansion coefficient of liquid aluminum and solid aluminum oxide is such as to assure continual cracking of the oxide layer during heating, while the rapid oxidation of aluminum exposed by cracking assures buildup of oxide along the cracks.

A last group of SEM photographs shows parts of the surface of the big agglomerate which can be seen near the center of Fig. 3.6. Figure 3.11 depicts a section of new surface with wrinkles which probably developed during cooling of the big mass of agglomerate. Figure 3.12 shows the original oxide layer joining new surface. Inasmuch as agglomeration results in a decrease in the surface-to-volume ratio the original oxide present on the individual spheres is now more than adequate to encapsulate the resultant agglomerate. This means that more and more of the original oxide is occluded in the developing agglomerate. Indeed, agglomerates have been found which were very hard to crush and which, upon crushing, produced a noise similar to breaking glass. The original aluminum spheres, on the contrary, are very soft and can be squeezed and cleaved without any trouble or noise. In Fig. 3.11, at low magnification,

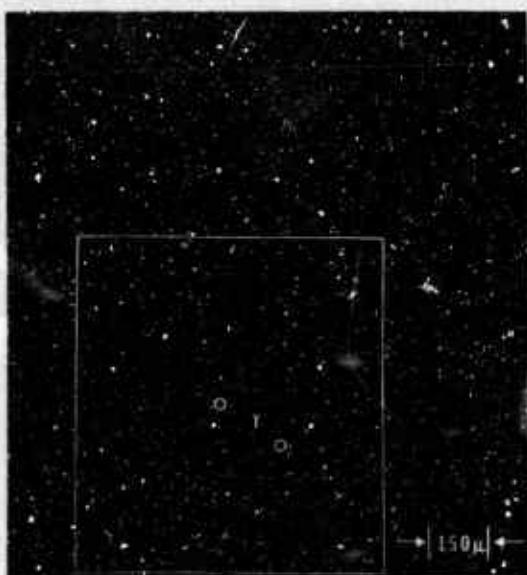


FIG. 3.6. Optical Microscope Photograph of Aluminum Particles After Heating to 1400°C and Cooling. O marks opaque, T marks transparent particles.



FIG. 3.7. SEM Photograph of Framed Section of Fig. 3.6. Opaque particles are marked with O, transparent particles with T.



FIG. 3.8. Magnification of Fig. 3.7. Arrow points to completely transparent particle.



FIG. 3.9. Magnification of Fig. 3.8. Transparent center particle is between two opaque particles which show broken oxide shells.

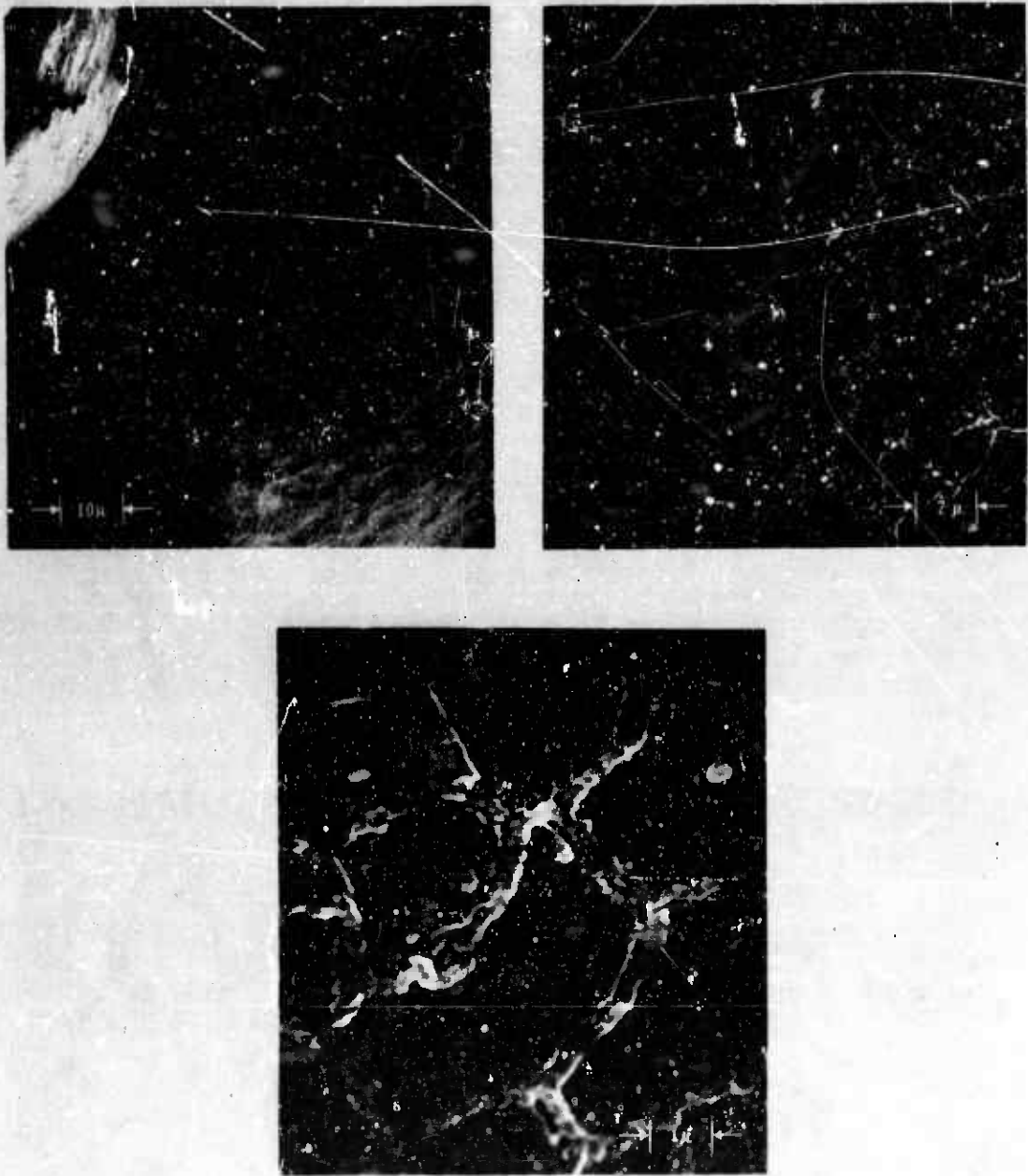


FIG. 3.10. Surface of the Transparent, Hollow Center Particle of Fig. 3.9. Three different magnifications.

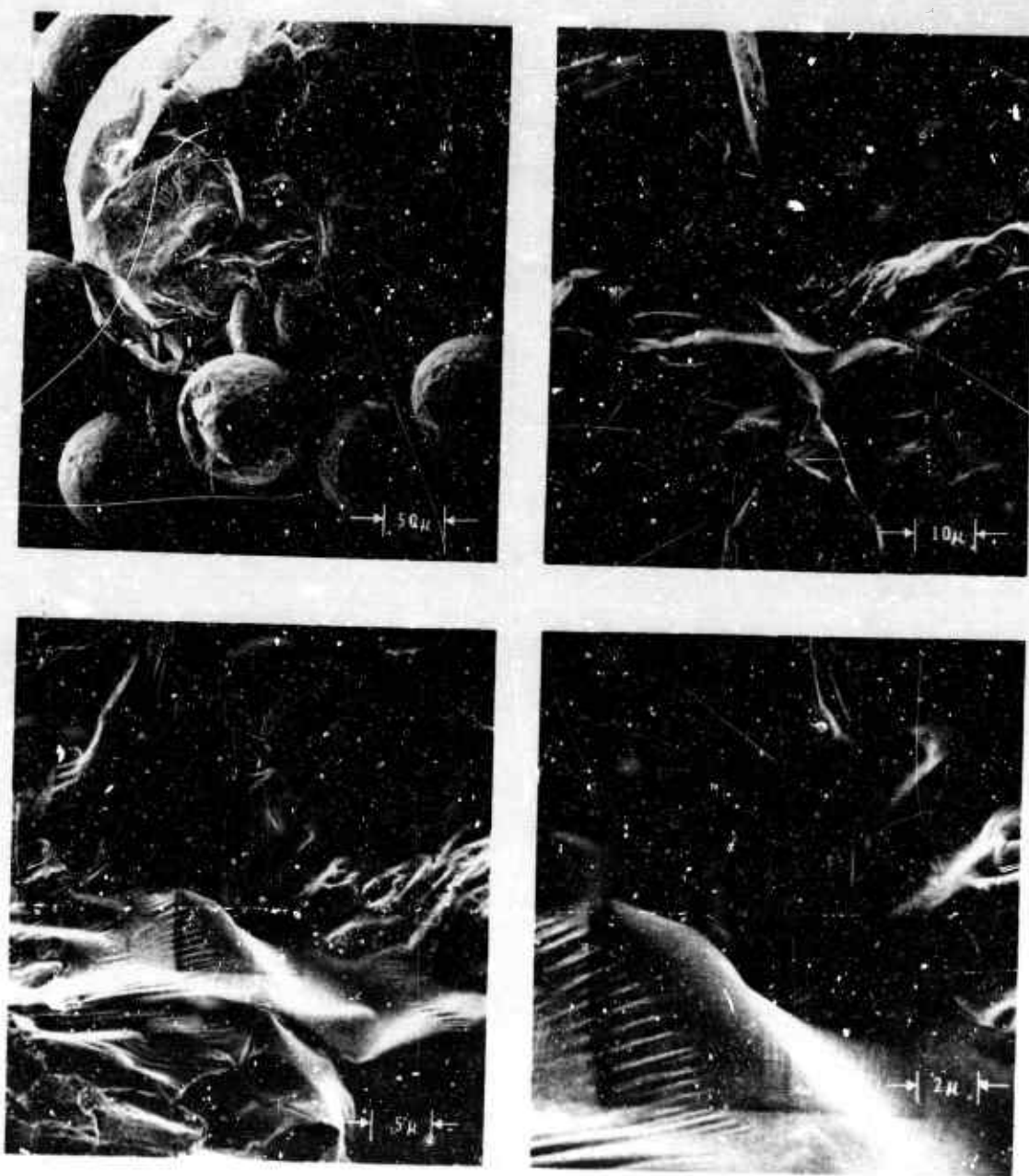


FIG. 3.11. Section of Surface of Large Aluminum Agglomerate. Four different magnifications.

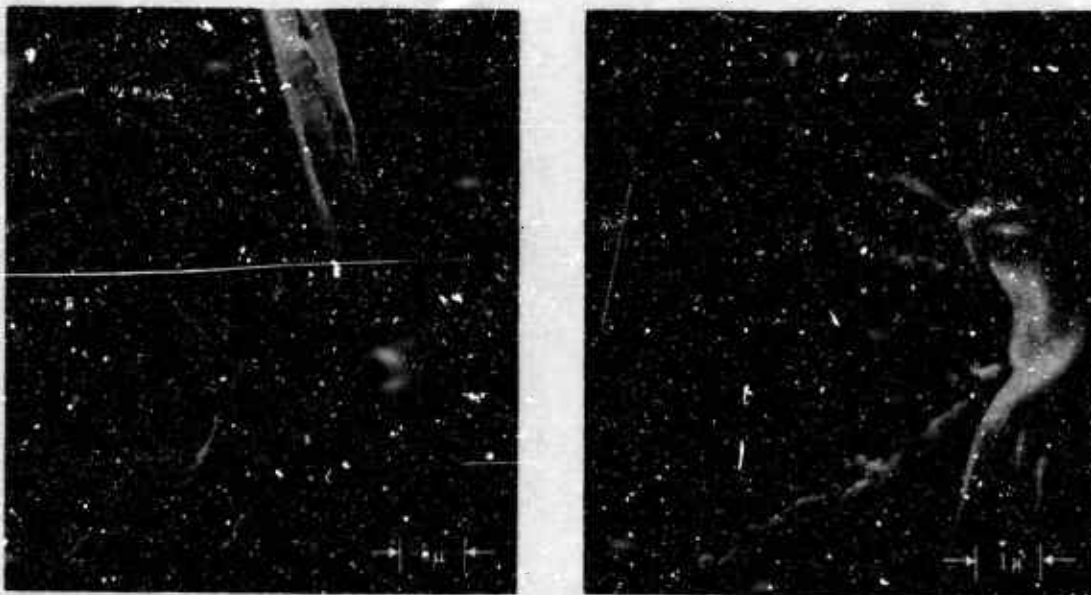


FIG. 3.12. Original Oxide Layer Joining New Surface on Large Aluminum Agglomerate.

two small particles can be seen joining each other and the big agglomerate. The process of agglomeration occurs here under a protective shield of self-healed oxide ( $\approx 1\mu$  thick).

The conclusions drawn from the photographic evidence are:

(1) The protective nature of the oxide layer of an aluminum particle is not maintained on heating.

(2) The molten metal can leak through the cracks and holes in the oxide.

(3) Aluminum particles can agglomerate well below the melting point of the oxide.

(4) There is a possibility that a significant amount of aluminum can evaporate into the gas phase even when the aluminum is well below its boiling point. This may be of importance with respect to the ignition of both particles and agglomerates.

### 3.3. RAPID HEATING OF ALUMINUM PARTICLES IN A BURNER FLAME

Spherical aluminum particles with diameters between 50-150 $\mu$  were passed through CO/O<sub>2</sub> or H<sub>2</sub>/O<sub>2</sub> burner flames. The burner is described in Section 2.1. The calculated flame temperatures were 2800°K for H<sub>2</sub>/O<sub>2</sub> flames and 3200°K for CO/O<sub>2</sub> flames. These temperatures should be considered as upper limits because they are adiabatic flame temperatures. Most particles ignited if they were given an ample stay time in the flame. Unignited aluminum particles were found in the residue which passed through the burner flame. The transition to ignition is a continuous but very fast process and it is difficult, if not impossible, to draw a sharp line between unignited and ignited particles. However, observation of residues indicated that all ignited particles had well developed smoke clouds around them. Particles judged to be unignited were at the most surrounded by a very thin and hardly visible deposit which probably arose from the evaporation of aluminum at high sub-ignition temperatures. Based on this rather rough criterion, particles which were collected below the general ignition level of the flame (see Section 2.6.1) by impingement quenching were considered as not ignited if no well developed smoke pattern was visible. Scanning electron microscope photographs were made from an unignited particle and of a particle which was assumed to have been in an early stage of ignition.

Figure 3.13 shows the surface of the unignited aluminum particle in two magnifications. An intact skin of oxide remained so well attached to the metal surface that cooling during the quenching process produced a net-like pattern of wrinkles. The network is irregular like the one shown in Fig. 3.10 but without any seams or cracks. However, when the smoke deposit is more pronounced around a quenched particle the skin no longer is fully intact. An example can be seen in Fig. 3.14. There are crack-like lines and isolated defect regions. Both have a granular structure and indicate the beginning of destruction of the oxide skin. Breaks in the skin can be roughly correlated with the smoke pattern around the quenched particle. This suggests that ignition is preceded by the exposure of fresh aluminum.

A comparison of the results in Section 3.2 with those in Section 3.3 shows that there are several temperature regions within which the aluminum oxide behaves in a characteristic way. In one region the oxide retains its rigid but vulnerable structure (see Section 3.2). Another region is characterized by the possibility of plastic flow. The capacity for self-healing increases and the granular structure of the surface becomes smooth. Finally, in a third region, the tendency to decrease the surface area because of surface tension of the oxide may force a very soft (liquid) oxide to contract to a configuration (caps for example) which is more favorable for exposing aluminum. During this process the oxide skin may locally become so thin that it breaks and exposes fresh metal surface to the gas phase. This last temperature region covers the transition to ignition and ignition itself and more work has to be done in order to permit more accurate descriptions of the limits within which ignition actually occurs.

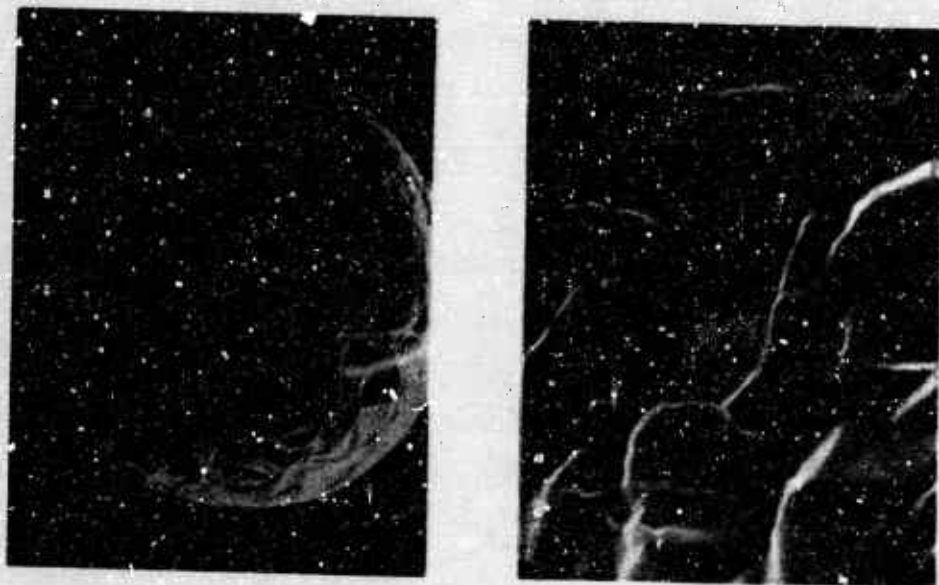


FIG. 3.13. Surface of Unignited Aluminum Particle.

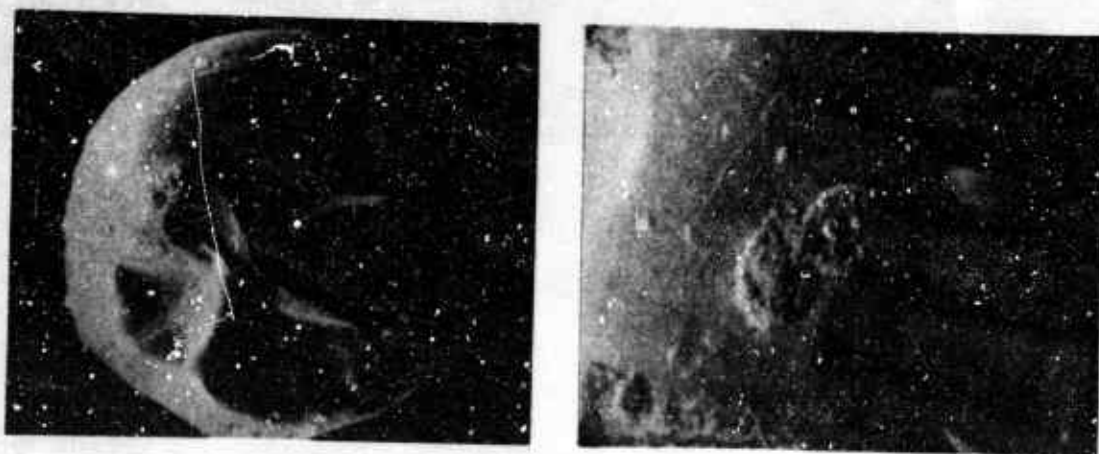


FIG. 3.14. Surface of Aluminum Particle Quenched Early in the Ignition Stage.

### 3.4. INTERPRETATION OF RESULTS

Different aspects of the preignition state and behavior of aluminum particles have been studied and a summary of the results is presented here.

(1) All aluminum particles used are covered by an oxide layer. This layer is very inhomogeneous and thin, about  $1\mu$  thick. Although the oxide may be protective at low temperatures, the protective nature is degraded by heating, particularly above the melting point of aluminum. Liquid metal can flow through cracks and holes in the oxide.

(2) Oxide bridges frequently develop at points of contact between aluminum particles when aluminum is heated above its melting point. These bridges are apparently formed by the flow of aluminum through cracks and subsequent oxidation of the molten aluminum. This is considered to be the key step in the agglomeration process.

(3) At least three temperature regimes can be distinguished within which the aluminum oxide behaves in characteristic ways. In the low temperature region, the oxide retains its rigid but vulnerable structure. The second temperature region may be characterized by the possibility of self-healing of the oxide layer and smoothing of its granular structure. In the third region, the surface tension of the oxide may cause a very thin oxide skin to break and contract to cap-like structures. This last region covers the transition to liquid oxide.

#### 4. IGNITION OF METALS

##### 4.1. DEFINITION OF IGNITION

A variety of ideas are associated with the concept of "ignition"; most are identified with concepts of ignition temperature or self-sustaining or runaway reactions. An ignition temperature is appealing because it appears as a unique property of the material involved. Unfortunately, measurements of temperatures associated with apparent attainment of ignition often depend upon environmental or other variables not uniquely related to the thermal state of the material to be ignited. This seems to be particularly true of metal particles, which may ignite spontaneously in room temperature air under some conditions (e.g., small particles of aluminum  $< 1\mu$  with clean surfaces) and yet fail to ignite at  $1500^{\circ}\text{K}$  in air under other conditions (e.g.,  $50\mu$  particles of aluminum with the usual protective coating of oxide). In the example, the attainment of self-sustaining reaction is highly dependent on the particle size and the character of the oxide layer that forms prior to, or during heating. In ignition of metals, one must anticipate such effects in developing the concept of ignition.

The practical outcome of ignition is the attainment of "self-sustaining combustion", which is understood to involve high temperatures and high rates of exothermic reactions. In proceeding to a more precise definition it is obviously necessary to specify what is meant by "high" temperatures and reaction rates. In relative terms, "high" refers to a comparison with temperatures and rates before an igniting stimulus was applied, while the term "self-sustaining" means continuation of high temperatures and rates after removal of initiating stimulus. The qualification to exothermic reactions is redundant, in the sense that self-sustaining combustion could not ensue unless exothermic reactions were involved.

There have been many efforts to arrive at precise definitions of ignition embodying the qualitative aspects described above. Most of them depend on the idea of a precipitous increase in reaction rates resulting from the tendency for chemical reaction rates to be exponentially temperature dependent. In the case of metal particles a factor sometimes of equal or greater importance is the effect of the surface oxide layer, which may lead to either greater or lesser temperature dependence of the reaction rate, depending on the properties of the layer. It seems clear that a proper definition of ignition should reflect an excess of heat generation rate over heat loss rate sufficient to assure

continued self-heating after the igniting stimulus is removed. Any exact definition may prove to be a handicap if applied indiscriminately to all metals in all oxidizing environments, because of the variety of ignition sequences occurring with different metals. In any case, it is the sequence of physical events that is sought, and the definition of a moment during that sequence is relatively unimportant.

#### 4.2. FACTORS GOVERNING CHARACTER OF IGNITION

When a metal particle is heated at the usual rates of ignition experiments, its temperature rises rather uniformly because of small size and high thermal conductivity. In an oxidizing atmosphere, a layer of surface oxide is either already present, or forms rapidly--usually before ignition is achieved. The subsequent reaction behavior is highly dependent on the properties of the oxide layer, such as its melting point, solubility in the metal, permeability, and thermal conductivity. These factors affect the diffusion rates of oxidizer to metal and metal to oxidizer, and often lead to sudden changes in diffusion rate when the protective character of the oxide layer breaks down due to melting, vaporization, or solution in the metal.

The simplest kind of ignition event with a metal would result if, as in the case of ignition of hydrocarbon droplets, the reaction products were gaseous and no oxide layer occurred. Then, depending on the boiling point of the fuel, the reaction would occur at the surface or in the diffusion region around the droplet and ignition would be achieved whenever the reaction rate produced sufficient heat to overcome heat loss from the reaction region. Such a state of affairs would usually be signaled by a subsequent rapid rise in temperatures approaching a quasi-steady-state combustion rate. None of the metals studied in this program ignite in this way in atmospheres with oxygen as the oxidizing agent, although boron combustion goes through a post-ignition transition at the boiling point of the oxide that resembles such ignition.

The most extensively studied ignition of metals is that of spherical aluminum powders ignited by gas burner flames. Particles normally have a highly protective coating of oxide which breaks down only at quite high temperature. The protective character of the coating results not only from its high melting point, but also from the fact that the volume of the oxide is greater than the volume of the metal from which it is formed, and the oxide is not soluble in the metal. These properties cause the oxide coating on the particle to be relatively impervious to diffusion of oxidizer to the metal surface for continued oxidation. Further, the oxide layer seems to often retain enough strength following melting of the metal to preserve the integrity of the "particle". Thus, ignition is delayed until conditions are attained that reduce the protective action of the oxide layer. The exact requirements for this are unknown, although there is no doubt that ignition is achieved by

the time the melting point of the oxide is reached because of lowering of the diffusion barrier to the metal surface. In this respect, ignition of aluminum is particularly well assured by the time the melting point of the oxide is reached because the oxide is not soluble in the metal, has a very high surface tension, and retracts into one or more discrete globules upon melting. Thus, the metal is decisively exposed at around 2315°K. Self-sustaining reaction may be achieved before this temperature is reached under some conditions, but most authors refer to an ignition temperature of single spherical particles of around 2315°K.

It should be understood that the foregoing discussion pertains almost exclusively to ignition of spherical or granular particles by heat transfer from burner flame gases or similar high temperature sources and does not apply to the case of flash ignition of aluminum foils. Flash ignition of foils results in molten droplets with exceedingly small quantities of oxide on the surface (Ref. 1, Fig. 5.3a) and, in fact, in the case of particles ignited in one atmosphere of a 20% O<sub>2</sub>-argon mixture, no oxide was found on the surface following ignition nor did any material accumulate on the droplet during burning. It can be stated then, that melting of an oxide shell is not a necessary condition for xenon flash ignition of aluminum foils.

When the oxide layer on a metal particle is porous, diffusion of oxidizer to the metal continues, and the metal may eventually be consumed completely at moderate temperatures. The meaning of ignition then becomes contingent on what is meant by "self-sustaining exothermic reactions", and occurrence of ignition may be sensitive to the diffusional situation without unique ignition temperature. A single particle may react exothermally and fail to become self-sustaining because of heat loss to the surroundings, while a cloud of particles may be self-sustaining because the proportional heat loss is less. It usually happens that a rapid acceleration in reaction rate eventually occurs somewhere in the reaction history, although it may occur after self-sustaining conditions are reached (e.g., boron in air, which can burn below the boiling point of the oxide, but usually self-heats to a higher temperature with transition to much more vigorous combustion above 2400°K or so).

#### 4.3. OBSERVATIONS OF IGNITION

The present experimental program has not dealt extensively with the details of ignition, primarily because the experimental technique was not designed for such studies. Some significant observations regarding the preignition behavior of aluminum were described in Section 3, and some details of ignition behavior in the gas burner are described in Section 5. High speed motion pictures of particle combustion in the gas burner usually show ignition events along with already ignited droplets. Particles proceed from nonluminous to fully ignited in a few frames (times of the order of 1 msec, as shown in Fig. 4.1). In the case of aluminum, the



FIG. 4.1. Sequence of Five Consecutive Frames From High Speed Motion Picture Showing a Typical Aluminum Particle Ignition in a 1:1 CO/O<sub>2</sub> Flame. Camera speed: 6500 fr/sec.

luminous region increases abruptly in size, indicative of establishment of the detached reaction zone. Under some conditions, the aluminum droplet appears to shed its pre-ignition oxide during the initial phase of burning (Section 5.2), an event that affects the course of the subsequent combustion.

The general experience with ignition of metal particles is as follows:

1. Aluminum particles in sizes from 50 to 150  $\mu$  were ignited in H<sub>2</sub>/O<sub>2</sub>, CO/O<sub>2</sub> and (CN)<sub>2</sub>/O<sub>2</sub> flames. Aluminum particles of 150  $\mu$  and greater diameter were difficult to ignite in H<sub>2</sub>/O<sub>2</sub> and CO/O<sub>2</sub> flames.
2. A limited number of experiments on beryllium combustion were performed using hydrocarbon-oxygen flames in the early gas burner facility. Considerable difficulty was experienced in igniting beryllium particles of approximately 100  $\mu$  diameter. The relatively low temperatures of hydrocarbon flames was no doubt responsible for the difficulty with ignition and as a result the combustion was marginal.
3. Particles of boron, titanium and zirconium could not be ignited with the xenon flash in cold carbon dioxide at atmospheric pressure.
4. Foils of aluminum, titanium and zirconium could be ignited quite easily in the flash apparatus at pressures of pure O<sub>2</sub> as low as 0.2 atmospheres.

A qualitative summary of the ignition behavior of the systems employed in this study is presented in Table 4.1. It should be noted that all burner flame ignition experiments were conducted at one atmosphere pressure. All nonflame entries in the table apply to flash heating

experiments. Blanks in the table indicate that those systems were not studied.

TABLE 4.1. Summary of Experimental Ignition Behavior

(Gaseous environment)	Metal				
	Al	Be	B	Ti	Zr
Air . . . . .	Ign.	--	Ign.	Ign.	Ign.
O <sub>2</sub> . . . . .	Ign.	--	Ign.	Ign.	Ign.
CO <sub>2</sub> . . . . .	Ign.	--	None	None	None
O <sub>2</sub> /Ar . . . . .	Ign.	--	Ign.	Ign.	Ign.
*CO/O <sub>2</sub> . . . . .	Ign.	--	Ign.	--	--
*(CN) <sub>2</sub> /O <sub>2</sub> . . . . .	Ign.	--	--	--	--
*H <sub>2</sub> /O <sub>2</sub> . . . . .	Ign.	--	--	--	--
*R/O <sub>2</sub> † . . . . .	Ign.	Marginal	--	--	--

\* It should be understood that the metal particles were ignited in the burnt products of these flame gases.

† R indicates hydrocarbon (propane or butane).

In the case of aluminum, considerable insight into the ignition process is provided by observations of particles that have been heated by a torch flame but have not achieved the steady-state burning configuration. By combining this technique with that of dropping particles on a heated sapphire plate in air (Section 3.2) certain significant factors have been identified. These techniques have revealed a capacity for progressive fracturing and "healing" of the oxide and have further shown that aluminum can escape from this oxide shell. The fracturing of the oxide coating and local oxidation seems inevitable in view of the relative thermal expansion characteristics of the metal and its oxide. The results of sampling "unignited" particles in flames (Fig. 3.13) indicate that the oxide becomes plastic before ignition. This plasticity doubtless alters the permeability of the oxide coating and its ultimate rupture (usually at multiple sites) leads immediately to ignition in terms of the usage developed here. Such interrupted ignition experiments hold promise for much more detailed and reliable information on the controlling processes of ignition and how they can be modified to advantage.

## 5. QUASI-STEADY COMBUSTION

### 5.1. SCREENING STUDIES

To obtain a broad perspective of the range of behavior associated with metal combustion, a number of metals were burned in a variety of oxidizing environments. Aluminum, boron, titanium and zirconium were studied in the flash ignition apparatus over the range of environmental conditions summarized in Table 5.1. Aluminum, beryllium and boron were examined in the gas burner apparatus. The flames used for ignition are summarized in Table 5.2. A brief comparison of the characteristics of the quasi-steady combustion of these metals follows:

a. Aluminum and beryllium - Boiling point of the oxide exceeds the boiling point of the metal and the oxide has negligible solubility in the metal. Surface oxide is relatively impermeable to the oxidizing gas. Burning primarily by vapor transport of metal to detached heterogeneous reaction zone.

b. Boron - Boiling point of the oxide is less than that of the metal and the oxide has negligible solubility in the metal. Burning predominantly by surface processes on solid or molten particle.

c. Titanium and zirconium - Boiling point of the oxide exceeds the boiling point of the metal; however, the oxide is soluble in the metal. Burning occurs predominantly on droplet surface.

The general character of the combustion expected for each of these groups has been discussed by Brzustowski and Glassman (Ref. 8), Markstein (Ref. 9), and Mellor (Ref. 10). The melting and boiling points of these metals and their oxides are given in Table 1.1.

Residues quenched from gas burner flames suggest that both aluminum and beryllium burn primarily by vapor phase transport of metal from the parent particle to a detached heterogeneous reaction zone. Aluminum combustion was described in considerable detail in the previous progress report (Ref. 1). An illustrative example of a beryllium particle quenched from a hydrocarbon-oxygen flame is shown in Fig. 5.1. Relative to aluminum in a similar environment (Fig. 5.2), the smoke cloud around the beryllium particle is more dense. It is seen that the diameter of the detached reaction zone in relation to the particle size in the case of beryllium combustion is less than that for aluminum under similar conditions. It is noteworthy that the large amounts of surface product commonly associated with aluminum combustion are observed to even a greater degree on the beryllium residues. Fragmentation of beryllium

TABLE 5.1. Experimental Conditions  
Used in Flash Ignition Studies

Metal	Variables			
	Particle size	Pressure (absolute)	Oxidizer type	Oxidizer concentration
Aluminum	(6) 275-460 $\mu$	1 - 4.4 atm	Air	20%
		0.2 - 1.0 atm	O <sub>2</sub> /Ar CO <sub>2</sub> O <sub>2</sub>	5-75% 100% 100%
Boron	177-250 $\mu$	1 - 4.4 atm	Air	20%
		0.2 - 1.0 atm	O <sub>2</sub> /Ar CO <sub>2</sub> O <sub>2</sub>	5-75% 100% 100%
Zirconium	(6) 238-388 $\mu$	1 - 4.4 atm	Air	20%
		0.2 - 1.0 atm	O <sub>2</sub> /Ar CO <sub>2</sub> O <sub>2</sub>	5-75% 100% 100%
Titanium	(4) 239-334 $\mu$	1 - 4.4 atm	Air	20%
		0.2 - 1.0 atm	O <sub>2</sub> /Ar CO <sub>2</sub> O <sub>2</sub>	5-75% 100% 100%

was not observed. Due to the ignition difficulty encountered, relatively little work was done on beryllium combustion in the gas burner apparatus. Some aspects of aluminum combustion will be discussed in detail in the subsequent sections of this report.

The studies of the combustion of flash-ignited boron particles, to be described in more detail below, suggest that boron burns by a surface process in agreement with Talley's observations (Ref. 11) on the combustion of oxide-covered boron rods. These latter observations showed that, when the boron temperature was below the boiling point of the oxide, combustion took place through a uniformly adherent covering of liquid oxide. At higher temperatures the surface of the particle was exposed to direct attack by oxidizing species, and combustion proceeded much more rapidly.

Titanium and zirconium have many phenomena in common. Flash-ignited particles of both of these metals exhibit catastrophic fragmentation when burning in air, will not sustain burning in room temperature CO<sub>2</sub> and blow oxide bubbles when burning in pure oxygen. The combustion of both metals has been discussed by Brzustowski and Glassman (Ref. 8). Nelson has made extensive studies of the combustion of pulse heated single particles of

TABLE 5.2. Experimental Conditions  
Used in Gas Burner Experiments\*

Flame composition Metal	Hydrogen/ oxygen	Carbon monoxide/ oxygen	Cyanogen/ oxygen	Hydrocarbon/ oxygen
Aluminum, spherical	ignition	ignition	ignition	ignition
Aluminum, granular	ignition	--	--	ignition
Magnesium filings	ignition	--	--	ignition
Boron crystalline granules	--	ignition	ignition	--
Beryllium, granular	--	--	--	marginal
Beryllium, spherical	no ignition	ignition	ignition	--

\* Blank in the table indicates no attempt made to study that system.

zirconium (Ref. 4). The details of the combustion of Zr and Ti in a variety of oxidizers have been studied in the flash heating apparatus in this laboratory and are described in Section 6 of this report.

## 5.2. ALUMINUM COMBUSTION

Considerable insight into the combustion of aluminum particles in atmospheres containing oxygen as the oxidizing species has been provided by earlier studies in this laboratory (Ref. 1, 12 and 13). Recent studies have provided more conclusive supporting evidence relative to the hypotheses advanced by that earlier work, as well as uncovering new details of combustion behavior. The principal combustion processes occur in a detached heterogeneous reaction zone, with some surface oxidation usually occurring concurrently on the metal droplet. Under many test conditions the original surface oxide is either severely limited in quantity (flash ignition) or is ejected shortly after ignition (CO/O<sub>2</sub> flame), and the droplet flame envelope then approaches the spherical configuration postulated in analytical models, at least during the early burning history. Under most test conditions, appreciable oxide accumulates on the surface as burning progresses, leading to a variety of phenomena not encompassed in analytical models and difficult to study in



FIG. 5.1. Nominal 100  $\mu$  Beryllium Particle Quenched While Burning in a Propane-Oxygen Flame at 1 Atmosphere Pressure.

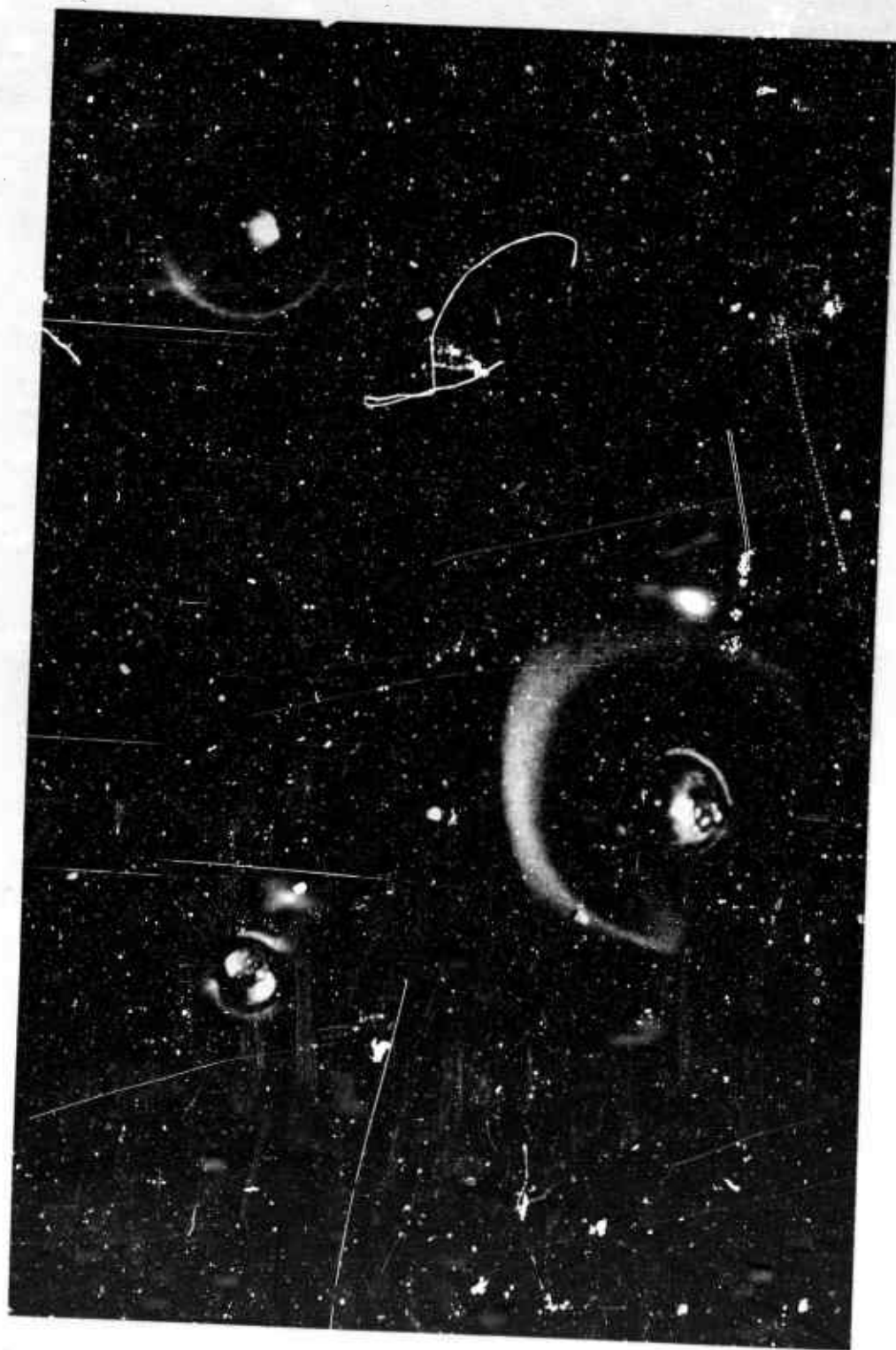


FIG. 5.2. Nominal 100  $\mu$  Aluminum Particles Quenched While Burning in a Propane-Oxygen Flame at 1 Atmosphere Pressure.

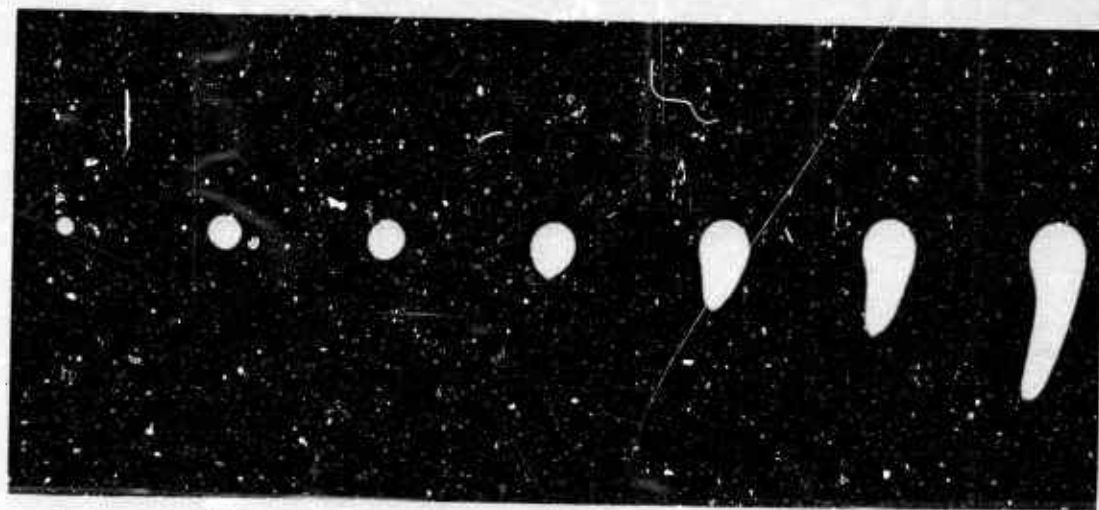
detail because of their complexity, transient character, and because of the small dimensions of the combustion zone.

High speed motion pictures of particle combustion made during gas burner experiments show that the detached reaction zone of the aluminum droplet is fully formed in approximately 0.1 to 1.0 millisecond after its first evidence (Fig. 4.1), with some variation in diameter continuing thereafter. The droplet flame envelope usually exhibits spherical symmetry early in burning, although it becomes comet-shaped if there is a motion relative to the environmental gas (Fig. 5.3).

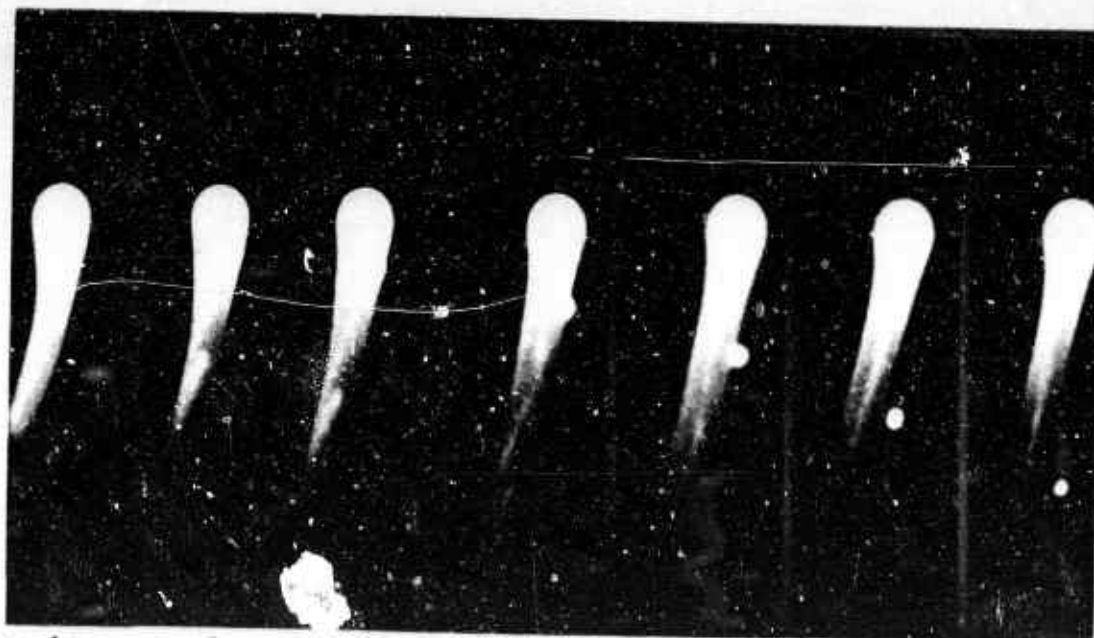
In the absence of convection the droplet flame envelope retains its apparent disc shape and is intensely luminous. High speed photography employing backlighting has shown that in the presence of convection the tail of the "comet-like" combustion zone is largely nonluminous (Fig. 5.4). This technique permits observation of the dynamics of the processes which had yielded earlier quench specimens showing "stretched" combustion envelopes.

As long as the smoke nuclei remain in the reaction envelope, continued heterogeneous reaction on their surface keeps them luminous. As the envelope is distorted through shearing action of the torch gases the material normally resident in the spherical envelope is drawn out into a tail and is cooled basically as a consequence of lowering the density of the reactants. Formation of much of the  $Al_2O_3$  occurs by heterogeneous reaction in the smoke cloud, with lower oxides forming  $Al_2O_3$  on the smoke nuclei at a rate limited by the ability of the droplet to lose the excess energy involved ( $Al_2O_3$  cannot form in appreciable concentration without heat removal and condensation). Because the reaction product ( $Al_2O_3$ ) is in the condensed phase, there is a net inward flow from the environment towards the smoke which tends to cause accumulation of the smoke in the vicinity of the aluminum particle.

While formation of  $Al_2O_3$  in the detached reaction envelope is well established and embodied in existing analytical models for aluminum combustion, it is quite clear that oxide or oxide-containing product can also form on the aluminum droplet surface (Fig. 5.5) and this aspect of the combustion does not yet appear to be adequately treated in the models which are extant. The oxide has negligible solubility in the metal and very high surface tension, with the result that it tends to retract upon melting, thus exposing the metal surface. The evaporation of metal and diffusion of the metal vapor from the surface are necessarily accompanied by some counter diffusion of oxygen as well as aluminum suboxides back to the surface, where the temperature is low enough to permit formation of liquid  $Al_2O_3$ . The simultaneous accumulation of oxide and decrease in metal as burning progresses usually leads to serious deviation of the combustion from that predicted by models treating the case of spherical symmetry. The detailed combustion behavior resulting from accumulation of surface oxide is highly dependent on the atmospheric environment, and will be discussed in more detail in the following.



a b c d e f g



h i j k l m n

FIG. 5.3a-n. Sequence of Selected Frames From High Speed Film Showing Development of Comet-Shaped Smoke Trail and Shedding of an Oxide Sphere. Particle burned in  $\text{CO}/\text{O}_2$  flame.

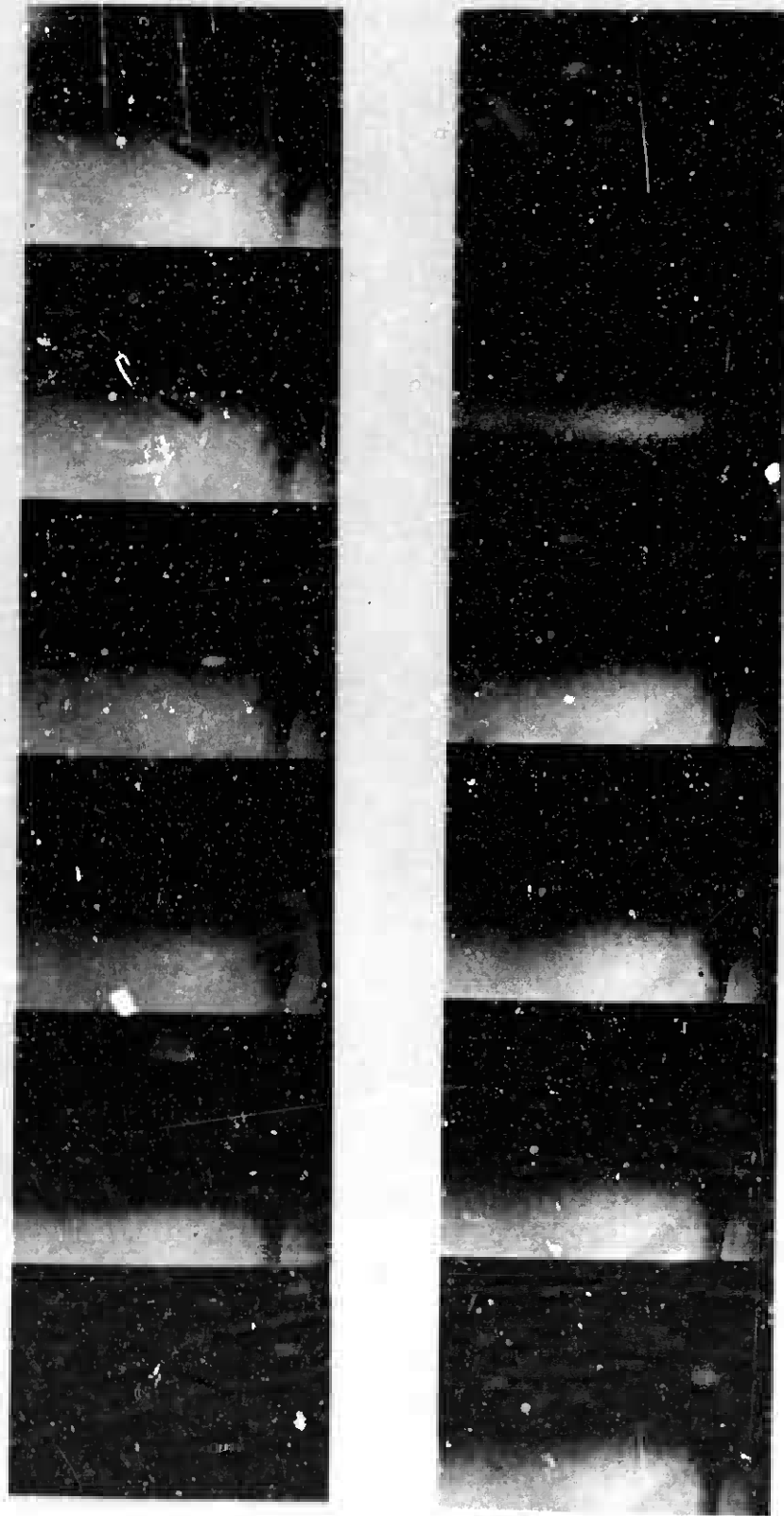


FIG. 5.4. Two Sequences of Consecutive Frames From High Speed Film With Pulsating Backlighting Indicating Nonluminous Smoke Cloud Associated With Aluminum Particles Burning in A Stoichiometric CO/O<sub>2</sub> Flame.

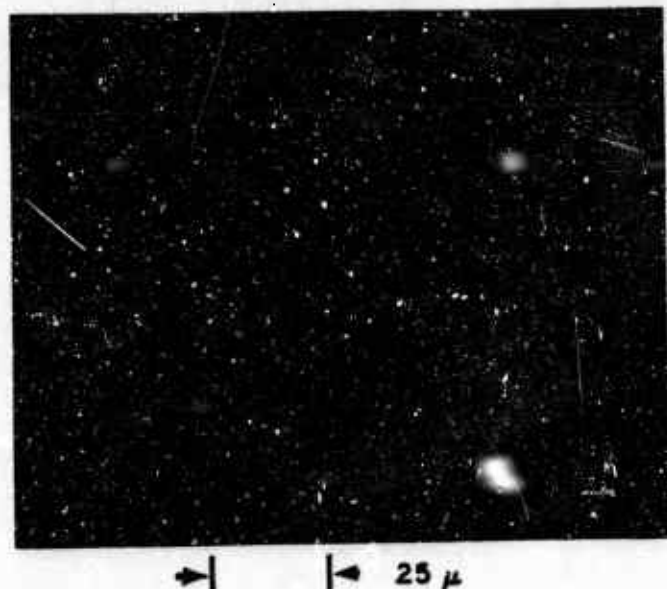


FIG. 5.5. Scanning Electron Microscope Photograph of a Nominal 100  $\mu$  Aluminum Particle Quenched from a Stoichiometric CO/O<sub>2</sub> Flame. Note that the hollow oxide csp has burst, revealing some cellular structure.

#### 5.2.1. Surface Oxide

While there is no doubt about the accumulation of product on the droplet surface during burning, the amount, composition and importance may be quite varied and are not fully known. Motion picture records of aluminum particles in both gas burner and propellant combustion studies (Ref. 7) clearly show the "bilobate" burning configuration of the metal droplets. The oxide is more luminous than the metal because of the high emissivity of the oxide. The retractile nature of the melting oxide is evident in both gas burner and propellant combustion experiments, but the presence of the oxide fog and absence of external illumination in the gas burner tests limits the resolution of the burning droplet to a luminous spot corresponding to the radiating oxide cap. The size of the luminous spot and its orientation relative to asymmetries in the detached reaction zone during spinning further support the identification with an oxide cap, an interpretation which is also consistent with the appearance of quenched samples (Fig. 5.6).

This type of combustion (with nonsymmetric accumulation of oxide and transition to spinning configurations) was usual in CO/O<sub>2</sub> flames with high CO concentration, in air counterflow in the gas burner, and in air atmospheres in the flash ignition experiment. In argon-oxygen atmospheres in the flash ignition no surface accumulation of product

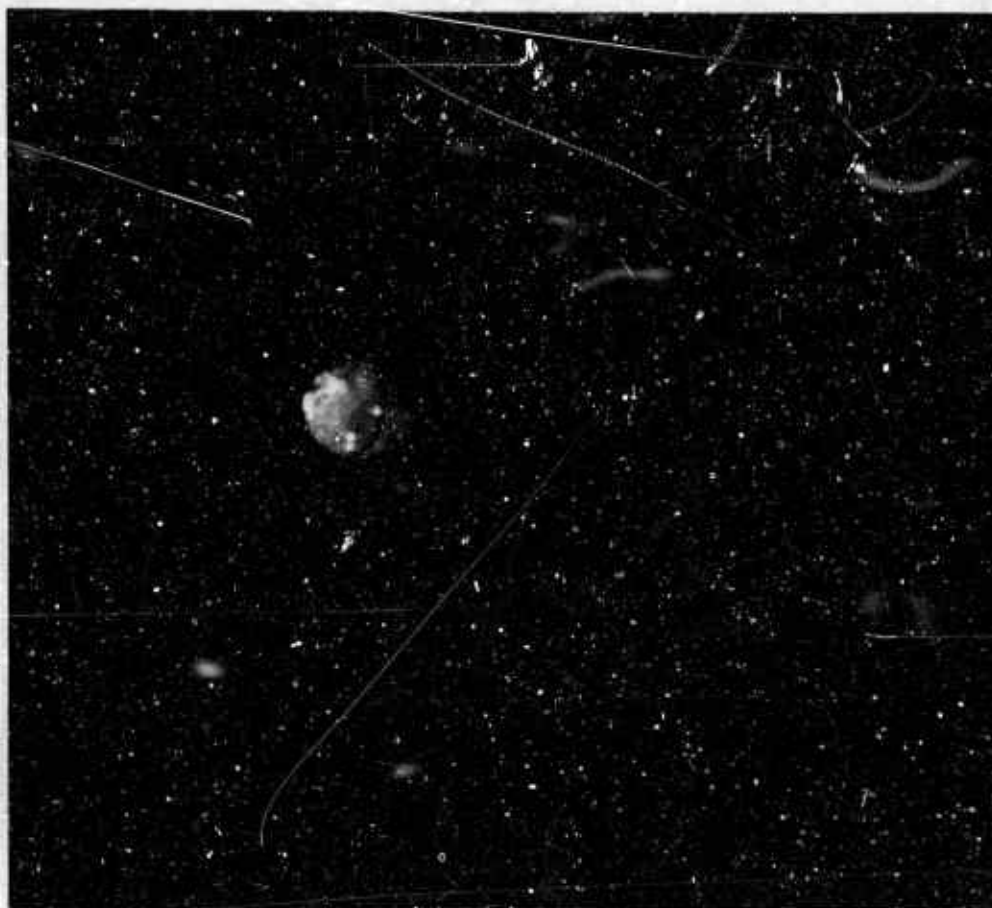


FIG. 5.6. Optical Photomicrograph of a Nominal 460  $\mu$  Xenon Flash Ignited Aluminum Particle Quenched While Burning in Ambient Air. Note the distortion of the smoke cloud associated with the vapor phase flame. Smoke is associated only with the exposed metal lobe of the droplet.

occurred and particles burning in  $\text{CO}/\text{O}_2$  flames with 1:1 volume mixture ratio showed evidence of accumulating oxide in only 50% of samples observed.

From the foregoing it is evident that the accumulation of product on the droplet surface is dependent on the composition of the atmosphere (Section 6.3 and 6.5). As an example of slightly oxygen-rich flames the 1:1  $\text{CO}/\text{O}_2$  flame provides a particularly interesting case, in which some particles appear to shed their original oxide in the form of a bubble and remain substantially free of oxide thereafter (Fig. 5.7). Other particles appear to retain (and possibly accumulate) oxide throughout burning. The occurrence of shedding of oxide is inferred by: (a) observing numerous quench specimens in which some particles are

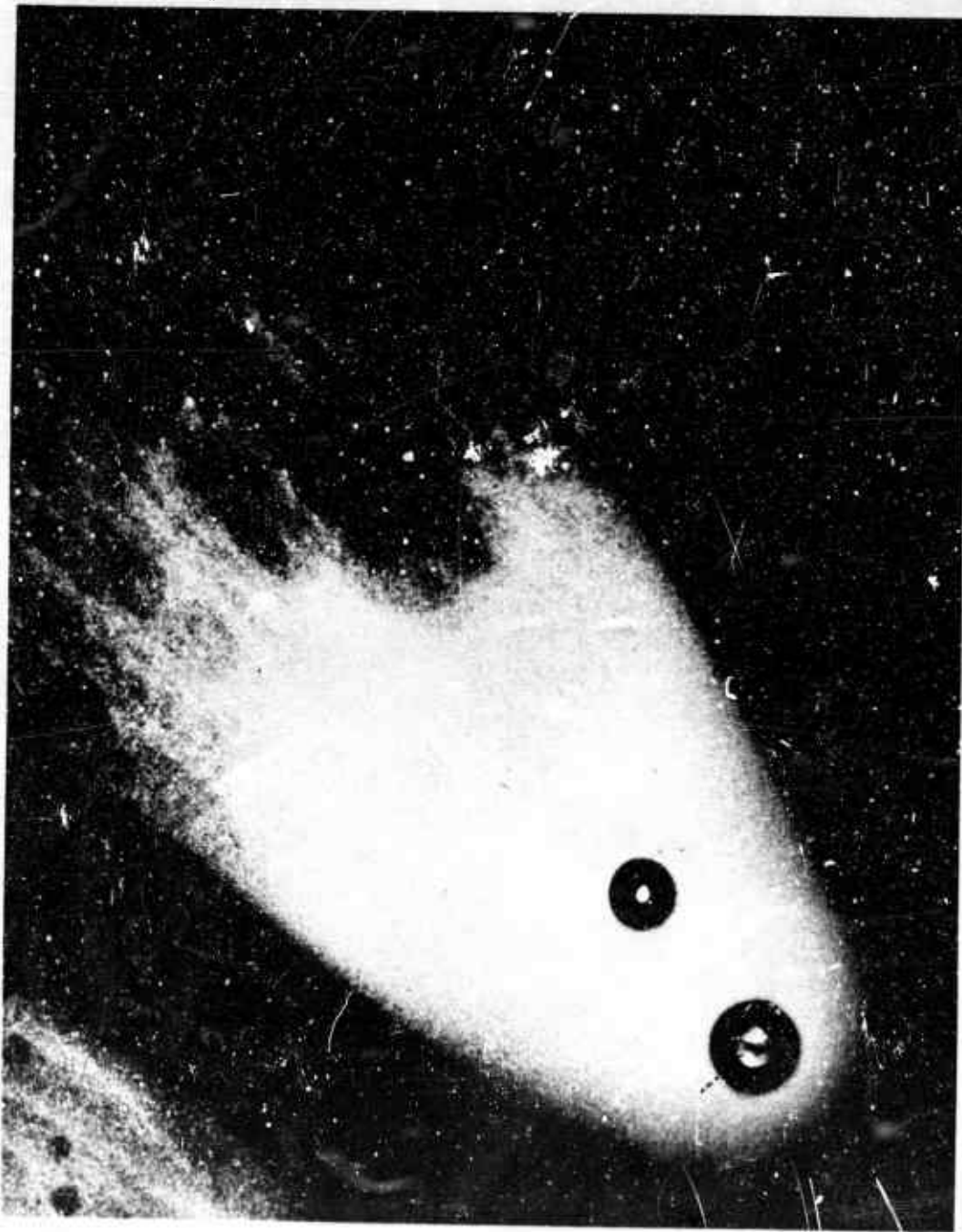


FIG. 5.7. Nominal 100  $\mu$  Aluminum Particle Quenched From a Near-Stoichiometric  $\text{CO}/\text{O}_2$  Flame. This particle has shed essentially all of its oxide in the form of a sphere, which is lying in the smoke field, and is burning in the nonspinning configuration.

definitely "b.lobate", having considerable nonsymmetric accumulation of product on the particle surface, while others seem to have shed virtually all of the oxide and retain their sphericity; (b) observing that most of the product which is collected below the burner flame consists of large, thin-walled oxide balloons; and (c) observing that many particles shed a large luminous object approximating the original droplet diameter (or slightly larger) whose color temperature is the same as that of the smoke cloud. Those particles which do not shed the luminous sphere proceed to spin, jet and fragment, while those shedding the sphere do none of these things.

Thus, in the 1:1 CO/O<sub>2</sub> flame, presence of surface oxide during burning is apparently contingent on retention of the original preignition oxide. It is possible that combustion in the CO/O<sub>2</sub> flame would be like that in argon/O<sub>2</sub> atmospheres in the flash ignition apparatus if the amount of surface oxide at the moment of ignition were the same.

### 5.3. BORON COMBUSTION

Boron particles have been burned in both the flash ignition apparatus and the gas burner. In addition, some aspects of the quasi-steady combustion have been investigated via a computational model (see Appendix A).

In the room temperature environment of the flash ignition experiment 177-250  $\mu$  boron powder could not be ignited in a mixture of 5% oxygen in argon. With 10% oxygen, slow combustion was achieved, characterized by sharp particle tracks (Fig. 5.8a). With greater than 20% oxygen, rapid combustion was achieved, characterized by broad particle tracks (Fig. 5.8b, c, e, f). In many instances, broadening of the track and an increase in color temperature occurs after appreciable burning time has elapsed, suggestive of a transition in combustion behavior. Particles quenched shortly after ignition retained the granular appearance of the starting material, indicating that they had not been melted. Particles quenched from that part of the trajectory where the broad track was observed were smoothly spherical, indicating that the particle in the latter burning configuration was melted.

The combustion in air under the same conditions appears similar to that observed in 10% oxygen/argon mixtures. Similar observations of boron particle combustion in the gas burner could not be made because the particles were obscured by the intense luminosity characteristic of burner flames containing boron compounds (green "fluctuation bands" of BO<sub>2</sub>). It is interesting to note the contrast between boron particles burning in torch flames and those burning in the cold ambient environment of the flash heating experiment. Flames containing boron powders always emit intensely in the green while flash-ignited particles burning in an atmosphere at ambient temperature do not emit the green BO<sub>2</sub> radiation in any of the oxidizers employed in this study. It seems reasonable to conclude then, that the high temperature burner flame not only keeps all the B<sub>2</sub>O<sub>3</sub>

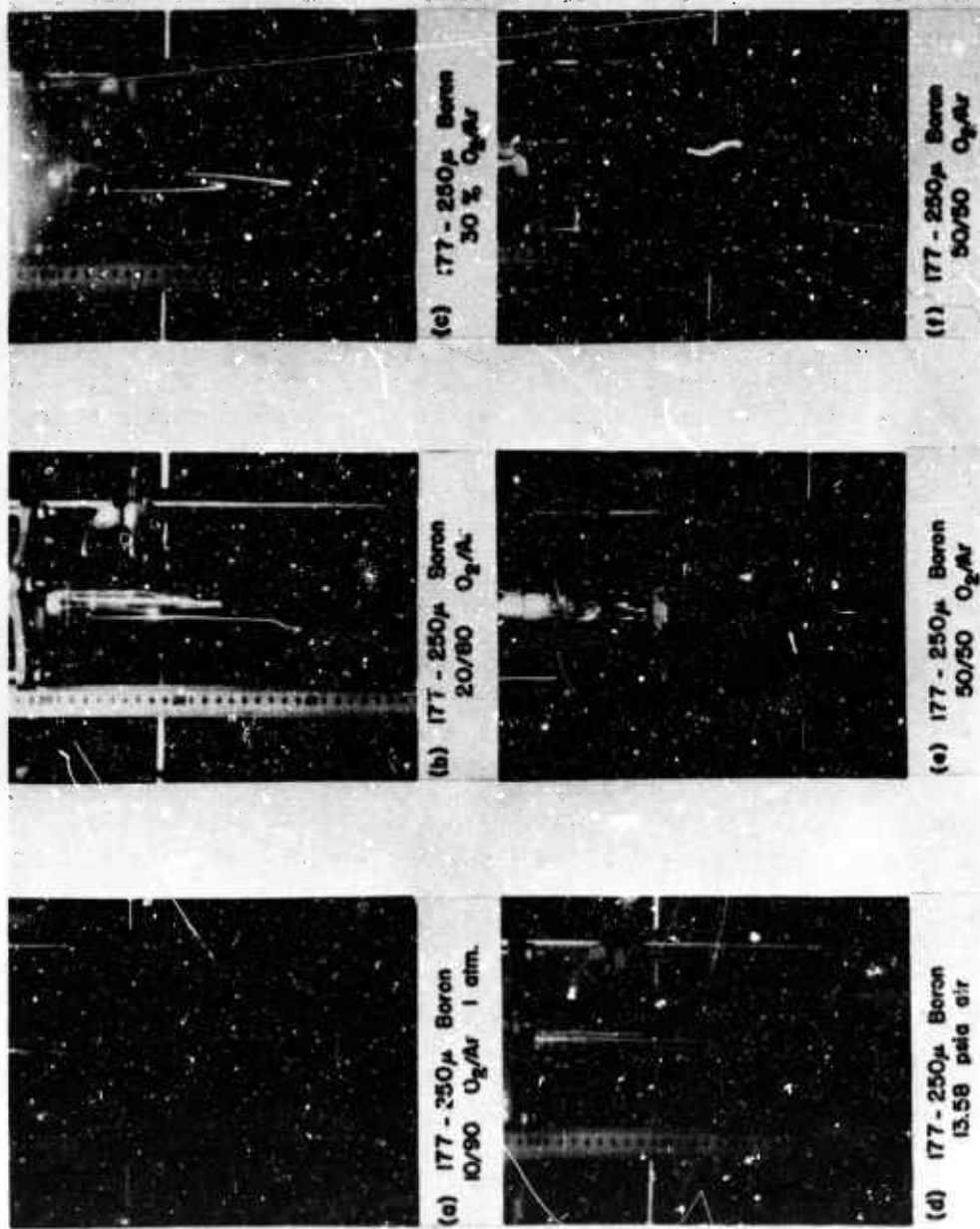


FIG. 5.8. Track Photographs of Flash-Ignited Boron Particles Showing Effect on Combustion of Varying Oxygen Content of O<sub>2</sub>/Ar Mixtures and Comparing this Behavior to Combustion in Ambient Air.

gasified but promotes the dissociative equilibrium leading to  $\text{BO}_2$ , while the cold environment of a flash-ignited particle promotes the rapid quenching of  $\text{B}_2\text{O}_3$  and grey-body radiation from either the parent particle or from the resultant fog of  $\text{B}_2\text{O}_3$  is all that is detected.

At low oxygen concentrations in the flash ignition apparatus where the narrow, sharply defined tracks are obtained, combustion no doubt takes place through a liquid oxide film on a solid particle. At higher oxygen concentrations the broad, diffuse track results from condensation of  $\text{B}_2\text{O}_3$  in a zone somewhat removed from the particle since the surface temperature then exceeds the boiling point of the oxide. Even under these conditions, due to the low vapor pressure of the metal, the parent particle is consumed primarily by surface reaction rather than by evaporation. The transition in burning behavior at the higher oxygen concentrations is a consequence of an increasing surface temperature which ultimately frees the surface of oxide, exposing the metal to direct attack by oxidizer.

The preliminary picture of boron particle combustion emerging from these flash heating experiments is in good qualitative agreement with the earlier postulates of Talley (Ref. 11), who studied the combustion of boron rods. A result unique to the flash heating experiments was the change in the appearance of the burning configuration which occurs at the higher oxygen concentrations. Based on the experimental evidence cited above and model calculations to be discussed below, it is inferred that for oxygen-argon mixtures containing more than 20% oxygen, combustion immediately following ignition occurs through a surface film of liquid  $\text{B}_2\text{O}_3$ . As combustion proceeds, the surface temperature increases to a value at which the surface film evaporates, exposing the surface to direct attack by the oxidizer, with correspondingly higher combustion rate.

When the particle surface temperature is less than the boiling point of the oxide, there is a net convection toward the particle. This convection tends to return any product which condenses in the region surrounding the particle back to the surface. The overall stoichiometry of the combustion of boron by oxygen is  $2\text{B} + 3/2\text{O}_2 \rightarrow \text{B}_2\text{O}_3$ . The convection is a consequence of the number of moles of the product being smaller, even without condensation, than the volume of oxygen that produced it. If the particle surface temperature is high enough so that back-diffusing fog particles evaporate before reaching the surface, the condensed  $\text{B}_2\text{O}_3$  tends to remain in a limited zone some distance removed from the particle. While the nonsteady aspects of fog accumulation cannot be handled by the steady-state model, certain aspects of the formation and evaporation of the fog were investigated to assess their effect on the particle surface temperature and the temperature gradients in the gas phase adjacent to the particle.

The particle tracks illustrated in Fig. 5.8 are produced by radiation from condensed phase species surrounding the particle, and thus are

evidence of the condensation of  $B_2O_3$  vapor. While not important as a heterogeneous reaction zone (because the boron partial pressure is too low), the luminescent cloud is analogous to the oxide fog characteristically surrounding burning aluminum particles. In the case of burning boron particles, however, the fog will be convected toward the particle until it reaches the surface and evaporates, or until it enters a region adjacent to the surface, of thickness  $\Delta t$ , where the partial pressure of  $B_2O_3$  vapor is less than the metal vapor pressure and where  $\Delta t$  is of such thickness that the  $B_2O_3$  has time to vaporize. Due to the high temperature exponent of the  $B_2O_3$  vapor pressure, the temperature of the fog cannot appreciably exceed the boiling point of  $B_2O_3$ .

Boron particle track photographs made on colored film indicate that as combustion proceeds the color temperature of the fog increases. Where the combustion is taking place through a surface oxide film, the surface will be the locus of highest temperature. Thus it is inferred that the increase in color temperature of the fog reflects an increase in surface temperature. At high oxygen concentrations particle luminosity is not apparent until a very broad track appears some time after initiation of the flash (apparent ignition delay). At high oxygen concentration the increased diameter and color temperature of the broad track suggests that the particle temperature is considerably higher than at low oxygen concentrations.

A computational model has been developed to provide a theoretical foundation with which to correlate the experimental observations of burning boron particles. The details of the model are described in Appendix A. This model allows exploration of the effects of oxide condensation and evaporation in the space around the particle as well as oxide formation on, and evaporation from, the surface of a parent particle in the steady-state, stagnant-film approximation. Oxide species other than  $B_2O_3$  have not been included in the model since in the temperature range of interest they are present only in minor concentrations.

The model calculations show that for very low oxygen concentrations, the reaction zone is at the surface. The nature of the relationship between oxygen partial pressure and surface temperature, neglecting the presence of the fog, is illustrated in Fig. 5.9. The discontinuity in the steady-state surface temperature is associated with the change of enthalpy accompanying the melting of the boron. On the basis of this model, for very low partial pressure, the product  $B_2O_3$  would collect on the surface. Since reaction would be forced to take place by diffusion through a continually increasing thickness of surface oxide, a lower limit in oxygen partial pressure is implied for self-sustained combustion to take place. It has been observed experimentally that for  $O_2$ /argon mixtures at 1 atmosphere, flash-heated boron powders do not exhibit self-sustained combustion at oxygen mole fractions less than about 0.09.

Another result of interest is that for oxygen mole fractions only slightly greater than the minimum necessary for self-sustained combustion,

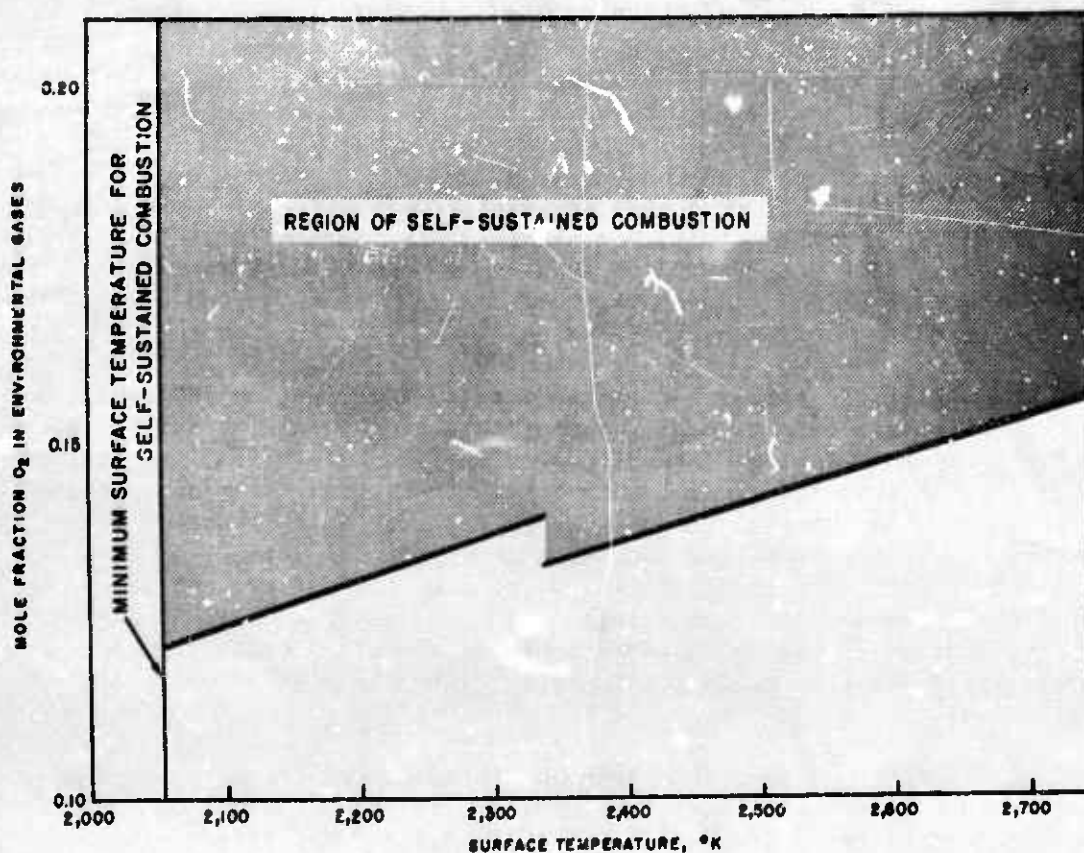


FIG. 5.9. Theoretical Relationship Between Surface Temperature and Oxygen Mole Fraction for Boron Droplet Combustion.

the model indicates that the parent particle should burn without melting; which is in qualitative agreement with experiment. With the values of the model parameters used here this would be at a mole fraction of oxygen less than 0.09. As pointed out in the Appendix, surface temperatures can be varied rather considerably by varying the model parameters over a range of reasonable values.

The surface temperature in Fig. 5.9 was computed on the assumption that boron burned with a clean surface whose location is defined by the zero of the oxygen partial pressure. Actual combustion must take place by heterogeneous reaction between the oxygen and the boron at the particle surface. As a consequence, the product  $B_2O_3$  is formed on the surface and must subsequently evaporate from the surface. The influence of the kinetics of the evaporation process on combustion has been investigated by assuming that the surface rate of reaction, as given by the flux of  $B_2O_3$ , is equal to the rate of evaporation of  $B_2O_3$  from the surface. For this boundary condition, the surface temperature becomes dependent on the diameter of the particle and offers an explanation for the increase

in surface temperature with decreasing particle size as inferred from the color of the particle tracks.

It is also worthwhile to examine how the combustion adjusts itself to accommodate perturbations from the steady-state. If it is assumed that a balance between reaction rate and  $B_2O_3$  evaporation rate were established on the surface at a temperature exceeding that corresponding to the partial pressure of  $B_2O_3$  over the surface, the burning surface temperature would be between the equilibrium temperature corresponding to the  $B_2O_3$  partial pressure (lowest) and the clean-surface temperature determined by the vanishing of the oxygen concentration (highest). The rate of reaction under these conditions would be limited by diffusion through a surface oxide film. The stability of this film can be illustrated by considering a given surface temperature and a surface oxide film of other than the steady-state thickness; if too thick, the reaction rate will be less than the evaporation rate leading to a decrease in thickness; if too thin, the reaction rate will exceed the evaporation rate leading to an increase in thickness.

In Talley's experiments the temperature of the oxide-covered boron rod was controlled by ohmic heating. At low rod temperature, combustion was limited by diffusion through a surface oxide layer. As this temperature was increased the surface layer was reduced in thickness as a consequence of the competition between the diffusion-limited reaction rate through the oxide film and evaporation of the film. At high rod temperature (approaching the oxide boiling temperature) the film disappeared, exposing the rod to direct attack by oxygen. In Fig. 5.10 this sequence is demonstrated for a typical model calculation where the surface temperature varies as a consequence of decreasing particle size.

#### 5.4. SUMMARY

This section on quasi-steady combustion describes in qualitative terms the wide divergence of combustion behavior of the metals studied and relates such combustion characteristics to the thermophysical properties of the metals and their respective oxides. The treatment shows that in many cases (notably aluminum), the combustion departs from ideality very early following ignition; this fact immediately invalidates any hydrocarbon droplet burning analogy and renders suspect all models treating the limited case of spherical symmetry. Indeed, it is such departures from ideality, including development of droplet asymmetry, spinning, jetting and fragmentation which give rise to the use of the term quasi-steady combustion.

Due to the wide range of experimental techniques employed by this laboratory this study is uniquely fitted to contrast the combustion of aluminum particles burning in the high ambient temperature of the gas burner ( $\approx 2900^\circ K$ ) in the presence of forced convection with that of single particles burning in a stagnant atmosphere at room temperature. This

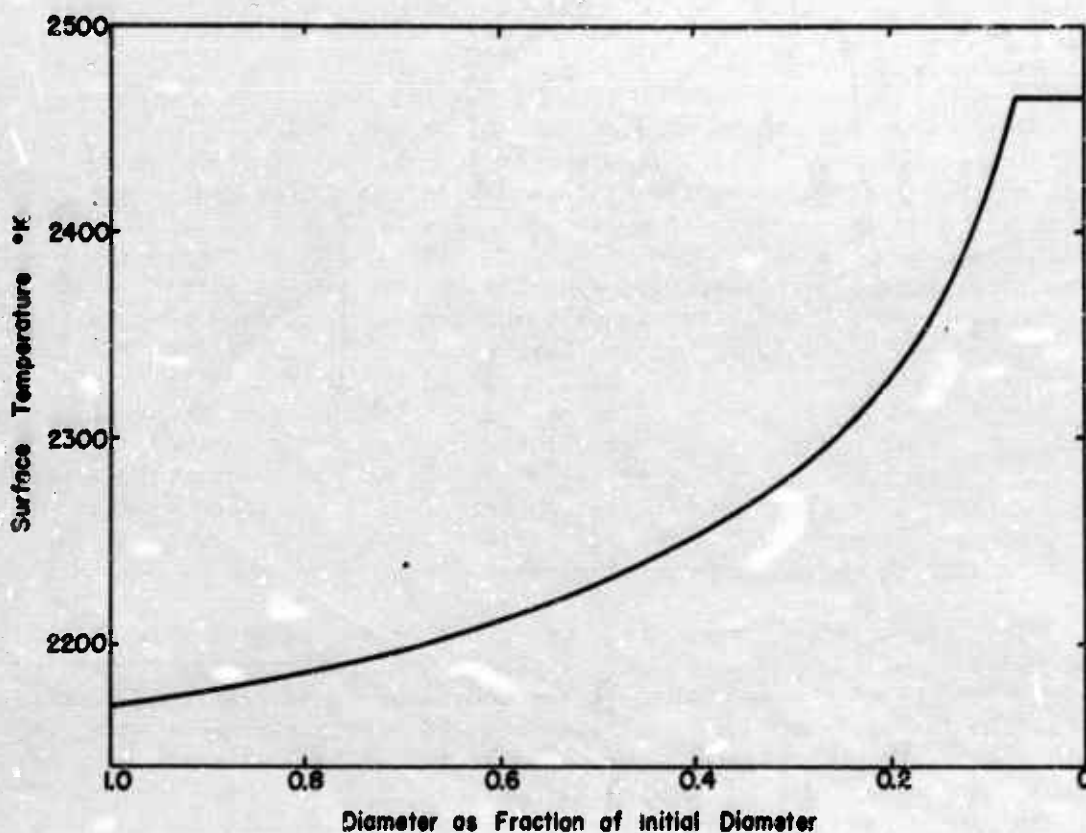


FIG. 5.10. Variation of Surface Temperature Versus Particle Diameter for Boron Burning in 15% Oxygen-Argon (Theoretical).

study is also able to show that the ignition mode can affect later quasi-steady combustion behavior by influencing the degree of surface oxidation at the time of ignition (See also Section 4.2).

Surface oxide, both original preignition oxide and that which accumulates during combustion have been treated in some detail. The discussion has sought to show how such oxide is indeed responsible for the anomalous behavior associated with the quasi-steady state and indicates, for aluminum, why one cannot really speak of steady-state combustion in the ordinary sense.

From the standpoint of combustion energetics, boron is a favored candidate in propulsion systems. Widespread interest in its potential and the ability of this laboratory to conduct controlled boron particle combustion studies in the flash ignition apparatus has led to significant emphasis in this section as well as in Appendix A. Boron combustion has been treated as a special case of a surface burning metal whose oxide boils at a temperature below the steady-state burning temperature. While boron combustion has been shown to exhibit on occasion certain

progressive characteristics (such as combustion with rising droplet temperature, beginning below and terminating above the metal melting point), it nevertheless can be described by a steady-state approximation and is amenable to analytical description and manipulation.

Section 6 of this report presents, from the experimental point of view, a quantitative or semi-quantitative picture of the unsteady aspects of the combustion of the metals already cited and indicates how the events affecting the quasi-steady combustion are the controlling factors in the terminal stage of combustion.

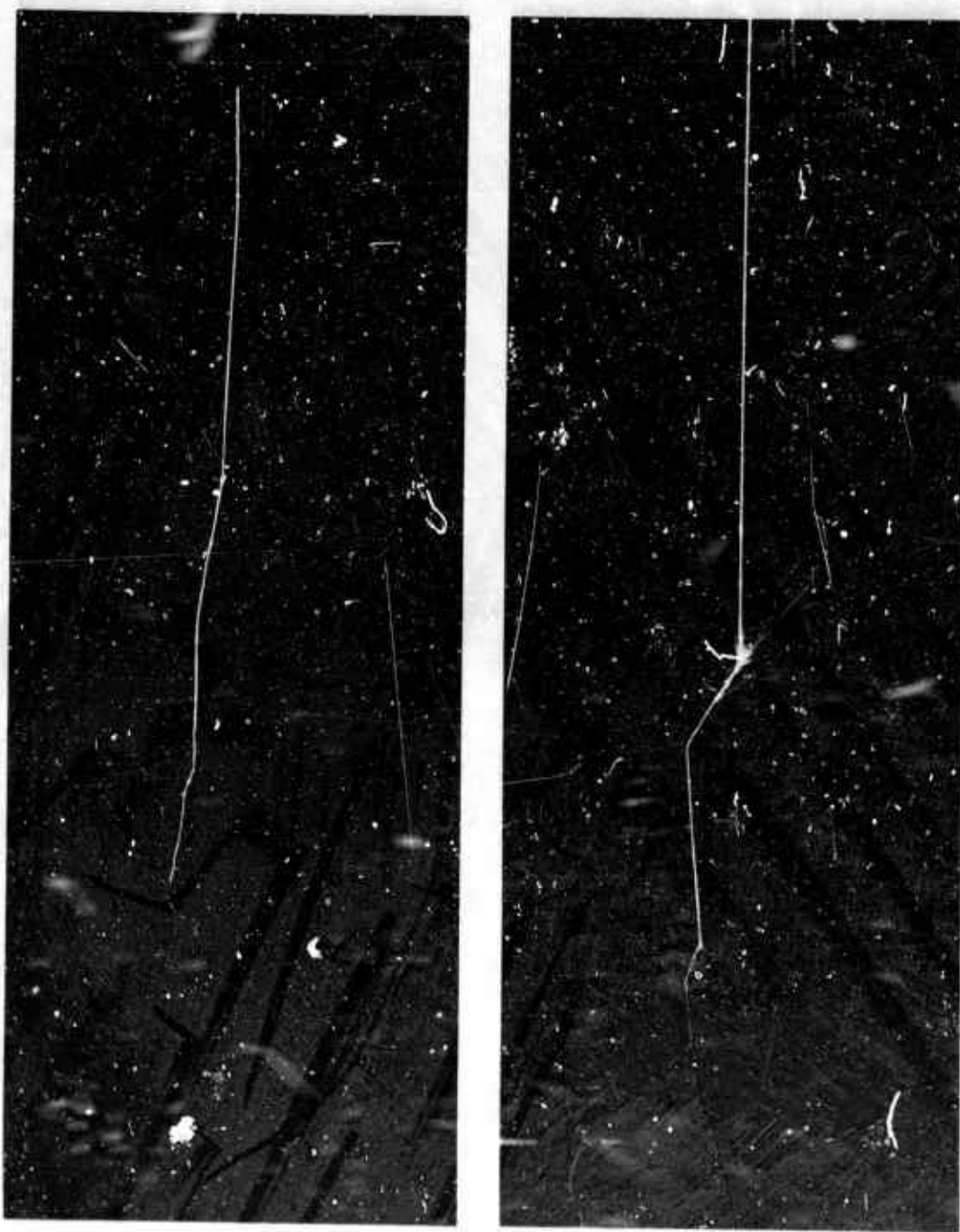
## 6. TERMINAL STAGES OF COMBUSTION

Aluminum, boron, titanium and zirconium are all of current interest as additives to propellant, pyrotechnic or photoflash formulations. Practical use is made of the vast difference in burning behavior between titanium and zirconium, representing surface burning processes on the one hand, and aluminum, as a representative vapor phase burner on the other hand. A very dramatic trait which all three metals have in common is the tendency for their burning droplets to terminate combustion by means of a catastrophic fragmentation of the particle when nitrogen is present in the environment. Boron appears to represent a rather special case of the surface burning mechanism as described in Section 5.3. Never, under the experimental conditions employed in the studies reported here, have boron particles been seen to fragment.

Considerable insight into the qualitative aspects of the overall combustion was gained from a study of the trajectories of burning particles where the factors controlling the terminal stage of combustion often manifest themselves. Such observations help to distinguish between the different basic types of combustion mechanism. Generally, information on particular traits of individual metals may also be gained from such studies. Figures 6.1, 6.2 and 6.20 are representative of the trajectories of burning particles of the four metals listed above. As examples of the types of behavior susceptible to such analysis and as an overview of the combustion phenomena to be described in detail in this section, the following brief general description is presented.

Due to the complex nature of the high temperature phase relationships between the metal and its oxide, burning droplets of titanium and zirconium maintain their spherical symmetry throughout burning by dissolving all surface reaction products as they are formed. Trajectories seen in track photographs of such specimens are, as a result, straight, sharply defined and exhibit no peculiarities throughout burning prior to termination. Termination, in this case, may either be simple consumption or droplet explosion, depending on the atmosphere.

Aluminum exhibits very erratic behavior, particularly when burning in torch flames, and such phenomena as oxide sphere shedding (balloons), spinning, jetting, puffing and fragmentation are familiar characteristics. As described later, all of the peculiarities in the particle track photographs of burning aluminum droplets can be traced to the presence of insoluble product on the droplet surface.



(a)

(b)

FIG. 6.1. (a) 461  $\mu$  Aluminum Particle Burning in Ambient Air-Xenon Flash Ignition, and (b) 308  $\mu$  Zirconium Particle Burning in Ambient Air. Flash ignition.



(a)

(b)

FIG. 6.2. (a) 239  $\mu$  Titanium Particle Burning in Ambient Air, Flash Ignition, and (b) 334  $\mu$  Titanium Particle Burning in Ambient Air, Flash Ignition.

Boron droplets burn without change of symmetry following ignition and the product does not dissolve in the metal. The surface of the burning boron droplet remains clean due to oxide vaporization once the steady-state combustion temperature is reached. As a consequence, trajectories of such droplets are quite devoid of the anomalies observed in aluminum combustion.

While metals are usually classed according to the particular combustion mechanism they affect, the classification could also be made with respect to the type of termination of burning. As an example, under the proper circumstances, burning droplets of aluminum, beryllium, magnesium, titanium and zirconium experience catastrophic fragmentation while those of boron and silicon do not.

Several metals were each burned in several oxidizers in this study, and each metal will be described separately. In addition to the flames described in Section 2.1, the environmental gases employed in these experiments were air, oxygen, carbon dioxide and various oxygen-argon-nitrogen mixtures. The behavior of flash-ignited specimens will be described first, followed by the gas burner studies.

#### 6.1. ALUMINUM

It is known that aluminum burns primarily by a vapor transport process. The stoichiometric oxide formed in the combustion process ( $\text{Al}_2\text{O}_3$ ) is insoluble in the metal and nonvolatile at temperatures occurring at the surface of the burning droplet. Some of the oxide accumulates on the surface of the droplet resulting in pronounced droplet dissymmetry. Marked physical, and possibly chemical, changes occur within the interior of the oxide lobe of the bilobate burning geometry as combustion progresses. The accumulation of product on the droplet has an overriding effect on the combustion behavior during the later stages of burning causing such phenomena as spinning, jetting and fragmentation.

The flash ignition experiments have demonstrated that there may be two completely different modes of termination of combustion depending on the presence or absence of product accumulation on the droplet surface. If the product accumulates, all of the above phenomena are likely to occur and termination is by droplet fragmentation. If the product does not accumulate on the droplet surface, as is the case for burning in  $\text{O}_2/\text{Ar}$  mixtures, none of the above phenomena are observed and termination is by simple burnout (i.e., complete consumption of the particle).

One advantageous feature of the flash ignition technique is the ability to produce ignited particles having virtually no surface oxide, in contrast to the gas burner method where appreciable oxide covers the entire droplet surface at the time of ignition. In the flash experiments particle size is accurately known and varied over a considerable range of diameters. The type of oxidizer and oxidizer partial pressure has

been varied extensively. System pressures were varied from 1 to 4.5 atmospheres absolute, and burning and explosion times of droplets were measured as a function of these variables.

#### 6.1.1. Flash-Ignited Aluminum Particles Burning in Oxygen-Argon Mixtures

Mixtures of gases containing 5, 10, 20, 50 and 75% oxygen in argon were employed in these experiments. Aluminum foils cut to produce molten droplets with diameters of 280 to 460  $\mu$  were used. Foils etched in the manner described in Section 2.2 ignited readily and vapor phase combustion was immediately established.

Aluminum particles which were burned in oxygen-argon mixtures behaved in a straightforward manner and probably represent as close an approximation to the idealized Brzustowski-Glassman spherical droplet burning model as can be found. Figure 6.3 shows the track photograph of a 461  $\mu$  aluminum particle burning in 1 atmosphere pressure of a 20/80 oxygen/argon mixture. Figure 6.4 shows a typical specimen quenched while burning in this environment. This figure clearly shows that no product accumulates on the droplet surface during burning. The burning time for aluminum particles in this gas mixture was found to be a linear function of the droplet diameter as can be seen in Fig. 6.5. This plot presents data for aluminum particles burning in both 20/80 oxygen-argon and in air. Since aluminum particles burned in  $O_2/Ar$  do not explode or fragment, the data in this plot are actually droplet burnout times. The data for aluminum particles burned in air are actually times to explosion or fragmentation of the particle. The two sets of data are plotted together here for comparison.

Increasing the oxygen concentration in these mixtures shortened the burning time, as would be expected, and increased the light emitted from the reaction. Aluminum droplets of the sizes employed here burned too slowly in a mixture of 5% oxygen in argon to make burning time measurements (insufficient length of reaction vessel). Combustion in  $O_2/Ar$  mixtures typically was terminated by burnout (complete consumption) and was indicated by the abrupt end to the track in photographs such as Fig. 6.3.

The behavior in oxygen/argon mixtures represents the simplest case for the aluminum-oxygen system; however, a variety of more complex burning characteristics are exhibited by aluminum powders burning in torch flames or flash-ignited particles burning in air.

#### 6.1.2. Flash-Ignited Aluminum Particles Burning in Air

The aluminum foils ignite readily in air and vapor phase combustion of the resulting droplets becomes fully established with barely detectable surface oxide present (Fig. 5.3a, Ref. 1). Still plate photographs of particle trajectories such as that shown in Fig. 6.1a reveal that aluminum droplets burning in air exhibit characteristics significantly different from those noted for droplets burning in 20% oxygen in argon.



FIG. 6.3. Flash-Ignited 461  $\mu$  Aluminum Particle Burning in a 20% Oxygen-Argon Mixture at 1 Atm Pressure.



FIG. 6.4. Optical Photomicrograph ( $\sim 50\times$ ) of Flash-Ignited Aluminum Particle Quenched While Burning in a 20% Oxygen-Argon Mixture at 1 Atm Pressure.

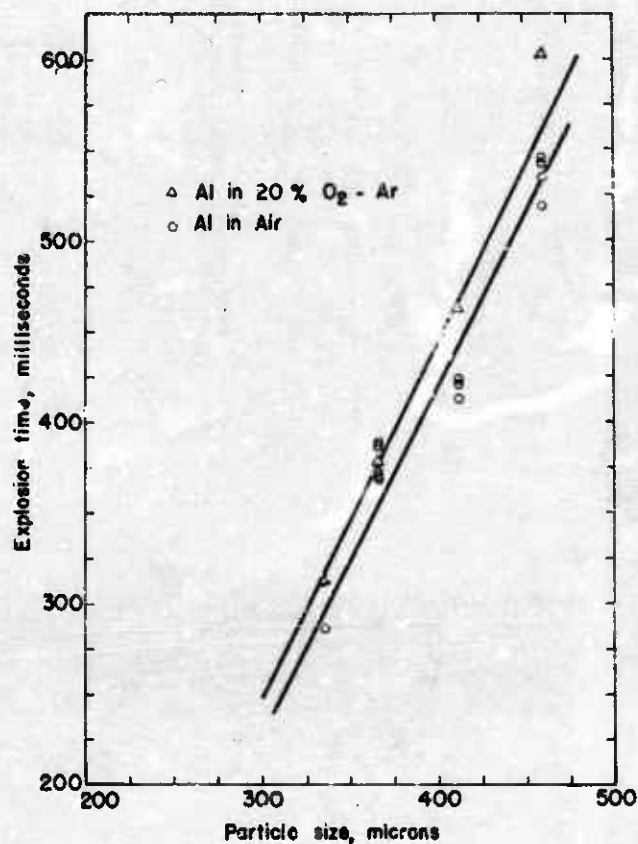


FIG. 6.5. Plot Showing Variation of Burnout or Explosion Time with Change in Particle Size. Data for Al in 20% oxygen-argon is actually time to burnout. Data for Al in air is time to explode. Combustion terminated in either case.

Examination of track photographs similar to Fig. 6.1a discloses that the aluminum particles spin vigorously following a phenomenon referred to as "puffing", represented by the bulge on the track about two-thirds of the distance down the length of the track. Subsequent to the puff the droplet is seen to jet some material and combustion is then terminated by a weak fragmentation.

The "puff" observed during the combustion of flash-ignited aluminum particles appears as a bulge on the track photographs and as a brilliant flash of light with a duration of 0.5 - 2.0 msec on high speed movies. These high speed movies indicate that the puff (flash of light) occurs reproducibly when 75% of the time from ignition to fragmentation has elapsed. This agrees with the result reported by Marshall and coworkers (Ref. 14). An interesting, but as yet unexplored finding is that aluminum particles puff in laboratory ambient air with approximately 35%

relative humidity but do not show any puffing when burned in dry air at atmospheric pressure. Particles are found to spin in both cases.

The plot in Fig. 6.5 shows the variation of the time from ignition to fragmentation of aluminum droplets burning in ambient air. The plot demonstrates that aluminum particles burn slightly faster in air than in 20/80 oxygen-argon.

Previous quenching studies (Ref. 1, Section 5.3) showed in detail the evolution of the particle geometry during burning. That study was made with the use of conventional low power optical microscopes and led to the view that the product lobe on the droplet did correspond to what has been referred to as a "lens-shaped cap". The use of the scanning electron microscope (SEM) has revealed additional details of the droplet geometry. Figure 6.6 is a SEM photograph which indicates clearly that the oxide globule more nearly resembles a fumarole than a "lens cap". When viewed at lesser magnification, specimens like that in Fig. 6.6 exhibit quenched smoke patterns around the particle indicating that oxidizable fuel vapor was issuing from the center of the oxide globule (Fig. 6.7).

By the time the oxide growth has reached the dimensions shown in Fig. 6.6 the frothiness described earlier (Ref. 1, p. 62) is encountered. Examination of these and similar specimens at a magnification of about 60X with an optical microscope reveals that the oxide contains numerous gas or vapor bubbles which appear to be percolating to the surface. Such interior details cannot be seen by the SEM.

Figure 6.8 is a composite of SEM photographs of the evolution of the burning geometry. This figure is composed of three specimens which were quenched at different times during the combustion. Each of the specimens is also shown greatly enlarged. These specimens span the range of configurations from a small oxide globule (representing little reaction) to that in which the oxide has encapsulated about 55-60% of the droplet. Total encapsulation of flash ignited particles has never been observed. The specimen shown in Fig. 6.7c was quenched at a time very shortly before expected fragmentation.

Figure 6.9 provides several views of two different particles quenched during the intermediate stages of combustion. These specimens indicate in some detail the nature of the change in the surface characteristics of the oxide globule and demonstrate the tendency of the oxide to fuse and for the fumarole to disappear.

Figure 6.10 shows several SEM views of another specimen quenched quite close to the fragmentation point. This is a terminal specimen which has impacted in the oxide-down position.

The opinion is widespread that the vapor phase flame of the aluminum particle creates and regulates the environmental temperature of the metal

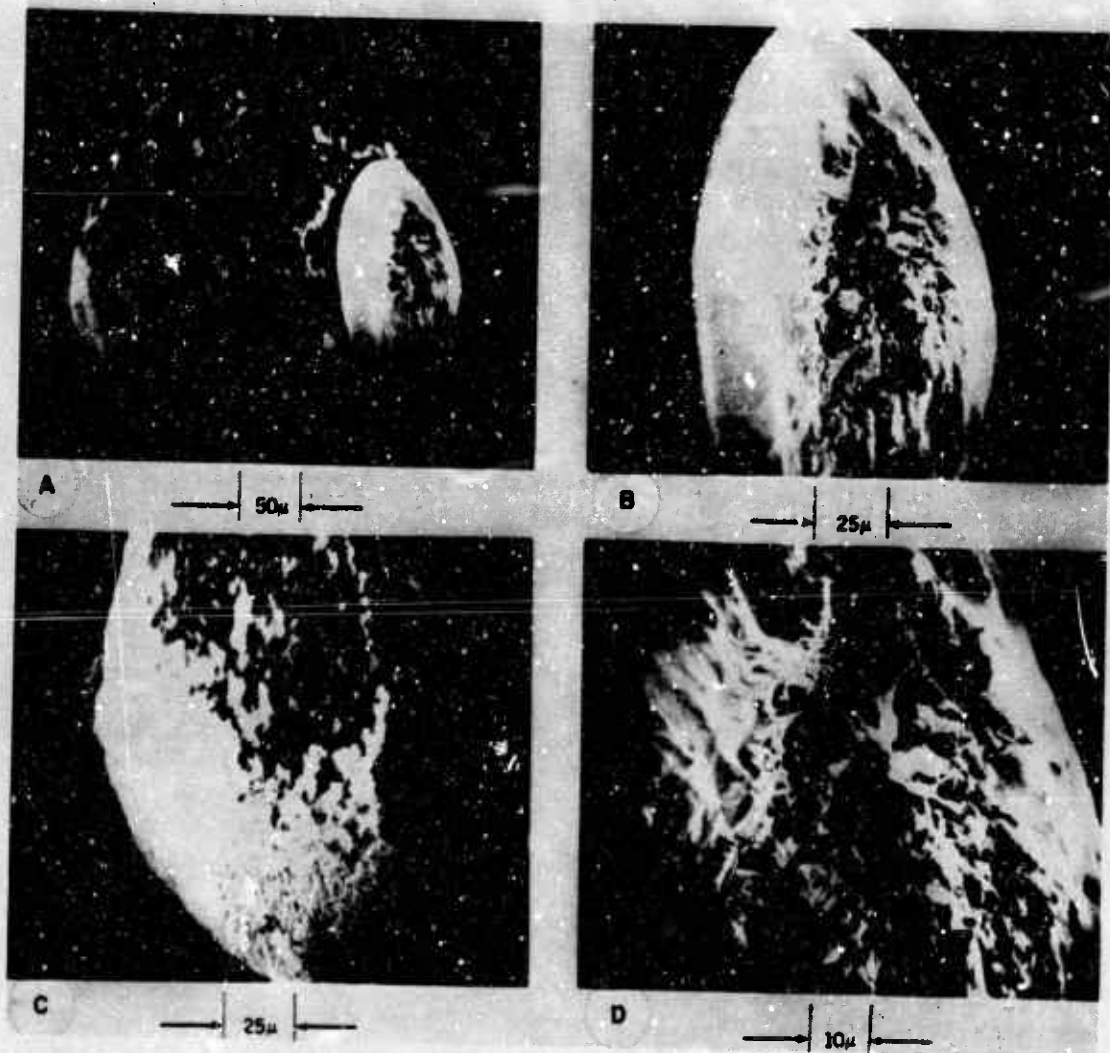


FIG. 6.6a-d. Scanning Electron Microscope Photographs at Various Magnifications Showing a  $461 \mu$  Flash-Ignited Aluminum Particle Which was Quenched While Burning in Ambient Air. Quenched at about  $0.3 t_{\text{freq}}$ .

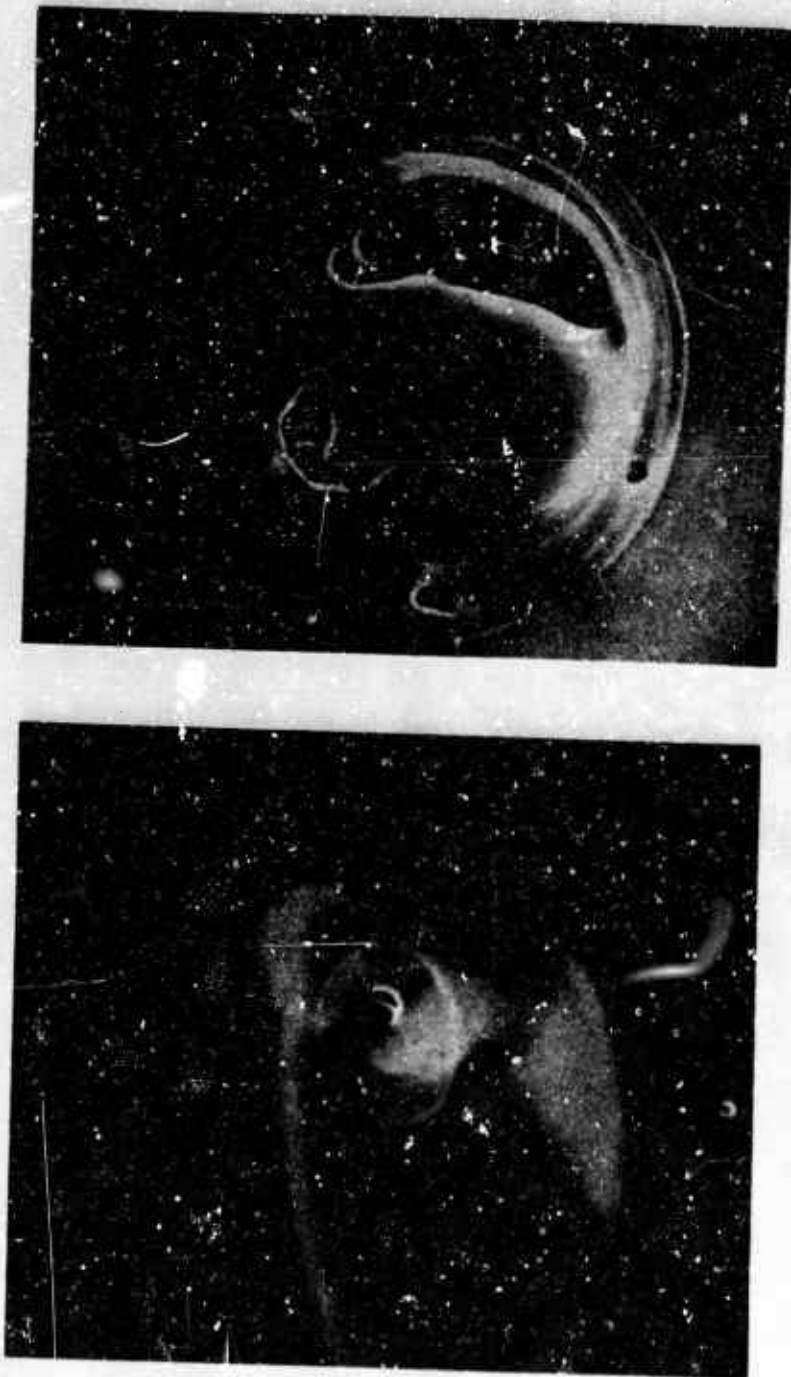


FIG. 6.7. Scanning Electron Microscope Photographs of a Nominal 100  $\mu$  Aluminum Particle Quenched While Burning in a CO/O<sub>2</sub> Flame. Particle has impacted metal-down. Note smoke associated with fumaroles in oxide cap.

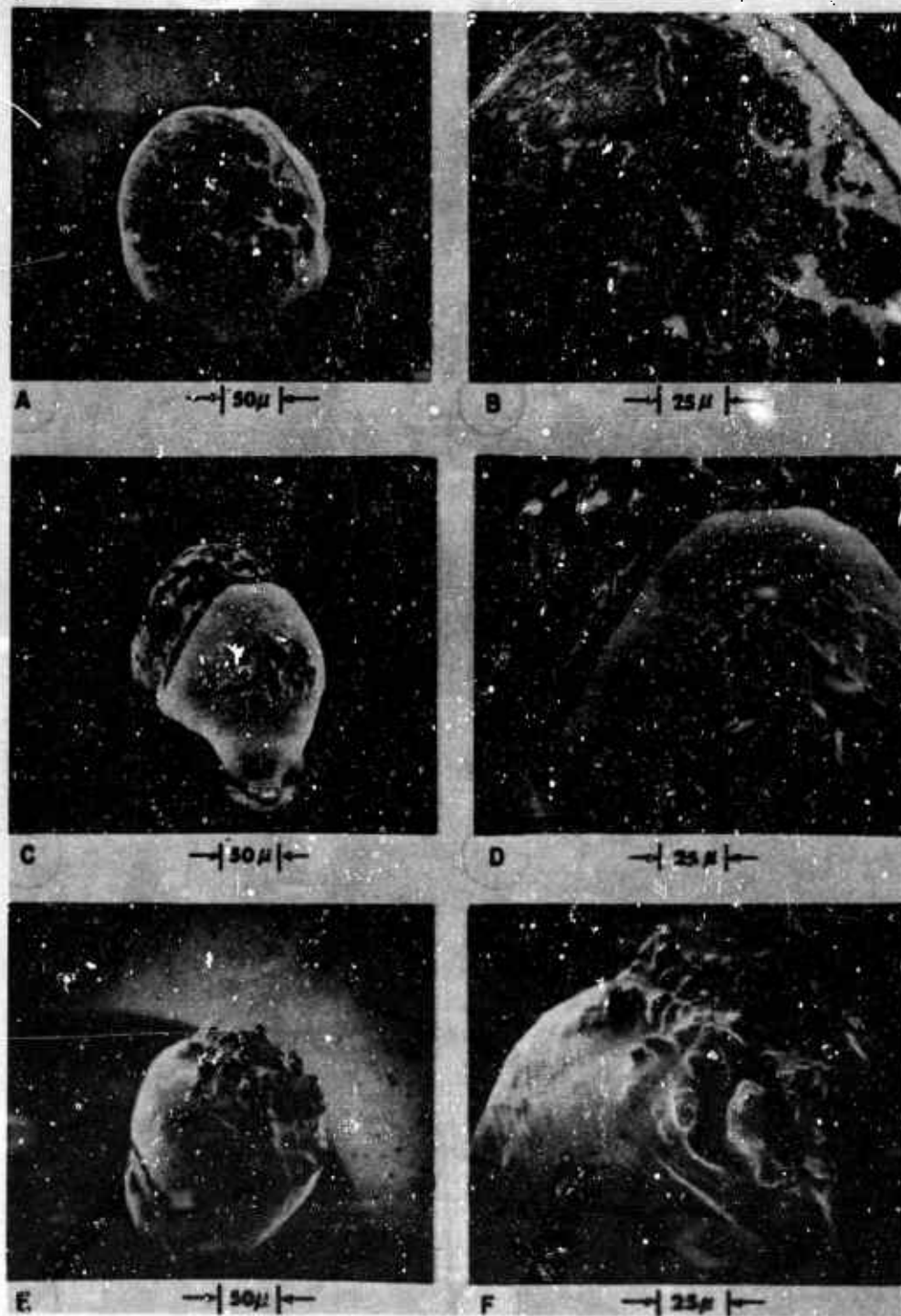


FIG. 6.8a-f. Composite of Several SEM Photographs Showing the Evolution of Burning Geometry of Flash-Ignited Aluminum Particles Burning in Ambient Air. Three different specimens are shown which were quenched at different times during the burning process.

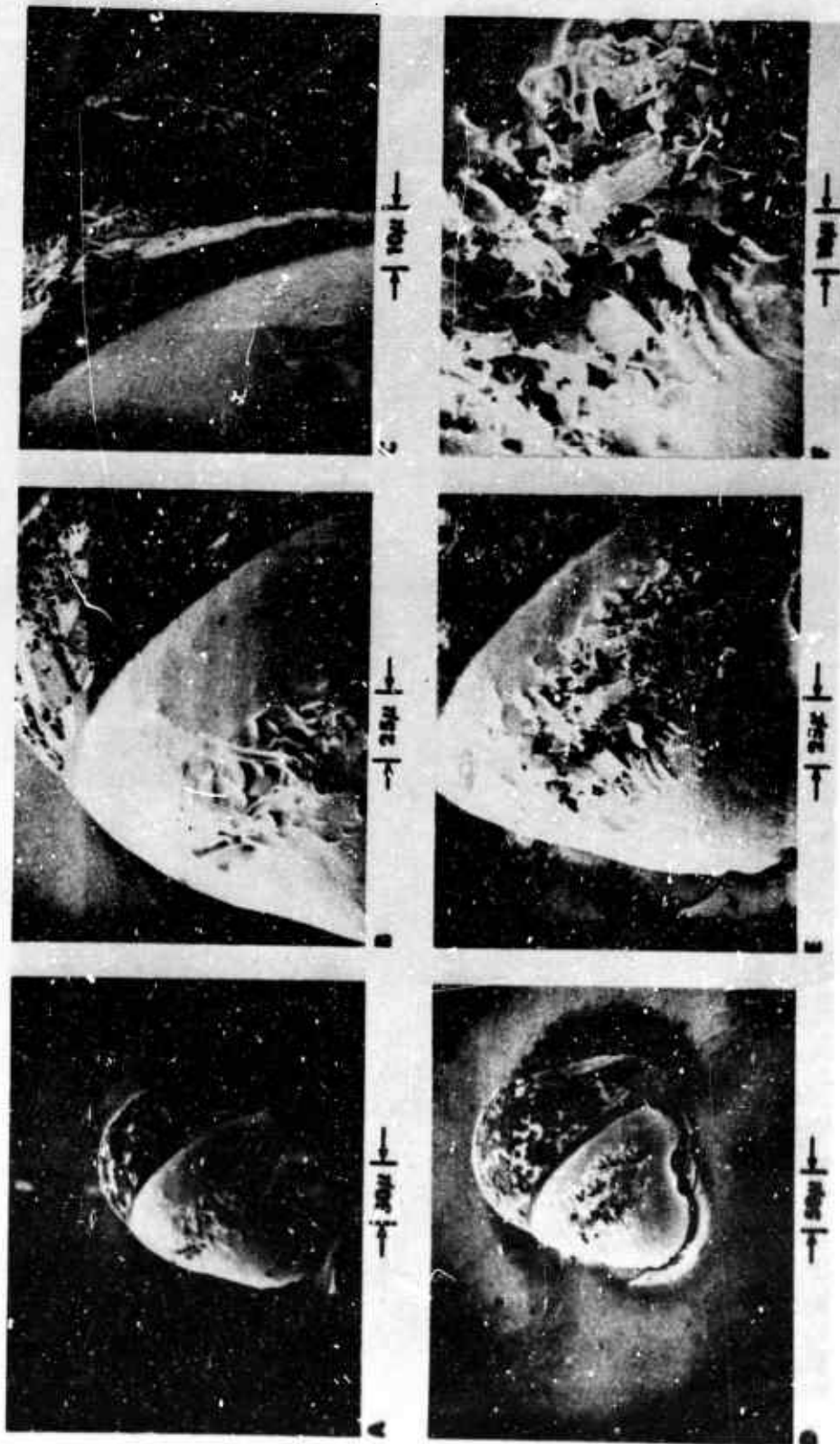


FIG. 6.9a-f. Composite Showing Several SEM Views of Two Different Aluminum Particles Quenched During Intermediate Stages of Burning in Ambient Air.



FIG. 6.10a-c. Flash-Ignited Aluminum Particle Quenched While Burning in Ambient Air. This is a terminal specimen quenched immediately before the expected fragmentation. Particle has impacted oxide-down.

droplet and therefore burning droplet temperatures are insensitive to ambient temperatures. Actually, this is strictly true only as long as the integrity of the spherical droplet flame is maintained. However, sufficient product accumulation occurs after one-third of the burning time has elapsed to destroy the spherical symmetry of the vapor phase flame and thus such thermal integrity or buffering is lost. Figure 6.11 provides evidence that aluminum particles burning in ambient air can cool by radiation from the oxide lobe. Note particularly the frozen oxide on the specimen seen in profile in Fig. 6.11b. This specimen and others like it indicate that the burning droplet is indeed sensitive to the particular ambient temperature of the experiment.

Figure 6.12 shows a 461  $\mu$  aluminum particle which was melted in argon by the xenon flash and allowed to quench. This specimen is offered in order to show the oxide-free metal surface.

The combustion of aluminum droplets in dry air was studied over a range of pressures up to 4.4 atmospheres (64 psia). The particles were found to fragment feebly in dry air at pressures up to about 2.4 atmospheres (35 psia). Fragmentation became quite weak and sporadic at this pressure and finally ceased as the pressure was raised to approximately 4.0 atmospheres. The time to fragmentation was found to be inversely proportional to the applied pressure. Fragmentation of aluminum particles in the cold gas atmosphere of the flash heating experiment generally is less violent than those occurring in the high temperature powder burning torch.

### 6.1.3. Flash-Ignited Aluminum Particles Burning in Oxygen-Argon-Nitrogen Mixtures

The marked difference in behavior between aluminum particles burning in 20% oxygen-argon and those burning in 20% oxygen-nitrogen (air) pointed strongly to the possibility of nitrogen playing an active role in the combustion of aluminum. Experiments were therefore conducted to assess this possibility.

When small percentages of nitrogen were added to mixtures of 20% oxygen-argon, particle spin was again observed in track photographs of the particle trajectories. When sufficient nitrogen was added particles were seen to spin and fragment exactly as in air. As little as 5% nitrogen added to a 20/80 oxygen/argon mixture was sufficient to cause detectable particle spin and sporadic fragmentation appeared when about 10% nitrogen was added.

These experiments have led to the conclusion that nitrogen, rather than being inert as had been supposed for some time, was an active participant in the combustion process. Nitrogen appears to be the responsible agent in causing the product to adhere to the droplet surface leading to the dissymmetry described earlier. Figure 6.13 compares specimens quenched from air and 20% oxygen-argon at comparable burning times. It

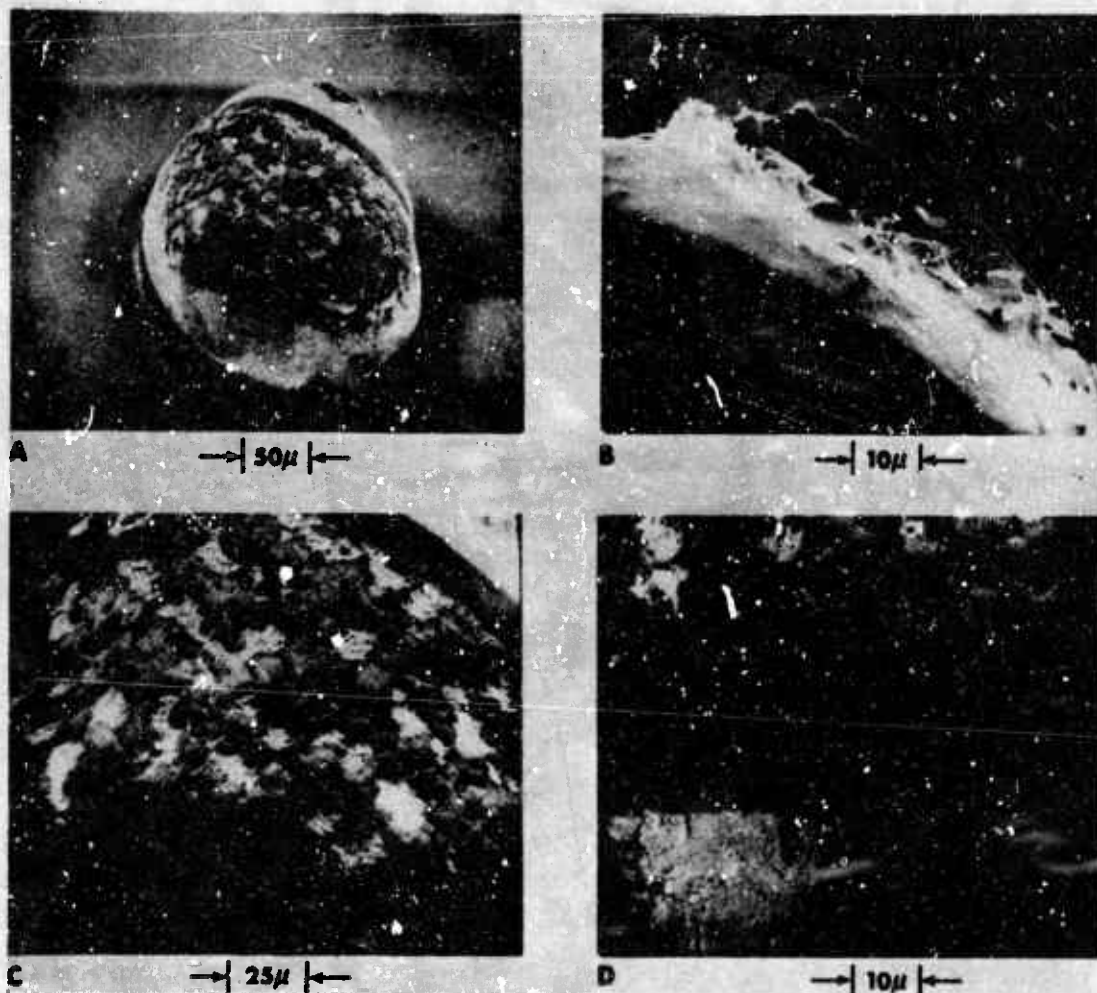


FIG. 6.11a-d. Composite Showing Several SEM Photographs of a 461  $\mu$  Flash-Ignited Aluminum Particle Quenched While Burning in Ambient Air. Note jagged nature of oxide which had frozen during free-fall which can be seen in profile in 6.6b. Particle quenched at ca.  $0.4 t_{\text{freq}}$ .

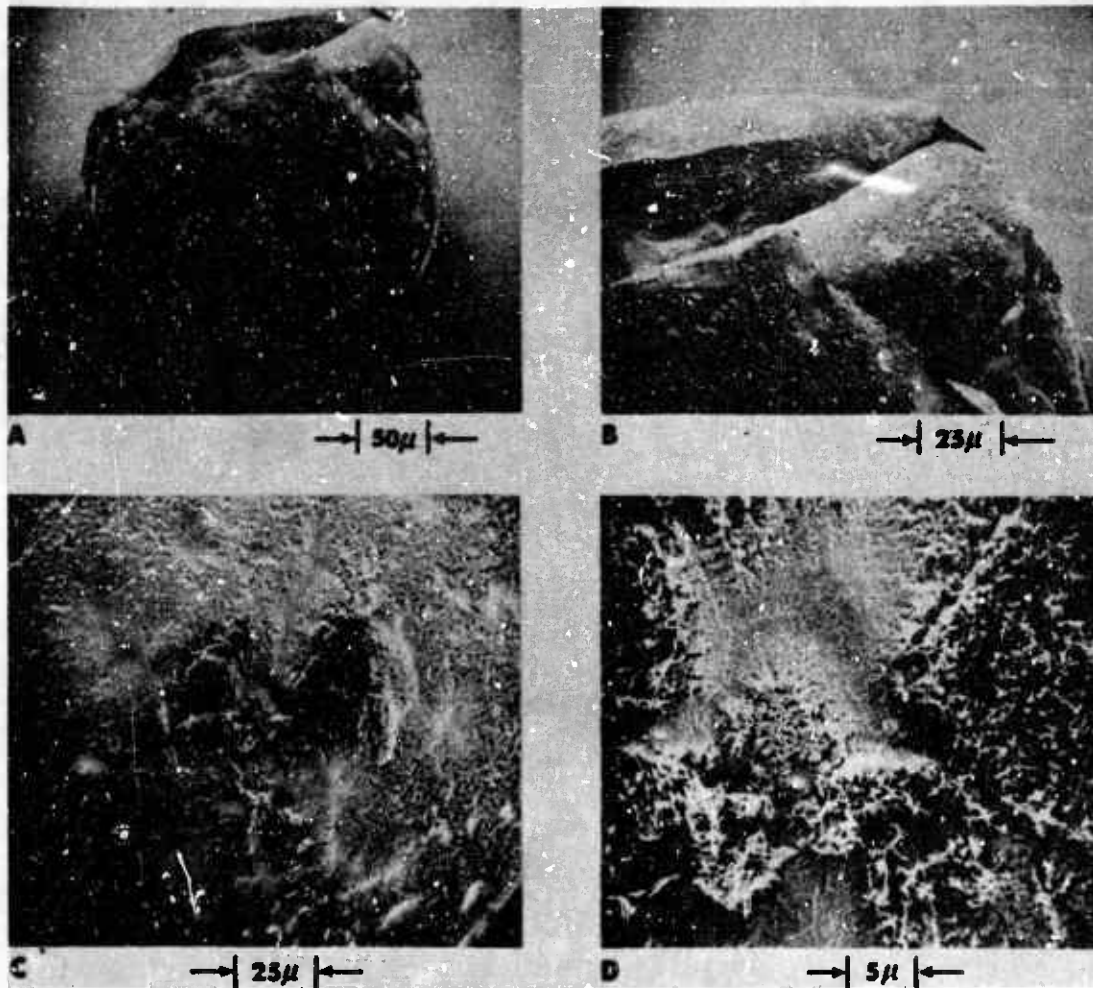
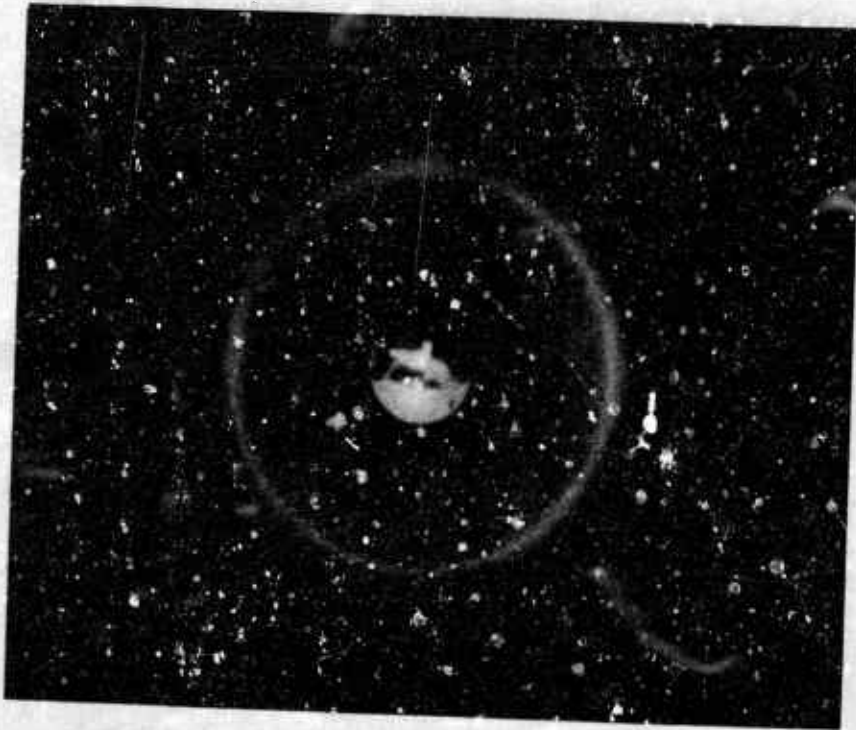


FIG. 6.12a-d. Composite of SEM Photographs Showing Unoxidized Surface of 461  $\mu$  Aluminum Particle Melted by Xenon Flash in Pure Argon and Permitted to Quench in Free-Fall.



(a) Burning in Ambient Air.



(b) Burning in 20/80 Oxygen-Argon

FIG. 6.13a-b. Comparison of Flash-Ignited 461  $\mu$  Aluminum Particles Quenched While Burning in (a) air, and (b) 20% Oxygen, Argon. Particles quenched at comparable burning time ( $\sim 0.65$  t<sup>burnout</sup>). Note absence of accumulated oxide on specimens (b).

is readily seen that the specimen burned in oxygen-argon possesses no accumulated product on the droplet surface and that the spherical symmetry of the vapor phase flame envelope is preserved. These specimens, when viewed in relation to their associated track photographs in Fig. 6.1a and 6.3, demonstrate conclusively that the presence of the oxide (or oxide-nitride) globule is responsible for the particle spinning and other erratic behavior.

#### 6.1.4. Flash-Ignited Aluminum Particles Burning in Carbon Dioxide

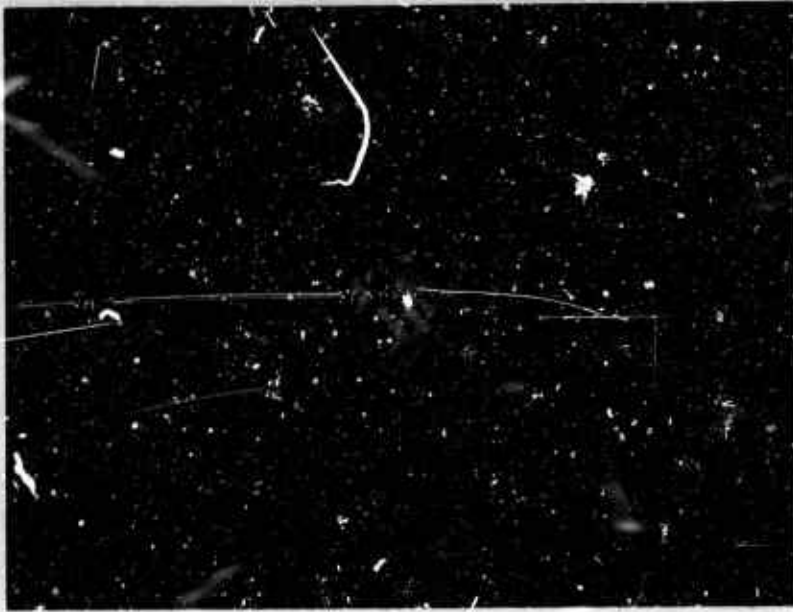
The most significant characteristic of aluminum particles burning in cold CO<sub>2</sub> is that they will not burn long enough to completely consume the particle. Examination of the photograph of the track of the burning particle in Fig. 6.14a shows only a straight, sharply defined track giving no evidence of droplet asymmetry, and indeed none is found in the quenched specimen shown in Fig. 6.14b. The oxide present on the surface appears as a very thin crust and the whole particle has the general appearance of a cinder. Termination appears to be caused by cooling as a consequence of inadequate heat of reaction to overcome heat loss from the system. No particles fragment in cold carbon dioxide.

#### 6.1.5. Flash-Ignited Aluminum Particles Burning in Pure Oxygen

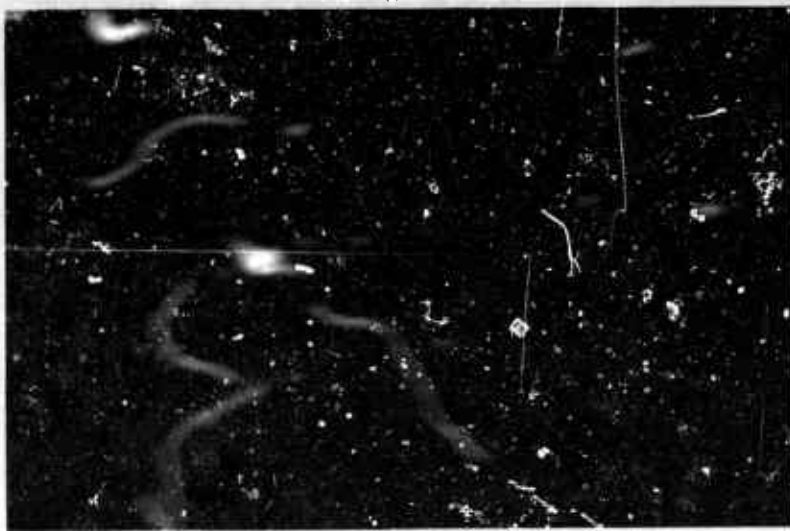
The burning times of even the largest particles used in this study were too short to be measured conveniently in one atmosphere of pure oxygen. The reaction was tremendously vigorous, consuming the metal very quickly and throwing off a shower of oxide globules in all directions. The major product of the burning of 461  $\mu$  droplets in this environment was found to be hundreds of tiny solid oxide beads ranging in size from 10-50  $\mu$  with a few hollow spheres as large as 275  $\mu$ . There was a dramatic increase in the intensity of the radiation from this reaction as compared to the reaction in other gases. Tracks of particles burning in 0.2 atmosphere pressure of pure oxygen are devoid of evidence of spinning or other phenomena associated with burning in air.

#### 6.1.6. Aluminum Particle Combustion in Carbon Monoxide-Oxygen Flames

The aluminum particle burning behavior was studied over a range of flame compositions, both with and without a counterflow of another oxidizing gas. Generally, the counterflow was either air or pure oxygen. The particles exhibited a range of behavior which was very dependent on the oxidizer/fuel ratio of the torch flame (see also Section 5.2). A summary of the aluminum particle burning characteristics in a CO/O<sub>2</sub> flame, without counterflow, is given in Table 6.1. The table shows that for flames on the oxygen-rich side of stoichiometry, oxide sphere shedding from the droplet seemed to be most characteristic, with minimal fragmentation occurring. On the fuel-rich side, sphere shedding (as described



(b)



(a)

FIG. 6.14a-b. Flash-Ignited  $461 \mu$  Aluminum Particle Burning in Cold  $\text{CO}_2$ .  
(a) Track photograph showing termination of combustion. (b) Particle quenched while burning in  $\text{CO}_2$ .

in Section 5.2) is absent, and fragmentation, puffing and spinning are dominant characteristics. The sphere shedding referred to here is not a terminal event, but the occurrence or nonoccurrence of this process does determine the method by which combustion is terminated.

The summary of observations in Table 6.1 does not represent the behavior experienced by all particles under a given set of flame conditions. Rather, it is a subjective averaging made necessary by the inhomogeneous nature of powder burning torches. Since particles ignite at various levels in the flame and thus burn out at various levels, such averaging is made necessary.

The results obtained with a counterflow of an oxidizing gas were also highly dependent on the oxidizer/fuel ratio of the flame itself. Considering stoichiometric or slightly fuel-rich flames, there is a significantly greater incidence of fragmentation when particles cross the interface into pure oxygen as compared to air. On the other hand, for flames which are somewhat oxygen-rich there appears to be no significant difference in the incidence of fragmentation when the particles are crossing the interface into either air or oxygen counterflow.

TABLE 6.1. Characteristics of Aluminum Particles  
Burning in 1 Atmosphere CO/O<sub>2</sub> Flames

Oxygen-Rich	Stoichiometric	Fuel-Rich
Ignition Shed 1 large sphere Some spin Little fragmentation	Ignition Puff - sphere(s) shed Vigorous spin Fragmentation	Ignition Puff Vigorous spin Fragmentation

#### 6.1.7. Summary

The studies reported here have shown that burning aluminum droplets may terminate combustion by two different methods. One burning mode, represented by flash-ignited aluminum burning in O<sub>2</sub>/Ar mixtures, is characterized by vaporization of the droplet with all reaction apparently occurring in a detached spherical reaction zone yielding a cloud of fine smoke as the product. Trajectories of such particles are straight and the combustion is unperturbed in any way prior to complete consumption of the droplet. With the exception of the fog of product which develops in the droplet flame envelope, such a process resembles a simple hydrocarbon droplet diffusion flame. Measurements on flash-ignited aluminum particles show a linear relationship between burning time and particle size for droplets burning in oxygen-argon mixtures. The second mode of burning, represented by flash-ignited aluminum particles burning in air

or spherical aluminum powders burning in torch flames, is characterized by erratic particle trajectories, spinning, puffing and fragmentation. Quenching experiments show that such particles have distorted smoke clouds and that the particle geometry deviates from the original spherical symmetry due to product accumulation on the surface.

A combination of photographic records of burning particles and photomicrographic examination of quenched specimens shows that the disposition of product(s) governs the route to termination of combustion. If the product does not accumulate on the droplet, particles burn unperturbed and termination is by simple consumption and burnout; if product accumulates in the droplet, termination is by fragmentation. Some particles burning  $\text{CO/O}_2$  flames appear to be able to rid themselves of nearly all of the surface oxide accumulation during the sphere shedding process. Consequently those particles do not spin and they are seen to burn out without fragmentation or any other irregularities.

The flash heating experiments have shown that the addition of nitrogen to nonfragmenting systems causes the product to adhere and accumulate on the droplet and, when sufficient nitrogen is added, droplet explosions occur. The time elapsed from the rise of the flash heating pulse to fragmentation of the particle has been found to be a linear function of the droplet diameter.

Particle fragmentations also occur in  $\text{CO/O}_2$  flames in the apparent absence of nitrogen, although the situation there is not clearly defined due to significant nitrogen pickup by flames operating in atmospheric air (Ref. 15). Carbon dioxide does not appear to be involved since flash-ignited aluminum particles would not burn to completion in  $\text{CO}_2$ , and no particles were ever seen to explode or fragment in this gas. Further, the bilobate geometry characteristic of fragmenting droplets is not formed in carbon dioxide. It seems more reasonable to conclude that carbon monoxide is active in promoting fragmentation in this case.

## 6.2. TITANIUM

Titanium is a metal which burns primarily by surface processes. Melting and boiling temperatures of metal and oxide in this system are so high that there is insufficient metal vapor pressure to support vapor phase combustion. (Vapor pressure of titanium at  $3000^\circ\text{K}$  is ca. 50 Torr.) Among the unusual properties of titanium having a bearing on its combustion is the ability to form interstitial solid solutions with various compounds or elements. In particular, solid solutions containing up to 40 atom percent of oxygen without the separation of an oxide phase can occur in both titanium and zirconium (Ref. 16). These interstitial substances are not stoichiometric compounds but phases of widely variable composition. In the titanium-nitrogen system, the phase represented by the formula  $\text{TiN}$  (theoretically 22.6% nitrogen) varies from about 12 to 22.6% N without phase change. Also  $\text{TiN}$  is isomorphous with  $\text{TiC}$  and  $\text{TiO}$ ,

and the interstices in these compounds may be simultaneously filled with nitrogen, carbon or oxygen with little change in dimensions or properties. The lattice parameters of TiO and TiN are reported to be identical (Ref. 17). It becomes a matter of paramount importance then to have reliable knowledge of the high temperature phase diagram of such a system if predictive understanding is to be achieved. Burning temperatures will also have to be known accurately in order to describe the instantaneous composition of the burning system. Diffusion in the condensed phase in such potentially conglomerate systems would be difficult to describe and is a subject for which very little data is presently available.

It is known that in addition to the solid solution of oxygen in titanium, at least three intermediate phases, TiO, Ti<sub>2</sub>O<sub>3</sub> and TiO<sub>2</sub> exist.<sup>2</sup> The combustion of titanium in air or in an atmosphere of propellant decomposition products would therefore be expected to be quite a complex process.

#### 6.2.1. Flash-Ignited Titanium Particles Burning in Air

Reactor Grade titanium metal purchased from the Wah Chang Corporation was employed in these experiments. Titanium foils were cut to sizes which would produce droplets of 239, 265, 306 and 334  $\mu$  diameter. The titanium was characterized by very easy ignitability in the flash apparatus followed by vigorous and reproducible burning and fragmentation behavior.

Figure 6.2 shows track photographs of typical titanium particles burning in air at 0.9 atmospheres (13.6 psia) pressure. In Fig. 6.2a the 239  $\mu$  droplet can be seen to undergo a single catastrophic fragmentation while in Fig. 6.2b a 334  $\mu$  droplet, burned in the same gas at the same pressure, experiences a series of periodic eruptions of significantly lesser magnitude. Oxide debris from specimens corresponding to Fig. 6.2a was usually made up of relatively large curved fragments with jagged edges, while that from specimens represented by Fig. 6.2b was made up mostly of small round beads of about 5-25  $\mu$  diameter.

The variation of time to explode versus particle size for titanium is shown in Fig. 6.15. Again, as was the case for aluminum, it is seen that the time for these titanium droplets to explode is a linear function of the droplet diameter.

A notable feature of the debris from all of the series of eruptions in the larger particle was that every fragment left a spearpoint track. These spearpoint tracks were reported by Nelson (Ref. 19) as a result of his study of zirconium droplet combustion. He showed that they were

<sup>2</sup> Research published while this report was in preparation indicates that noncongruent evaporation occurs in the Ti/O<sub>2</sub> system with a trend toward Ti<sub>3</sub>O<sub>5</sub> (Ref. 18).

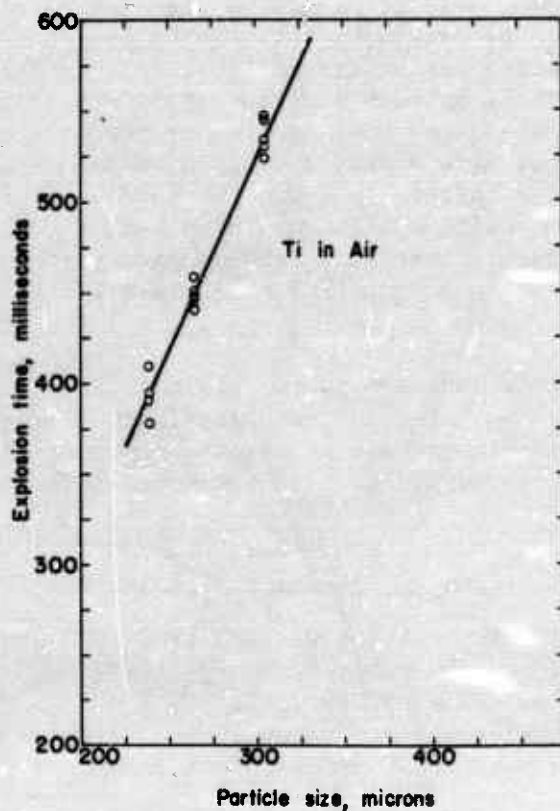


FIG. 6.15. Variation of the Time to Explode with Change in Particle Size for Flash-Ignited Titanium Particles Burning in Ambient Air.

due to a phenomenon known as the "Blick" effect, in which fragments from the exploding droplet may become supercooled by as much as  $500^{\circ}\text{C}$  below the freezing point of the oxide ( $\Delta T \approx 0.18 T_{\text{mp}}$ ). The supercooling is accompanied by a diminution of the particle radiation. At the onset of freezing the particle temperature abruptly rises again to the freezing temperature and the radiation experiences a corresponding precipitous increase followed by a second decay in both temperature and radiation to the final extinction.

Occurrence of the "Blick" effect as the cause of spearpointing suggests that the larger  $334 \mu$  droplet was molten at the instant of fragmentation while the smaller  $239 \mu$  droplet had at least solidified at the surface. It is possible that the difference in behavior may be attributed to the difference in radiative ability of the two particles. The smaller particle, having the greater surface-to-volume ratio, is more capable of cooling by radiating its heat away. The onset of freezing would also be expected to drive any dissolved gases out of solution and thereby contribute to a greater driving force which is evident in the explosion of the smaller particle.

Systematic impingement quenching similar to that for aluminum was not done for titanium and zirconium because reproducible results are difficult to achieve. This was partly due to a tendency on the part of the molten droplets to splatter and partly due to the longer times required to quench titanium and zirconium which prevents instant freezing of both droplet and reaction.

#### 6.2.2. Flash-Ignited Titanium Particles Burning in Oxygen-Argon Mixtures

Titanium was found to ignite and burn very readily in a 20/80 oxygen-argon mixture. Titanium droplets burning in such a mixture were observed to terminate combustion by a fragmentation of much reduced force as compared to air. Burning and explosion time data versus particle size in this gas mixture are incomplete at this time because the burning time of the largest particles exceeded the limits of measurement of the apparatus. Chamber lengths of nearly two meters are required to provide sufficient time for the particles to burn to completion. Sufficient data are available, however, to indicate that the titanium droplets burning in a mixture of 19.4% oxygen in argon terminate combustion 5-10% sooner than in air over the range of particle sizes from 239-334  $\mu$ .

The product from these droplet explosions was found to be mostly dense opaque white spheres of about 125  $\mu$  diameter together with an occasional metallic-looking sphere of nearly the same size. The peculiar spearpoint particle tracks described earlier were produced by all the fragments from all particle sizes of titanium burned in this gas mixture, and thus indicate that all the material was molten at the time of fragmentation.

#### 6.2.3. Flash-Ignited Titanium Particles Burning in Carbon Dioxide

The titanium particles employed in this study could not be successfully burned in cold carbon dioxide. Combustion of the particles could be initiated but the combustion would not sustain itself.

The particles retrieved from the bottom of the reaction vessel were found to be shiny dark gray spheres, the surface of which appeared glassy looking. These particles are not smoothly spherical but appear rather lumpy, and are found to be about 250  $\mu$  in diameter as compared to an initial molten particle size of 239  $\mu$  diameter.

#### 6.2.4. Flash-Ignited Titanium Particles Burning in Pure Oxygen

As in the case of flash heated aluminum droplet combustion in pure oxygen, the titanium was consumed too rapidly to make meaningful measurements of burning times at one atmosphere pressure of pure oxygen. The reaction of titanium droplets in pure oxygen was extremely fast. The

reaction was characterized by emission of intense radiation and by a shower of oxide spheres. The oxide product from the combustion of 334  $\mu$  droplets in pure oxygen consisted almost exclusively of hollow translucent spheres of about 50  $\mu$  diameter with a few as large as 350  $\mu$ .

### 6.3. ZIRCONIUM

Zirconium, like titanium, is a metal which burns primarily by a surface process, yielding a soluble, nonvolatile oxide. Reaction is controlled by oxidizer diffusion into the droplet. Zirconium, like titanium, is also able to dissolve large quantities of oxygen and form solid solutions of varying composition with its oxide and nitride.

Undoubtedly, the most comprehensive study of zirconium particle combustion reported to date has been done by Nelson (Ref. 4). The single particle zirconium burning reported in this investigation was done with some of the same oxidizers as Ref. 4 but at pressures of 1 to 4.5 atmospheres.

#### 6.3.1. Flash-Ignited Zirconium Particles Burning in Air

Zirconium foils cut to produce droplets ranging in size from 260-388  $\mu$  were used in this investigation. Zirconium, like the titanium, is characterized by easy ignitability and vigorous and reproducible combustion and droplet explosion.

Figure 6.16 shows track photographs of several 308  $\mu$  zirconium droplets burning in one atmosphere air. These specimens represent typical behavior in this particular environment and demonstrate the violence of the droplet explosions. The specimens in Fig. 6.16b and 6.16c, in particular, suggest the rupture of a gas-charged core as a mechanism for the explosion. It appears from Fig. 6.16b that most of the droplet remains intact after the eruption and continues to radiate for some time, even following the glancing collision with the wall. This asymmetric eruption suggests that a gas blister has formed and burst on one side of the droplet and suggests that the quenched remains of such a specimen might resemble a cored apple. Examination of the debris in Fig. 6.17 shows this to be the case.

The ricochet traces shown in Fig. 6.16b and 6.16c suggest that the particle or at least its surface was solid at the time of collision. The jagged nature of the oxide debris shown in Fig. 6.17 also suggests a solid or partly solid colliding particle. These observations point to the probability that the droplet was solidifying at the onset of explosion, or that the solidification itself was perhaps responsible for triggering the explosion.

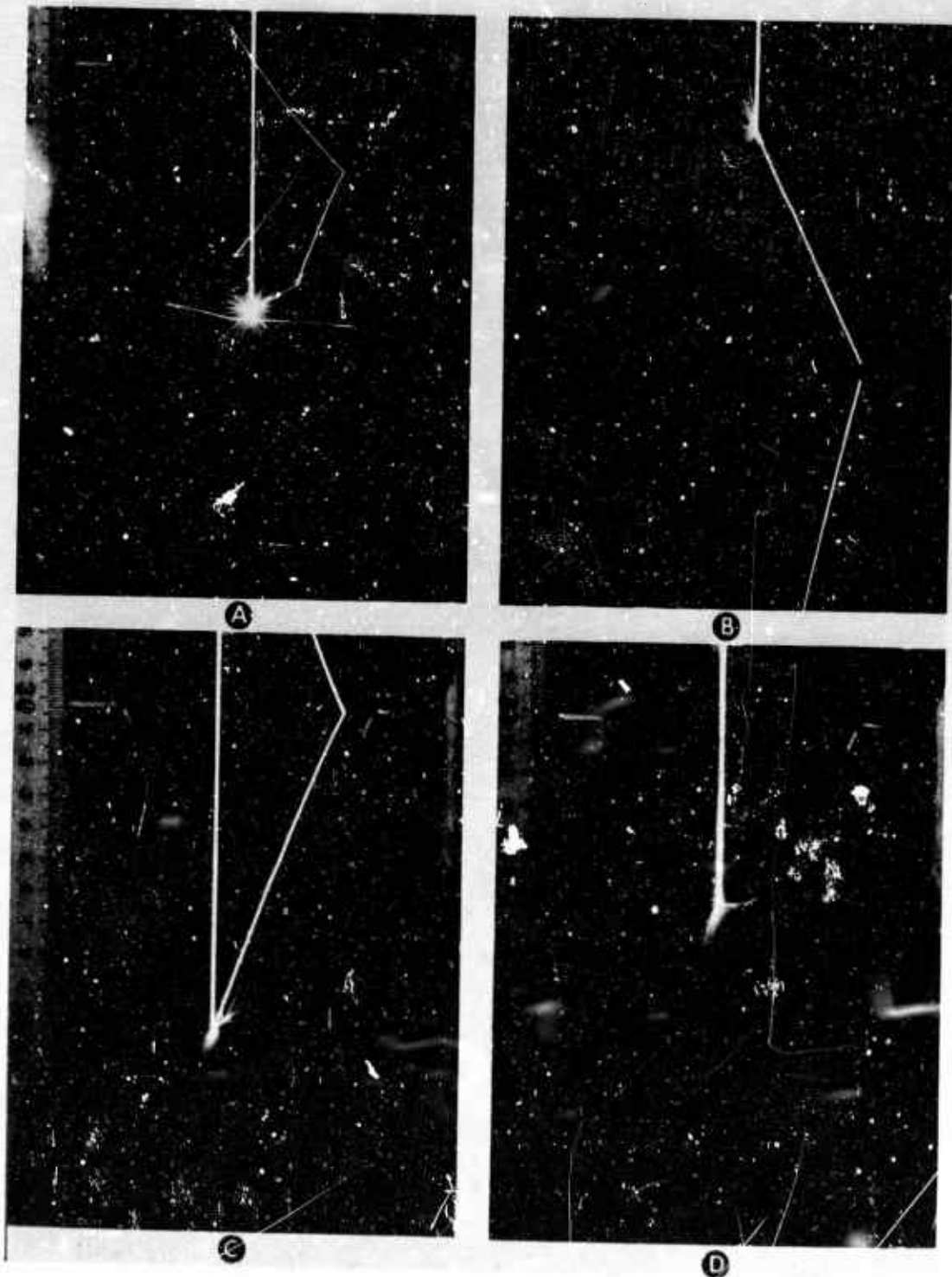


FIG. 6.16a-d. Some Representative Droplet Explosions of Flash-Ignited  $308 \mu$  Zirconium Particles Burning in Ambient Air.

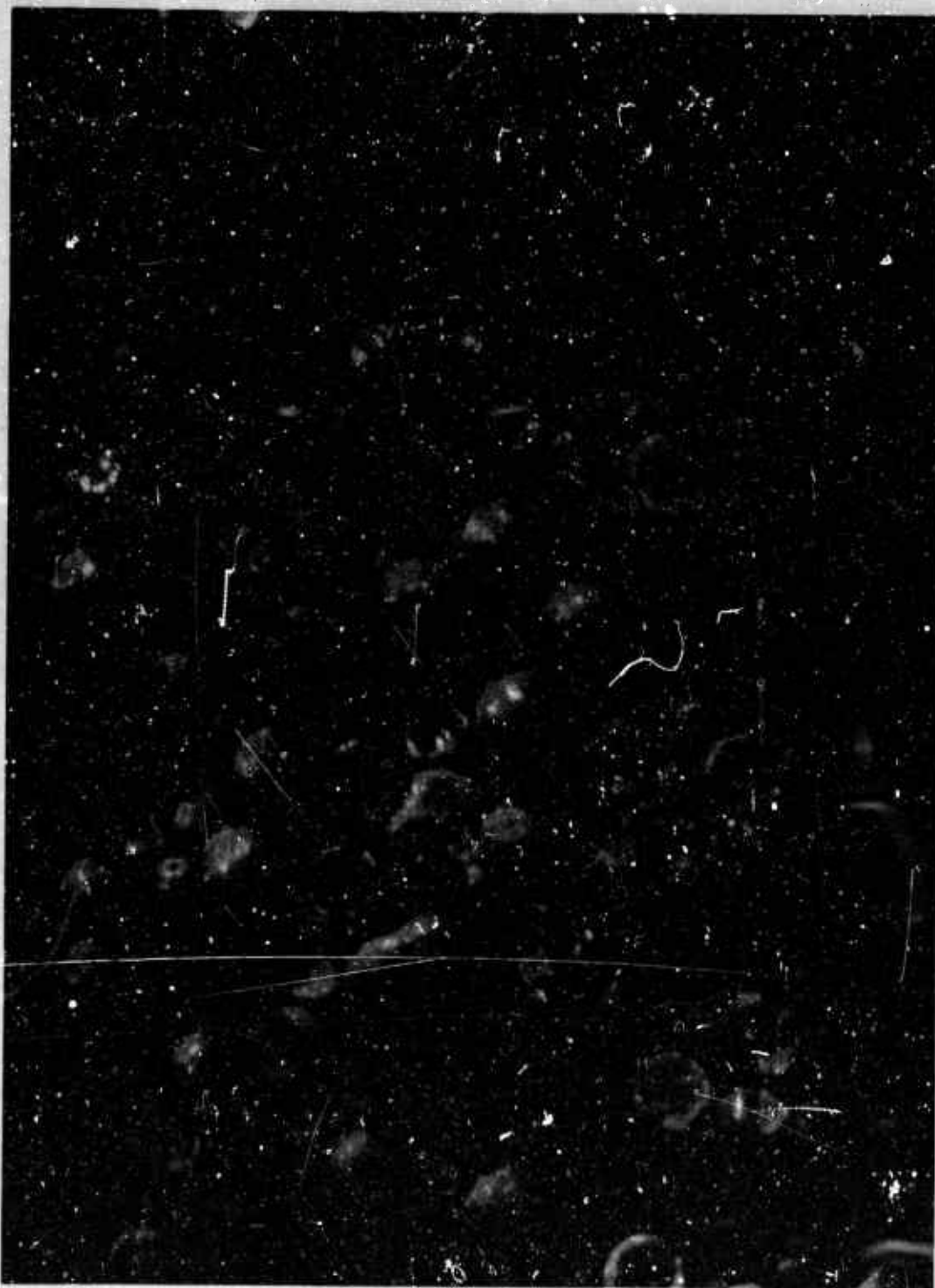


FIG. 6.17. Debris From Droplet Explosions of Flash-Ignited Zirconium Particles Burning in Ambient Air ( $\sim 50X$ ).

The variation of the elapsed time from ignition to explosion for these zirconium particles can be seen from Fig. 6.18 to be a linear function of the particle size. The variation of explosion time is inversely proportional to the pressure for Zr burning in dry air and seems to be roughly linear, although scatter in the data is considerable. At pressures approaching 60 psia droplet explosions become desultory, indicating that the threshold for nonfragmentation is quite close. In Fig. 6.19 the variation of explosion time with particle size in air for Al, Ti and Zr is plotted for comparison.

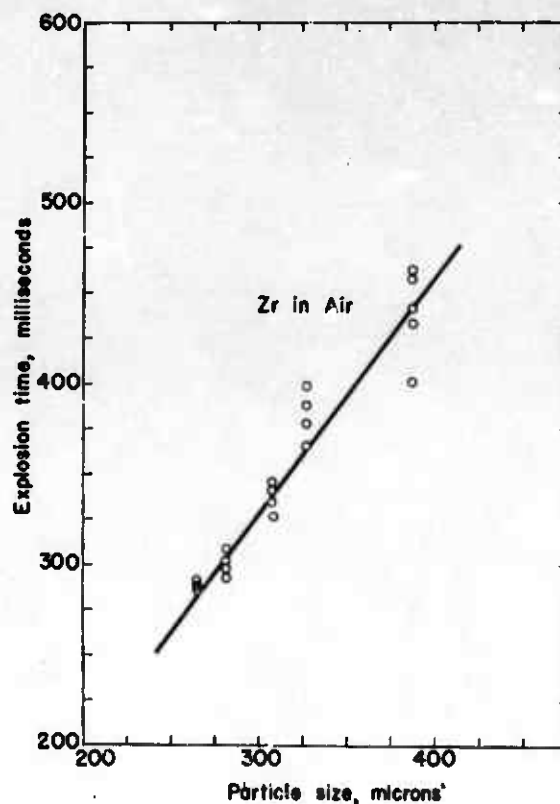


FIG. 6.18. Variation of the Time to Explode With Change in Particle Size for Flash-Ignited Zirconium Particles Burning in Ambient Air.

### 6.3.2. Flash-Ignited Zirconium Particles Burning in Oxygen-Argon Mixtures

The zirconium droplets ignited and burned very readily in a 20/80 oxygen-argon mixture. The time to explode for zirconium droplets burned in this atmosphere was found to be 33% longer than in air, which compares favorably with the value of 30% reported by Nelson (Ref. 4). The scatter in the data from these experiments is greater than in air.

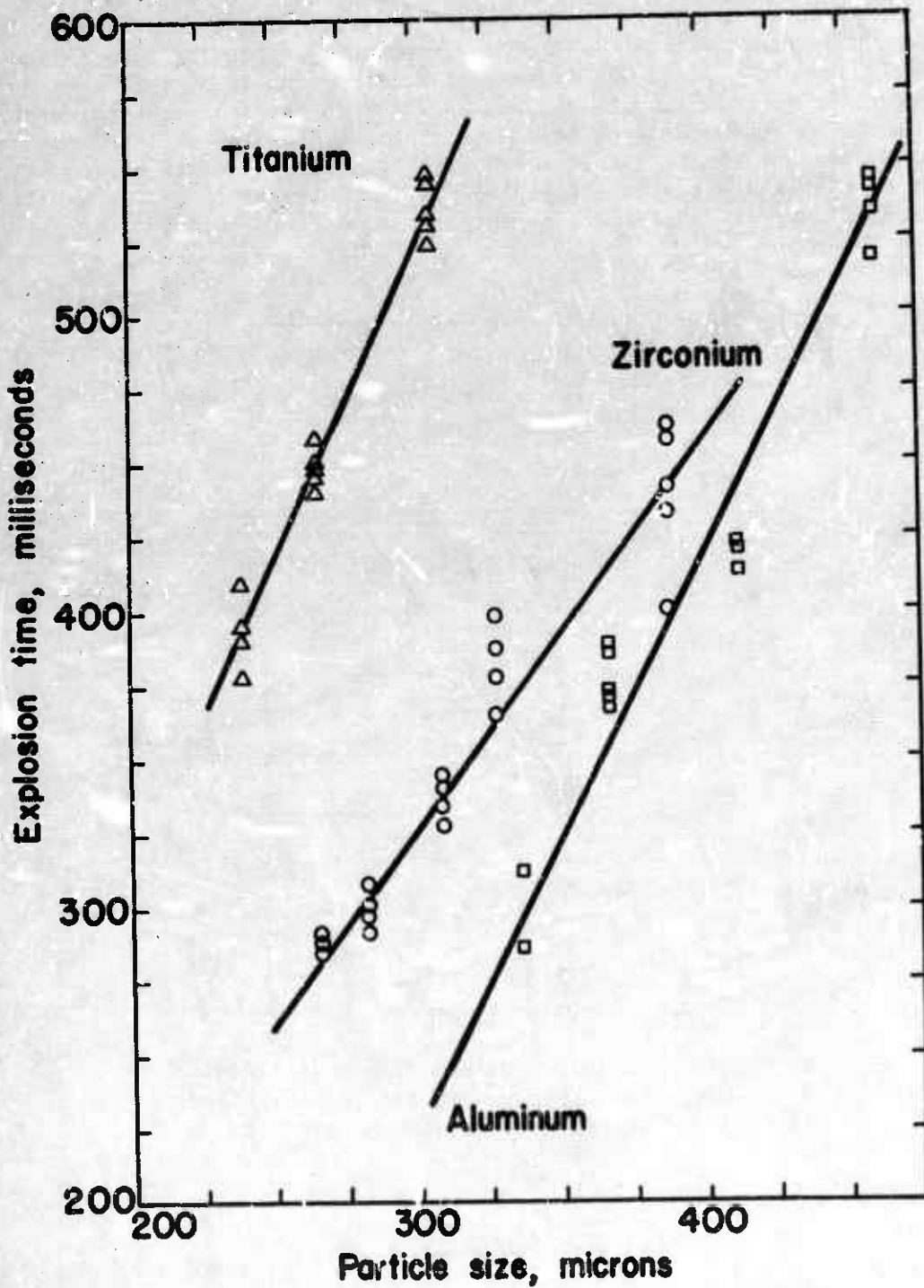


FIG. 6.19. Plot Comparing the Variation of the Time to Explode Versus Particle Size for Flash-Ignited Particles of Al, Ti and Zr Burning in Ambient Air.

The major product from these droplet explosions was found to be large numbers of tiny oxide bubbles while a few large teardrop-shaped balloons or sacs were found ranging in size from 250-275  $\mu$  when particles of 308  $\mu$  original diameter were burned.

The spearpoint tracks described earlier for titanium and attributed to the "Blick" effect were found to be characteristic of zirconium droplet explosions in this gas mixture, but not in air. Since the system was molten at the instant of explosion, the individual pieces of debris from the explosions are more accurately described as globules rather than fragments.

A noteworthy feature of these explosions in oxygen-argon is the very much reduced intensity or vigor of the event. For example, the experiments show that the material thrown from the site of the explosion in this gas mixture typically travels about 3 cm, while many fragments from explosions in air are hurled nearly a meter away.

#### 6.3.3. Flash-Ignited Zirconium Particles Burning in Carbon Dioxide

As with the titanium, combustion of the zirconium droplets could be initiated in cold CO<sub>2</sub>, but could not be sustained. The tracks of the particles looked virtually identical to those of titanium. The free-fall quenched particles also looked dark gray with a glassy surface and had increased in diameter about 5% due to a small amount of reaction having occurred, as was the case with titanium.

#### 6.3.4. Flash-Ignited Zirconium Particles Burning in Pure Oxygen

Systematic burning time measurements for zirconium droplets burned in 1 atmosphere of pure oxygen were not made because the particles usually were consumed very rapidly in a portion of the apparatus inaccessible to photographic measurements.

Combustion of zirconium in oxygen led to a profusion of small oxide bubbles typically of 5-30  $\mu$  diameter with some white teardrop-shaped sacs slightly smaller in diameter than the original droplet.

### 6.4. BORON

The boron used in the combustion studies reported here was Trona Polycrystalline granular powder with a purity of better than 99% and screened to give particle size fractions of 53-62, 88-105, 125-149 and 177-250  $\mu$ . The larger particles proved most convenient to study due to their longer burning time and most of the work in this study was done on this material.

#### 6.4.1. Flash-Ignited Boron Particles Burning in Air

With an energy input to the particles of about  $40 \text{ joules/cm}^2$  only the smaller particles ignited immediately; however, once ignited, all particles burned to complete consumption. Some of the larger particles studied ( $177\text{-}250 \mu$ ) exhibited an apparent ignition delay. Figure 6.20 shows the significant features of the tracks of  $177\text{-}250 \mu$  boron particles burning in air at one atmosphere pressure.

The most conspicuous aspect of the boron combustion in air was that the particles do not explode. Figure 6.21 shows a typical quenched specimen. The continuously changing color temperature of the tracks of many particles suggest a continuously rising particle temperature throughout the burning. The group of burning particles shown in Fig. 6.20 represents a comprehensive cross-section of boron particle combustion. There are represented in this figure nearly all types of combustion noted in Section 5.3. A peculiar characteristic of the boron particle tracks in Fig. 6.20 is that each of the specimens seems to reverse direction immediately prior to burnout. This phenomenon appears to be common to all particles which have achieved steady-state burning (see also Fig. 5.8). Time has not permitted an investigation of the cause of the phenomenon and no explanation is available at this time.

Examination of the quenched specimen in Fig. 6.21 shows that the particle surface was still somewhat irregular, as though it had become round by burning off the surface prominences rather than through bulk melting of the particle. On the other hand, smaller particles ( $\sim 50\text{-}100\mu$ ) obviously are spheroidized through bulk melting and even the largest particles, if quenched late enough in the burning process, were seen to be very smooth spheres.

Another notable feature is the thick ring-shaped accumulation of oxide on the quench plate next to the particle. This oxide ring is often thick enough to cast a shadow when illuminated by a microscope projection lamp at grazing incidence. The large diameter uniformly thin layer of smoke surrounding the particle is sufficiently hygroscopic that it will dissolve and become transparent (thus seeming to disappear) within a period of less than eight hours, leaving the boron particle and the thick inner ring. Nothing has yet been done to characterize these two apparently different types of oxide.

Track photographs which include the quench process indicated that burning boron particles take longer to cool than aluminum for example. Many burning particles were observed to hit the quench plate and bounce. Figure 6.22 shows that burning particles which hit the quench plate and immediately bounce and then impact the plate again do not leave the thick oxide ring just described at the site of the original impact. Depending on the time available for cooling between impacts bouncing particles may or may not leave a ring of oxide deposit at the final site.

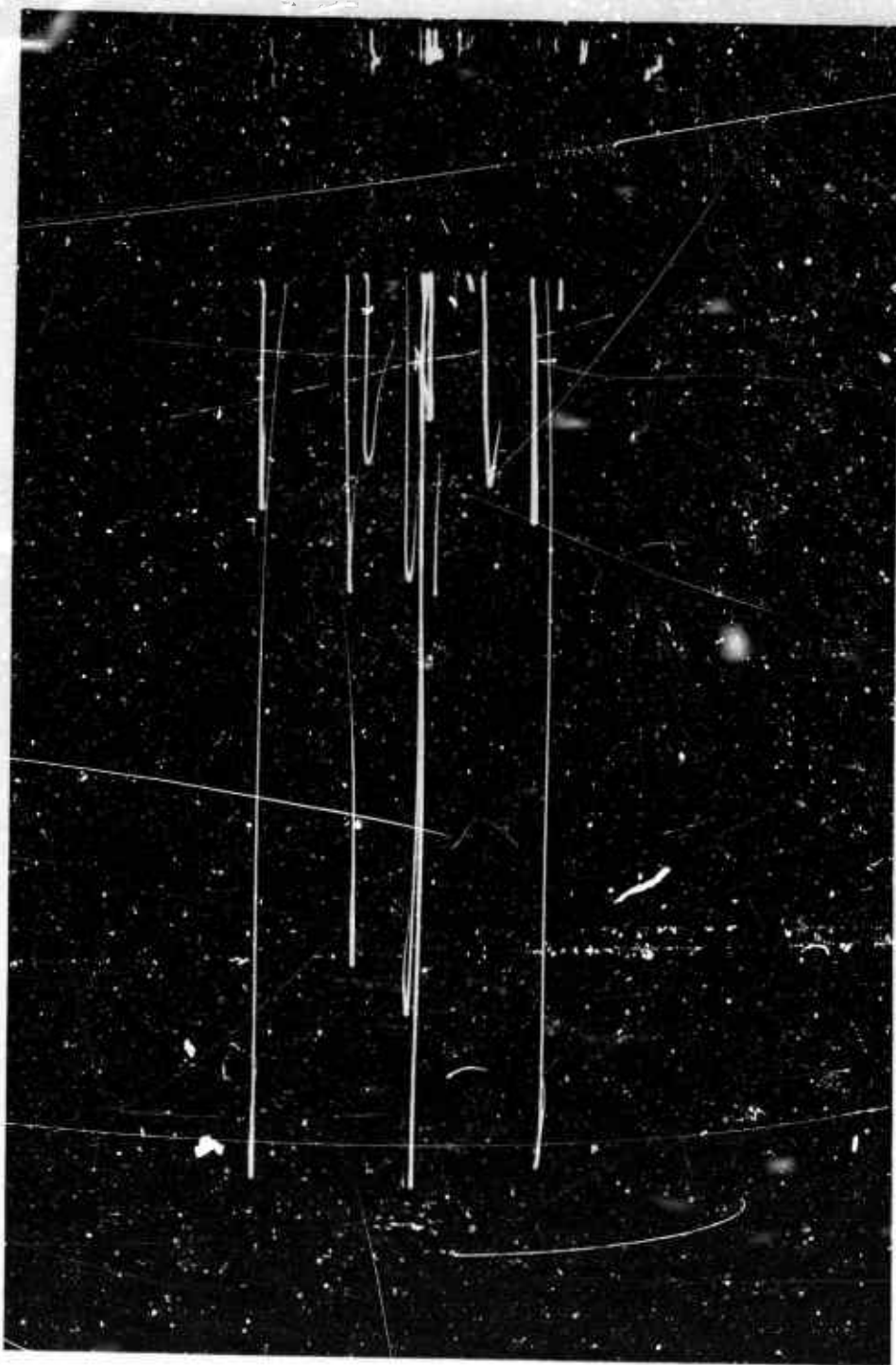


FIG. 6.20. Flash-Ignited Boron Particles (177-250  $\mu$  Screen Fraction) Burning in Ambient Air.

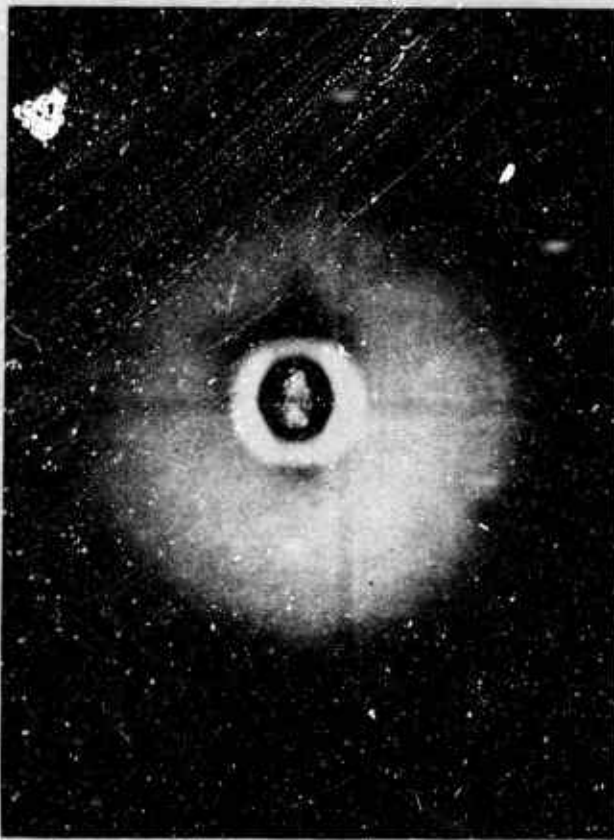


FIG. 6.21. Nominal 200  $\mu$  Boron Particle Quenched While Burning in Ambient Air. Xenon flash ignition. Note thick ring of oxide immediately adjacent to the particle.

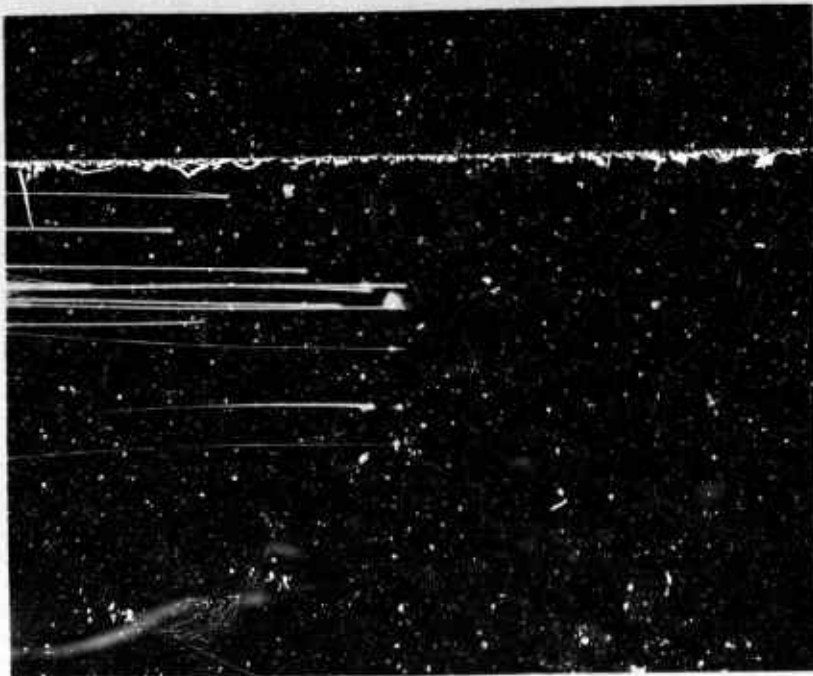
6.4.2. Flash-Ignited Boron Particles  
Burning in Oxygen-Argon Mixtures

While there appeared to be no significant difference in burning times, particles burned in 20/80 oxygen-argon appeared very much brighter than those burned in air. A 10/90 oxygen-argon mixture gave results which were qualitatively indistinguishable from air. As would be expected, increasing the concentration of oxygen in the atmosphere markedly increased the vigor of the reaction and greatly intensified the radiation from the particle.

Increasing the oxygen concentration to 30 mole percent led to a condition in which many particles exhibited what appeared to be a pronounced ignition delay. Such particles fell without radiating beyond the burnout point of others flashed at the same time, suddenly began to radiate intensely, and burned fiercely for a shorter time than their companions (see also Section 5.3).



(b)



(a)

FIG. 6.22 (a) Track Photograph Showing the Impact, Quenching and Bouncing of Some 177-250  $\mu$  Boron Particles Burning in Ambient Air, and (b) Quenched Boron Particle at Rest After Having Bounced From the Position of the Upper Smoke Cloud. Note particularly the absence of thick smoke ring at site of original impact and beginning of formation of a ring at final site. Smooth surface of particle quenched late in burning indicates boron was molten.

A limiting oxygen concentration was found below which combustion would not occur. Particles as small as 53-62  $\mu$  would not burn in a mixture containing 4.5% oxygen in argon at one atmosphere total pressure. Combustion of the boron failed to sustain itself at an oxygen concentration between 4.5 and 9%.

6.4.3. Flash-Ignited Boron Particles  
Burning in Carbon Dioxide

None of the boron particles employed in this study could be ignited in cold CO<sub>2</sub>. Particles as small as 53-62  $\mu$  and pressures as high as 4.4 atmospheres (64 psia) were tried unsuccessfully.

6.4.4. Flash-Ignited Boron Particles  
Burning in Pure Oxygen

The boron ignited readily and burned with great vigor in oxygen. The larger particles (177-250  $\mu$ ) were found to burn to completion about 60% faster than in dry air. Most of the boron particles burned out essentially while in the lamp area and the great quantities of boric oxide smoke generated in such a confined space prevented making measurements of particle burning times. Steps are being taken to solve this problem and the measurements will be repeated. Experiments in reduced pressures of pure oxygen are also planned.

6.5. DISCUSSION OF DROPLET FRAGMENTATION  
PROCESSES AND MECHANISMS

It has been pointed out earlier that, of the four metals studied, the burning droplets of aluminum, titanium and zirconium were found to explode, while those of boron did not. Nothing can be said at this time with regard to the importance of the phenomenon to practical metal burning systems except to note that results from propellant combustion tests in high pressure strand burning bombs have not shown fragmentation to be a prominent process. Additionally, the single particle burning experiments described in Section 6.1-6.4 in this report indicated that the process ceased for aluminum and was inhibited for both titanium and zirconium at elevated pressures. The phenomenon is, however, widespread in the combustion of metals at atmospheric and subatmospheric pressures and could be of considerable importance to the control or improvement of combustion efficiency in pyrotechnic or photoflash formulations which normally burn at reduced pressures common to high altitudes. The fragmentation phenomenon has attracted considerable attention in the metal combustion literature although little has been done other than to speculate concerning its origins. Considerable experience has been gained in this laboratory with burning and fragmenting metal particles. That experience now permits the definition of some necessary conditions for droplet fragmentation and makes possible the identification of the most probable mechanism for the phenomenon.

It will prove worthwhile to summarize briefly here the salient features of the combustion and/or explosion of the metals studied before proceeding to a discussion of mechanisms thought to be responsible for such features. The values of melting and boiling temperatures for selected metals and oxides found in Table 1.1 will be referred to in this discussion.

1. Aluminum burns primarily by a vapor transport process to a detached reaction zone, although a significant quantity of oxide-nitride or oxide-carbide product accumulates asymmetrically on the droplet following ignition. As burning progresses this oxide lobe tends toward encapsulation of the droplet.

Zirconium and titanium represent systems whose melting and boiling points are so high (very low vapor pressure) that they burn primarily by surface processes. Because the oxides and nitrides or other product species are soluble in the melt, original droplet symmetry is maintained throughout the burning.

Boron particles appear to begin combustion at a temperature below the melting point of boron. Boron has a negligible vapor pressure ( $\approx 10^{-5}$  atm) at its melting point and would thus be expected to burn by a surface process. Boron track photographs indicate progressively increasing droplet temperatures during burning. Once steady-state combustion is established the droplet remains free of oxide since the combustion temperature is greater than the oxide boiling point.

2. The time interval between the rise of the flash heating pulse and the explosion of droplets of Al, Ti and Zr was found to be a reproducible linear function of the droplet diameter. The time to explode was found to be roughly inversely proportional to applied pressure for these three metals. A pressure threshold existed, however (e.g., 4 atm for Al in air), beyond which particles refused to fragment.

3. Addition of nitrogen to nonexploding systems ( $O_2/Ar$ ) in percentages as low as 5-10% was sufficient to cause explosions. Removal of nitrogen from exploding titanium and zirconium systems caused explosions to become very feeble and sporadic.

4. Burning aluminum droplets appeared to be at least partially molten at the time of explosion in the flash experiment, while high ambient flame temperatures (2500-3000°K calculated) in the gas burner experiment would be expected to assure that all product residue would remain molten. Flash-ignited aluminum droplets gave evidence that the oxide had begun to solidify when they exploded in ambient air, but these same aluminum droplets did not explode in 20/80 oxygen-argon.

Fragments from flash-ignited titanium and zirconium droplets exploding in cold air suggest that the surface at least had begun to solidify (cf. Fig. 6.16, particularly wall collision) while those exploding in 20/80 oxygen-argon are totally molten.

The important conclusion is that the explosions can occur with or without a solid phase associated with the droplet, i.e., solidification is not a necessary condition for explosions.

5. The evidence for oxide solidification cited above and the pyrometric and spectroscopic measurement of droplet temperatures reported by Nelson for zirconium (Ref. 4) indicated that flash-ignited Al, Ti and Zr droplets burning in ambient air were capable of cooling during their fall, particularly just prior to explosion. Boron, which does not explode, and whose oxide is gaseous at the combustion temperature, on the contrary, appeared to increase in temperature during burning. The tracks of burning boron particles (177-250  $\mu$ ) seen in colored photographs characteristically were a dull red at initiation and progressed to dazzling white prior to burnout.

6. With only rare exceptions, most of the metal appears to have been consumed at the time of explosion. Measurements on flash-ignited aluminum particles quenched just prior to fragmentation in air indicated about 90% of the metal has been consumed. Nelson's gravimetric studies on zirconium showed that explosions occur at droplet compositions of  $ZrO_{1.25-1.96}$ .

7. Combustion of aluminum droplets was only marginally successful in cold carbon dioxide, while titanium and zirconium particles, once initiated, would not continue to burn and boron particles appeared not to ignite at all. No droplets exploded in  $CO_2$ .

8. As would be expected, all the metals burned appreciably faster in a pure oxygen environment. The combustion of Al, Ti and Zr in pure oxygen resulted almost exclusively in great quantities of small (~50  $\mu$ ) oxide spheres. The only exception was the formation of a small number of oxide balloons of a size equal to or greater than the original Al, Ti and Zr droplets.

The flash heating experiments indicated that the catastrophic fragmentation characteristic of Al, Ti and Zr burning in air was not common in pure oxygen.

Three different mechanisms for metal droplet fragmentations have been considered in the metal combustion literature. These will be discussed individually below along with applicable experimental evidence.

#### 6.5.1. Rupture of a Metal Vapor-Inflated Oxide Shell

This mechanism was originally proposed by Fassell, et al (Ref. 20) for the case of aluminum particle combustion to account for their observation of hollow translucent oxide spheres, fractured specimens of which sometimes contained tiny globules of unburnt metal, which were found in the residues from aluminum powder burning in torch flames. This mechanism envisions diffusion through a liquid oxide layer

surrounding the metal droplet as the rate-controlling step, and that metal boiling causes expansion of the oxide shell and accounts for the hollow translucent spheres. When forces due to the metal vapor pressure overcome the oxide surface tension forces, the shell is presumed to rupture resulting in the droplet explosion.

Since its formulation, considerable experimental evidence has accumulated which is contradictory to the predictions of this model. For example, Drew (Ref. 21) has shown that hollow oxide spheres may or may not be produced in all flames commonly employed, such condition being determined principally by flame stoichiometry (temperature), and further, that only about 30% of the original metal appears in the oxide balloon. Brzustowski (Ref. 22) has shown that predictions from the model of Fassell, et al, regarding product configurations are not supported by their own data. Prentice (Ref. 12) has shown conclusively that the oxide accumulates unsymmetrically on flash-ignited droplets subsequent to ignition and that complete encapsulation does not occur during burning, indicating that complete encapsulation is not a necessary condition for fragmentation.

Drew (Ref. 1) has shown that these hollow spheres are blown asymmetrically from the oxide lobe of the bilobate burning geometry and that fragmentation of the same droplet can follow such a bubble blowing event. Additionally, Prentice, Drew and Christensen (Ref. 13) have shown that the particle spinning and erratic trajectory is due to this particle dissymmetry. If the integrity of an oxide shell is maintained until the moment of fragmentation then it is difficult to visualize how a spherical droplet would experience the violently spinning, often erratic, trajectory seen prior to fragmentation in high speed motion pictures (Ref. 13). On the other hand, if the oxide shell bursts and the accompanying sudden release of vapor provides the propulsive force for particle spinning ( $10^4$  rev/sec) and translation (1000 cm/sec) then it is difficult to see how a second and later rupture in this skin can result in the catastrophic fragmentations which often hurl debris several thousand particle diameters away from the site.

#### 6.5.2. Superheating

In the classical case, a superheated system is one which has been heated above its boiling temperature, at that pressure, without ebullition. Fundamentally, this means that the heating has been done in such a fashion that equilibrium between the liquid and vapor has not been established and that the onset of ebullition, when it finally occurs, generally does so explosively. This, then, is one mechanism postulated for droplet explosion.

The superheating hypothesis has most often been applied to the case of aluminum droplet combustion (Ref. 23, 24, and 25) where it is imagined that accumulated oxide on the particle, acting as a site for heterogeneous reaction, exists at a temperature above the boiling point of the metal and feeds heat into the metal lobe in such a manner as to superheat the droplet.

Since actual measurements of the temperature of burning aluminum droplets have not been made use must be made of the values in Table 1.1 as upper limit temperatures. The boiling point of  $3800^{\circ}\text{K}$  for  $\text{Al}_2\text{O}_3$ , of course, is not a true boiling point but a decomposition temperature. The superheating hypothesis then requires that the oxide cap be at a temperature near  $3800^{\circ}\text{K}$  and that it has, as a result of heat transfer to the droplet through the contact interface, raised the metal lobe to a temperature in excess of  $2700^{\circ}\text{K}$ .

Such temperatures do not appear likely, however, since calculations by Kuehl (Ref. 26) using a modified form of the Brzustowski-Glassman analytical droplet burning model showed that the quasi-steady state solutions consistently converge on droplet temperatures significantly less than the aluminum boiling temperature. Additionally, the experimental evidence cited in Section 6.1.3 indicates that the particles need not be heating prior to explosion but are in some cases (Fig. 6.11) cooling. In the case of aluminum, Kuehl's work indicates that this cooling appears to closely approach the oxide freezing temperature of  $2315^{\circ}\text{K}$ .

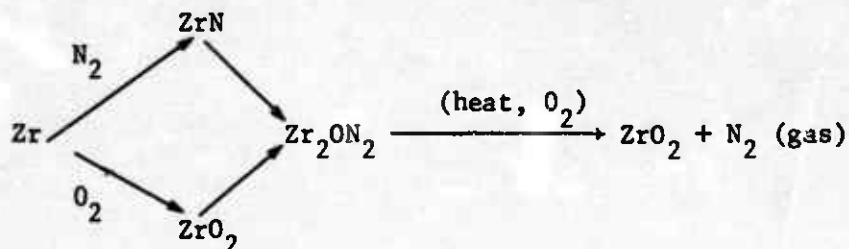
Calculations (Ref. 27) show that droplets of the sizes used here will not support large temperature gradients and that temperature equilibration will occur in the metal in times of the order of 1 ms. Thus, in the case of flash-ignited aluminum particles the metal droplet temperature would equilibrate with the temperature of the oxide globule immediately following its appearance at  $t/t_{\text{frag}} = 0.3$ . The system would then have to be in the unstable superheated state for the major portion of the burning time, typically 200-400 milliaoseconds.

A characteristic feature of superheated systems which is often overlooked in the application of this hypothesis to droplet explosions is the fact that such systems are exceedingly unstable toward nucleation. Such nucleation is characteristically a random phenomenon which is easily triggered by any number of miniscule perturbations. Therefore, it seems certain that the frothing of the oxide described earlier in this report or any one of the jetting events (seen in Fig. 5.4b of Ref. 1 from our earlier work), which are of such vigor as to impart a recoil to the particle, should have been sufficient to nucleate a superheated system, and yet they do not produce fragmentation. The reproducible linear relationship between explosion time and droplet diameter for all the metals studied here also militates against the superheating hypothesis.

### 6.5.3. Gas-Driven Fragmentations

As a result of his early work on the low pressure (0.1-0.85 atm) combustion of zirconium droplets Nelson (Ref. 4 and 28) postulated that the droplet explosions were gas-driven, and furthermore, that the gas was a permanent gas. He demonstrated that nitrogen, hydrogen, and possibly CO could cause droplet explosions in zirconium. The present work has duplicated Nelson's results with zirconium and  $\text{N}_2$  and has demonstrated a similar role for nitrogen in the fragmentation of burning aluminum droplets.

In brief, Nelson's mechanism proposes that the explosions are gas-driven by the forcing out of solution or expulsion from a melt of a permanent gas ( $N_2, H_2, CO$ ) which had been chemically combined with the zirconium early in the combustion but which had been liberated by disproportionation during the later stages. The process may be visualized as occurring in air by a reaction sequence like the following (unbalanced):



The free energy functions reported in the JANAF Thermochemical tables indicate that zirconium (also titanium and aluminum) is able to react simultaneously with both the nitrogen and oxygen in air at combustion temperatures to produce a nitride and an oxide. Once formed, these latter two then react to give an oxynitride of composition  $ZrO_xN_y$ . Oxynitrides are characteristically unstable in high temperature oxidizing environments and thus these species are only transitory intermediates. Nelson has argued that either by continued reaction or by droplet cooling the solubility of nitrogen in the particular ternary Zr - O - N system is exceeded and the resulting gas pressure explodes the droplet.

It should be emphasized that the foregoing description is an idealization and is therefore somewhat oversimplified. For example, the species ZrN,  $ZrO_2$  and  $Zr_2ON_2$  probably do not exist as such in the melt, but instead there is a range of Zr-O-N alloys formed as the oxidation progresses which precipitates these crystal phases when quenched.

Application of Nelson's mechanism to aluminum droplet explosions has been slow due to uncertainty about the formation and stability of aluminum nitride on the burning droplet surface. Only recently has systematic data on the formation and properties of aluminum oxynitrides become available which lends strong support to the hypothesis made here, that aluminum particle fragmentations arise as a result of similar processes to those cited by Nelson for zirconium combustion.

Long and Foster (Ref. 29) have shown that aluminum nitride is a refractory for aluminum at temperatures as high as  $2300^\circ\text{K}$ , which is nearly equal to the melting temperature of aluminum oxide. The sublimation temperature of AlN has recently been reported (Ref. 30) to be  $2673^\circ\text{K}$  and the JANAF Thermochemical Tables report a temperature of  $2790^\circ\text{K}$  for the point at which aluminum nitride decomposes thermally. This is seen from Table 1.1 to compare closely to the metal boiling point. Moreover,

since aluminum nitride decomposes to gaseous aluminum and molecular nitrogen, its thermal dissociation pressure would be expected to remain reasonably low when burning in air where the atmosphere is four-fifths nitrogen. Further, since the plot in Fig. 6.5 shows that aluminum burns slightly faster in air than in a mixture of 20% oxygen-argon it may be safely assumed that AlN will be formed and can survive on the metal droplet surface long enough to engage in reaction with the Al<sub>2</sub>O<sub>3</sub> forming there.

Long and Foster (Ref. 31) appear to have been first to demonstrate the possibility of condensed phase reaction between Al<sub>2</sub>O<sub>3</sub> and AlN to yield an oxynitride. They demonstrated that fusion of  $\alpha$  aluminum oxide containing a small amount of added aluminum nitride gave x-ray powder diffraction patterns similar to the  $\delta$ -alumina obtained from the calcination of alumina monohydrate in dry air. About 1% nitrogen (3% AlN) was adequate for complete conversion of the  $\alpha$ -phase to the  $\delta$ -phase.

LeJus (Ref. 32), and Leprince-Ringuet, LeJus and Collongues (Ref. 33) performed the synthesis and x-ray crystallographic study of the oxynitrides of aluminum. These investigators report the existence of three types of oxynitrides of the form Al<sub>10</sub>xN<sub>y</sub> containing respectively 30% Al<sub>2</sub>O<sub>3</sub> (oxynitride X), 67 to 86% Al<sub>2</sub>O<sub>3</sub> ( $\gamma$  oxynitride of the spinel type), and 95% Al<sub>2</sub>O<sub>3</sub> ( $\delta$  oxynitride of the  $\delta$ -alumina type).

These oxynitrides were synthesized by several different means. Most recently, Michel, Perez y Yorba, and Collongues (Ref. 34) have obtained the same aluminum oxynitrides by melting a mixture of Al<sub>2</sub>O<sub>3</sub> and aluminum in air with an induction heater. The strong similarity of their system to the one reported here suggests that the reaction product which accumulates on aluminum droplets burning in the presence of nitrogen is some aluminum oxynitride species of as yet undetermined composition. Studies reported elsewhere, particularly for the high temperature air oxidation of tantalum (Ref. 35), show that the formation of a metal oxynitride is responsible for the adherence of the oxide to the metal. This phenomenon appears to be general enough that a commercial process has been patented (Ref. 36) which utilizes nitrogen to improve the adherence of flame-plated refractories. The quenched specimens contrasted in Fig. 6.13 showing product accumulation on the droplet surface for burning in 20% oxygen-nitrogen (air) and no product accumulation for the specimen burned in 20% oxygen-argon are taken as indicative of the involvement of an aluminum oxynitride intermediate. Preliminary x-ray studies in this laboratory showed that the oxide formed on high purity aluminum wires heated to high temperature in pure oxygen was  $\alpha$  - Al<sub>2</sub>O<sub>3</sub>, while oxide debris from flash-ignited aluminum particles burning in air was provisionally identified as  $\delta$  - Al<sub>2</sub>O<sub>3</sub>. Further work on the x-ray characterization of intermediate species is needed and is being performed.

Additional evidence which appears directly related to the aluminum droplet burning studies is the work of Meyer (Ref. 37), who passed small granules of Al<sub>2</sub>O<sub>3</sub> and ZrO<sub>2</sub> through an argon plasma torch and found that

when these molten droplets were quenched in free-flight in air large hollow spheres were produced from the alumina, while the large teardrop sacs reported in Section 6.3 and elsewhere (Ref. 4) were produced by  $ZrO_2$ .

Meyer found that when melting the alumina granules in an argon plasma and cooling by air quenching pores were first formed in the droplet followed by considerable frothiness. The sequence of events in the froth development described by Meyer is virtually identical to that reported in Section 5, Ref. 1, for aluminum combustion in air. The degree of porosity and frothiness depends on both the nitrogen content of the gas (in cases where mixed argon-nitrogen plasma was used) and the length of the flight time through the air. Particles impacting a glass plate after traveling 20 cm in air result in droplet bursting very much like the gas-charged specimen of Drew's cited earlier (Ref. 1, page 54). Chromatographic analysis of crushed spheres disclosed molecular nitrogen in the contents. X-ray analysis of these specimens showed the presence of  $\gamma$ -alumina.

Decomposition of the labile oxynitride would be expected to begin with the accumulation of product on the aluminum droplet surface and the nitrogen thus liberated, plus some entrained aluminum vapor, would give rise to the frothiness in the oxide described in Section 6.1.2 and lead ultimately to fragmentation of the droplet.

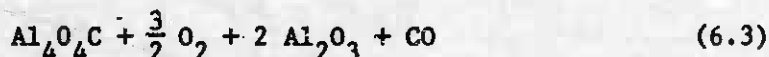
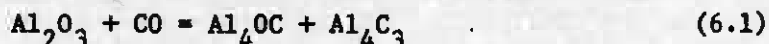
Explosion of aluminum droplets burning in a  $CO/O_2$  flame in the absence of nitrogen or water requires that a carbon-bearing species be sought as the agent providing the driving force for the fragmentation. It is unlikely that carbon dioxide will cause the explosion because flash-ignited aluminum droplets do not explode in  $CO_2$  and titanium and zirconium would not sustain combustion in that gas.

Various experimental studies have shown that carbon monoxide can also act in a role similar to nitrogen to produce internal pressures leading to bubble blowing or droplet fragmentation. Hollow spheres have been observed during the flame spraying of steels (Ref. 38) and attributed to carbon monoxide formed when atmospheric oxygen reacts with the carbon contained in the steel. It has been shown that during grinding on an abrasive wheel, sparks thrown from iron that contains more than 0.1% carbon will explode, while those formed from pure iron will not (Ref. 39). Hunger and Werner (Ref. 40) have shown thermodynamically that carbon monoxide released within such small iron droplets can provide gas pressure adequate to cause fragmentation.

A mechanism similar to the oxynitride mechanism of Nelson is proposed here to account for the explosion of aluminum droplets in burner flames (particularly  $CO/O_2$ ) and is based on the following experimental evidence.

Studies of the carbothermic smelting of aluminum (Ref. 41) have shown that aluminum oxycarbides, more volatile than metallic aluminum,

are readily formed in the presence of  $\text{Al}_2\text{O}_3$  and CO. These oxycarbides are volatile at temperatures as much as  $100^\circ\text{C}$  below the melting point of aluminum oxide. The equations listed below indicate likely reaction routes.



The tetraoxycarbide in Eq. 6.1 seems to be the favored oxycarbide under smelting conditions, although both species are unstable in the presence of excess oxygen.

The decarburization process (Eq. 6.3), yielding CO in the melt, could quite easily lead to jetting and aluminum droplet explosions in the manner demonstrated recently by Baker (Ref. 42) and Baker, et al (Ref. 43-44) for iron carbide droplets burning in oxygen. In that work on the decarburization of iron-carbon droplets in pure oxygen, carbon monoxide bubbles have been shown to nucleate in the droplet and CO pressures prior to droplet fragmentation as high as 50 atmospheres have been calculated (Ref. 45). Two results of that work are of particular interest: (1) very small quantities ( $\sim 0.5\%$ ) of carbon are required for fragmentation and (2) a linear relationship exists between the time required for fragmentation and the droplet diameter. Molten iron-carbon droplets containing 5% carbon falling through pure oxygen were found to exhibit what was referred to as a carbon "boil" as the carbon content was reduced. This so-called carbon "boil" possessed the characteristics of the phenomenon we have referred to as "jetting" with respect to aluminum combustion. When the carbon content was reduced to about 0.5% (through formation of CO) the droplets exploded.

Operation of the oxycarbide forming process during aluminum combustion would naturally be expected to yield aluminum vapor, gaseous oxycarbide and CO, all of which would make a contribution to the overpressure. Such a view is consistent with the experimental observation of oxidizable aluminum species present during venting or jetting through fumaroles formed in the product globule (see Fig. 6.7). Additionally, the flash of light and expansion of the droplet flame envelope associated with the "puff" event described in Section 6.1.2 (which is a noncatastrophic venting of overpressure) is also evidence for the presence of oxidizable aluminum species. This mechanism would predict that partially nitrated or carbided metals burning in pure oxygen or 20/80 oxygen-argon (normally nonfragmenting system) should be expected to explode. This point was checked in a very limited way as follows. Aluminum foils

were treated with a 5 wt. % solution of hydrocarbon grease (Apiezon N) in ether. Following evaporation of the solvent the foils were ignited by the flash lamp and allowed to burn in a mixture of 20% oxygen in argon. Particles treated with the grease exhibited spinning and fragmentation while untreated particles burn in this mixture without spin or fragmentation (Fig. 6.3). Nelson has observed such behavior for the combustion of zirconium droplets (Ref. 4).

The effect of hydrogen (or water) on the combustion of aluminum particles has been cited earlier (Ref. 1 and Section 6.1 of this report). Hydrogen has also been shown to be capable of playing a role in zirconium droplet explosions (Ref. 4). It was pointed out earlier that Drew was able to almost completely convert the product from aluminum powder burning in a hydrogen-oxygen flame into large hollow spheres (Ref. 21). The incidence of fragmentation is markedly reduced in this flame, perhaps as a result of the preferential shedding of most of the oxide in the form of both balloons and solid spheres (Fig. 4.10 and 4.11, Ref. 1). This suggests a decreased viscosity of the oxide attributable to its reaction with the water, making the whole oxide-metal system much more able to accommodate internal pressurization without violent rupture. Diamond and Drago (Ref. 46) and von Wartenburg (Ref. 47) have shown that when molten  $Al_2O_3$  and  $ZrO_2$  solidify in an atmosphere saturated with water vapor violent bubbling occurs, ostensibly due to either a marked decrease in the solubility of water on freezing or perhaps molecular hydrogen originating from decomposition reactions between water and the melt.

In conclusion, it can be stated that explosions or catastrophic fragmentation of burning metal droplets are gas-driven and this study suggests that for the case of aluminum particles metal vapor is a prominent constituent of the driving fluid with the major force provided by nitride-derived nitrogen for the case of combustion in air. Alternatively, oxycarbide-derived CO appears to be the working fluid for explosions in CO/O<sub>2</sub> flames. Final judgement is reserved, however, pending more thorough x-ray certification of the proposed intermediates. For aluminum droplet explosions to occur there must be an adherent oxide cap on the particle since explosions do not occur in the absence of a cap or if the adherence criterion is not met. The adherence of the oxide is an important aspect since fragmentation appears to be initiated in or under the cap. If the oxide is shed as a balloon, fragmentation does not ensue.

The fragmentation mechanism postulated by Nelson appears to account quite well for the bulk of the experimental evidence for titanium and zirconium although it does not adequately explain the ability of droplets of these two metals to burst (however feebly) in oxygen-argon mixtures. (Private communication with Dr. Nelson indicates that if zone-refined metals are used instead of the Reactor Grade employed here, the droplet bursting in O<sub>2</sub>/Ar can be eliminated).

Boron, the one specimen among those studied whose burning droplets did not explode is unique in several respects. The fact that the oxide

is insoluble in the metal and gaseous at combustion temperatures as well as the fact that the nitride melts at  $2600^{\circ}\text{K}$  and is therefore unlikely to survive on the surface at those temperatures precludes the occurrence of processes similar to those held responsible for droplet fragmentations in the other metals studied, and thus boron particles do not explode.

## 7. STATUS OF THE METAL COMBUSTION PROBLEM

This summary of the metal combustion problem is intended to point out those areas which seem to be adequately understood and to cite areas needing further research. By "adequately understood", it is meant that a qualitative understanding has been achieved. Where possible, experimental or theoretical approaches are suggested to resolve the areas of uncertainty.

Inasmuch as the metal combustion problem is an exceptionally complex interdisciplinary one, and further, since many different metals of varying characteristics are being investigated it is beyond the scope of this report to treat all possible or known cases. This discussion will concentrate on aluminum, since it has been studied the most extensively in this laboratory. Many remarks of a more general nature made concerning aluminum will also apply to metals collectively. Metals representing all presently known types of droplet combustion mechanism have been burned in this laboratory and such experience provides a broad perspective with which to make judgments concerning the state-of-knowledge.

### 7.1. PREIGNITION-AGGLOMERATION

The details of the physical process seem to be adequately documented (see Section 3) for the simple case of the agglomeration of aluminum particles in oxygen-containing environments. Other metals known to agglomerate in propellant matrices, notably beryllium, have not been studied in this laboratory. Agglomeration of metal particles has not yet been studied with high heating rates approximating those in rocket combustion nor has the process been studied in the complex oxidizing atmospheres found in propellant combustion. Research within these areas would appear to warrant early consideration.

A number of approaches have been suggested previously to prevent agglomeration, including use of fluxing agents, alloying, surface coating and increasing the heating rate of the particles. Most of these suggestions have some merit, but very little has been done to study them in a systematic way. Since the work described in Section 3 of this report indicates that agglomeration ensues immediately following melting of the metal, it seems that anything which would shorten the time interval from metal melting to particle ignition would be very helpful. The time constants of these processes may also exert a controlling influence on the processes governing the metal's effect on propellant combustion instability.

Additionally, any surface coating ( $\leq 1\%$  of the particle diameter) which would not fracture and allow bridge-building by molten metal when aluminum particles contacted each other during the transition to ignition would minimize the agglomeration.

## 7.2. IGNITION

To make a distinction between preignition and ignition may seem arbitrary and artificial, particularly in view of the discussion given in Section 4; however, it serves a useful function in that it focuses attention on two different but equally important aspects. On the one hand, the most important phenomenon in the preignition phase is agglomeration, while an ignition study must deal with the establishment of ignition limits as a function of the preignition condition of the particle. No systematic study of metal particle ignition has yet been done and this would seem to be both an important next step as well as a logical extension of the agglomeration studies currently under way.

## 7.3. QUASI-STEADY COMBUSTION

The qualitative aspects of the combustion of particles of many metals can be satisfactorily explained. The extent of quantitative understanding is poor. Routine prediction of burning rates as a function of metal type, particle size and oxidizer pressure is not yet possible.

The means by which oxide or other product accumulates on aluminum droplets during burning is uncertain. The term "back-diffusion" has been applied to indicate a mechanism for oxide transport to the droplet surface. Some authors have held this to mean diffusion of gaseous oxide ( $\text{Al}_2\text{O}_3$ ) from the detached reaction zone back to the droplet followed by condensation, while others have meant the diffusion of gaseous suboxides of aluminum from the "flame front" back to the droplet surface where further reaction with oxidizer yielded the condensed stoichiometric oxide. In any event, the actual process is unknown and the need to clarify the concept of back-diffusion is important.

Researchers have begun to re-evaluate the arguments about metal combustion mechanisms and are beginning to question mechanisms formerly felt to be well established. Examples include the low pressure combustion of calcium and magnesium. Recent investigations in various laboratories have cast doubt on the heterogeneous mechanisms usually invoked and the question of homogeneous or heterogeneous kinetics remains uncertain. Increasing attention is being given to excited peroxides, metal dimers (or higher polymers) and three-body collisions as intermediate stages in these low pressure combustion studies. The lack of accurate knowledge of reaction intermediates in the combustion of most metals has seriously hampered development of the kinetics of the relevant processes. More explicitly, the question of whether the reactions are kinetics-limited or transport-limited cannot be answered unequivocally.

A problem of perhaps overriding importance to the quasi-steady combustion (particularly of aluminum) has to do with the part played by condensation. Next to nothing is known about the mechanics of the process in metal combustion nor about its influence on the course or rate of the overall reaction. It would appear that the concept of thermophoresis should receive some consideration since there appears to be some experimental evidence for the existence of the process in aluminum burning studies; e.g., the dark zone surrounding the oxide sphere in the smoke field in Fig. 5.7 of this report. Thermophoresis may be very important to the movement and condensation of the oxide.

#### 7.4. TERMINAL STAGE OF COMBUSTION

Particles of some metals terminate combustion by a catastrophic fragmentation. Flash heating experiments in this laboratory indicate that fragmentation is suppressed at elevated pressures. Since fragmentation of metal particles in high pressure propellant strand burning studies has not been reported the process is probably also suppressed during rocket motor combustion. The phenomenon might be used to advantage in practical metal burning systems operating near atmospheric pressure to increase the combustion efficiency if made to occur shortly following ignition. This might be done by prenitriding or carbiding the metals of interest.

#### 7.5. THERMODYNAMICS-HIGH TEMPERATURE CHEMISTRY

High-temperature chemistry and thermodynamics are both disciplines which are vital to quantitative understanding of metal combustion. This report has indicated something of the complicated nature of the chemistry of the quasi-steady combustion of several metals, from which it can be seen that a great need exists for accurate phase diagram data on high temperature metal-oxygen-nitrogen-carbon systems. Water is known to alter the combustion of many metals; however, little is known beyond the semi-quantitative or qualitative effect on particle burning time and no systematic study of the kinetics or mechanism of the reaction at droplet combustion temperatures has been reported.

Until recently researchers have been guided by the postulate that "steady-state" metal combustion temperatures were limited to the boiling points of the respective metal oxides. The intent of the postulate, which has been subject to misinterpretation, was that such boiling temperatures should be understood to be upper limit temperatures. In practice, such temperatures (Table 1.1) have come to be accepted and quoted as the actual steady-state combustion temperatures. The need is now apparent for a re-examination of the whole concept of oxide "boiling point". Many values reported are not in fact "boiling points" but are instead decomposition temperatures whose value depends on the identity and partial pressure of species above the melt. Important questions about the composition of the

condensed phase product in metal particle combustion remain to be answered and there is a great need for research in the area of vaporization and decomposition of oxide species and high temperature phase diagrams of metal-oxygen-nitrogen-carbon systems.

#### 7.6. COMBUSTION MODELING

The Brzustowski-Glassman droplet burning model and its later modifications have proved of considerable value in developing the understanding of metal particle combustion, although the models do not treat surface burning metals like titanium and zirconium whose combustion products are soluble in the droplet. Additionally, these models have not been elaborated to satisfactorily accommodate accumulation of product on the droplet surface (aluminum and beryllium). Existing particle combustion models are restricted to treating the case of spherical symmetry while the combustion of particles of some metals is demonstrably non-symmetric (notably aluminum). With but a scant exception, modeling studies have been confined to a qualitative description, in general terms, of the quasi-steady droplet combustion while giving insufficient attention to predicting particle burning times or other quantitative data.

Theoretical descriptions of metal droplet combustion have thus far failed to come to grips with the question of the effect of oxide condensation on the course of combustion. An exception is the treatment of boron given in Appendix A, but this is an unusual case in which the oxide is gaseous at temperatures below the "metal" melting point.

#### 7.7. SUGGESTIONS FOR FUTURE WORK

To recapitulate, the areas requiring the greatest research effort in the near future are the following.

1. Agglomeration. Significant first steps have been taken toward understanding the mechanics of the process. A study of the effect of surface coating which would contain the molten metal until ignition appears to offer the greatest chance for success in reducing agglomeration. On the other hand, coatings or alloys might be developed which would alter the surface in such a way as to substantially lower the metal particle ignition temperature and thus reduce agglomeration.

2. Ignition. Experiments designed to establish ignition requirements as a function of the nature and extent of surface pre-oxidation or other coating are necessary. Flash heating experiments on single particles can be used to establish threshold ignition criteria for cases of variable surface oxidation, surface coating, oxidizer type and incident flux.

3. Quasi-Steady Combustion. Reaction kinetics, oxide condensation and transport processes are the areas in greatest need of study. The difficult problem of chemical kinetic studies of metal combustion systems might be profitably approached by use of the combined techniques of molecular beams and mass spectrometry. Such an experimental approach would permit control and identification of reactants and intermediates including polymeric metal species. In this experiment the geometry of the reaction zone can be well described and spectroscopic spatial resolution of the reaction could be employed to study the kinetics. Concentration of reactants could be controlled at levels which would maintain oxide concentrations within tolerable levels to permit study of the condensation processes by laser light scattering. Supporting research on refractive indices of refractories would probably have to be undertaken.

No systematic studies of metal particle combustion in halogen or mixed oxygen-halogen oxidizers have been undertaken to date. Further, the effect of water on the rates and mechanisms of particle combustion has not been adequately characterized. An experimental apparatus is newly available in this laboratory which incorporates a pulsed infrared laser (1.06  $\mu$ ) and an electrostatic particle levitator which will be used to conduct single metal particle combustion experiments in halogenated oxidizers as well as wet gases in the near future.

4. Terminal Stage of Combustion. There is no pressing need at present for further research in this area. The termination is usually determined by events occurring early in combustion.

5. High-Temperature Chemistry. More work is necessary on the thermodynamics and phase diagrams of high temperature metal-oxygen-carbon-nitrogen systems. Metal droplet burning temperatures and reaction kinetics will remain unknown or uncertain until reliable experimental information is gained on the vaporization-decomposition of metal oxides as well as the composition of the condensed phase in these systems. Such experiments are exceedingly difficult to perform because of sample contamination by container materials at high temperatures ( $> 2000^{\circ}\text{K}$ ). Nonetheless, some very valuable research is being done in this area and it should be supported at a greater level and with emphasis on systems of interest to metal combustion.

6. Droplet Combustion Modeling. The need is apparent for theoretical studies to devote greater effort to cases of particle combustion not possessing spherical symmetry. Oxide condensation and transport in the reaction zone should receive more realistic treatment.

Finally, more quantitative experiments in the future are necessary if the above requirements are to be satisfied. The increasing use of experimental techniques providing close control over relevant variables such as the latest techniques employing pulse heating (flash lamps, lasers) is an encouraging sign.

Appendix A<sup>3</sup>A COMPUTATIONAL MODEL FOR THE STUDY OF BORON PARTICLE  
COMBUSTION AT LOW ENVIRONMENTAL TEMPERATURES

In an attempt to supplement the experimental studies of boron combustion, a computational model has been developed. The model has been conceived with considerable flexibility to investigate otherwise unobservable details of the combustion employing a steady-state, stagnant-film approximation. Except for minor variations necessitated by the peculiarities of the specific application, the approach draws heavily from combustion models developed by Coffin and Brokaw (Ref. 48) and by Brzustowski and Glassman (Ref. 8). For brevity in presentation, the reader is referred to Ref. 48 and 8 for specific discussion of the origin of relations which have been used. Spherical symmetry has been assumed throughout.

## GOVERNING EQUATIONS

For gaseous specie  $j$ , its mole fraction is given by  $x_j$  and its radial flux in moles/second given by  $W_j$ . Since the temperatures of interest are relatively low, only three gaseous species are considered: an inert,  $j = 1$ ;  $O_2$ ,  $J = 2$ ; and  $B_2O_3$ ,  $j = 3$ . Where condensed  $B_2O_3$  is considered, its flux in moles/second is denoted by  $W_3^c$ . By its definition as an inert,  $W_1 = 0$ . If  $W_B$  is the consumption rate of boron in moles/second under steady-state burning conditions  $W_2 = -3/4 W_B$  and  $W_3 + W_3^c = 1/2 W_B$ .

For the gaseous species, their mole fractions are related to their fluxes through the diffusion equations

$$\sum_{j=1}^3 (x_j W_i - x_i W_j) / \beta_{ij} = dx_i / du \text{ for } i = 2, 3 \quad (A-1)$$

(see Ref. 48, Appendix D). Here  $\beta_{ij} = 4 \pi D_{ij} P / RT$  where  $D_{ij}$  are the binary diffusion coefficients for species  $i$  relative to  $j$ ,  $P$  is the total pressure,  $R$  the gas constant,  $T$  the absolute temperature, and  $u$  is the

<sup>3</sup>Contributed by R. H. Knipe of the Research Department.

reciprocal distance from the center of the particle. Since essentially qualitative information is desired from the model, it is assumed that all  $\beta_{ij} = \beta$ . Where the condensed phase is considered as droplets detached from the particle surface, it is assumed that the droplets move with the bulk gas velocity  $v = -u^2(D/x_1)dx_1/du$  (Ref. 8).  $(D/x_1)dx_1/du$  is evaluated from Eq. A-1 with  $i = 1$ , whence  $v = -u^2RT(W_B/4 + W_3^2)/4\pi P$ . Denoting the gross density of condensed  $B_2O_3$  in the region around the particle in moles/cc by  $\rho_3^*$ ,  $W_3^2 = 4\pi\rho_3^* v/u^2$  or the bulk gas velocity is

$$v = \frac{-u^2 W_B / 16\pi}{(P/RT + \rho_3^*)} \quad (A-2)$$

The negative sign indicates a velocity towards the particle as implied by the stoichiometry of the combustion. As a consequence, it is implied that  $B_2O_3$  droplets which are formed by condensation will be swept by the bulk gas motion towards the surface until they evaporate or reach the surface. While the conclusion is not a consequence of the steady-state model, it puts a severe limitation on the steady-state model in low temperature environments. In particular, where condensation of the product takes place at some distance from the particle, the condensed product will either be swept to the surface, or evaporate, diffuse outward and recondense. In either case  $B_2O_3$  will collect in the neighborhood of the particle. If this collection is on the particle surface, the burning rate will be a function of depth of the film collected. If the collection is in a fog surrounding the particle, the situation will be similar to the fog collection around aluminum particles. As in the case in aluminum particle combustion, the fog would be at a temperature near the boiling point of the oxide, but differing from the aluminum combustion in that the combustion reaction occurs in a high temperature region on or at least nearer the particle surface.

In order to investigate some aspects of the behavior of the condensed phase the kinetic aspects of the evaporation and condensation of  $B_2O_3$  in the fog have been considered, though only in a crude way. In this model, nuclei are introduced at a variable distance from the particle surface and allowed to grow or evaporate at the Langmuir rate, specifically neglecting any effect of particle size on evaporation or condensation rate. Where  $\tau$  is the radius of a fog particle,  $n$  is the number of particles per unit volume and  $\rho_3$  is the density of  $B_2O_3$  in the particle,  $\rho_3^* = n\rho_3 (4\pi\tau^3/3)$ . Assuming the fog particles to be moving with the bulk velocity as they evaporate or grow, the dependence of the particle radius on reciprocal distance is given by  $d\tau/du = \gamma (P_T - P_{x_3})/u^2\rho_3 v\tau^2$ . For  $B_2O_3$ ,  $\gamma = 5.32$  times the accommodation coefficient (Ref. 48) and  $P_T$  is the equilibrium vapor pressure at temperature  $T$ . It is assumed that the nucleation of the fog is localized, so that where there is fog, the flux of nuclei is given by  $f = 4\pi n v/u^2$ , a constant value which is less than 0 since  $v$  is negative. Using Eq. A-2 for  $v$ ,  $n = -(fP/RT)/(W_B/4 + 4\pi f\rho_3\tau^3/3)$ , and

$$d\tau/du = -(\gamma/u^4) (P_T - P_{X_3}) (4\pi P/\rho_3 RT^{3/2}) / (W_B/4 + 4\pi f\rho_3 \tau^3/3) \quad (A-3)$$

In the steady-state approximation the enthalpy transport is given by

$$\sum_{i=1}^3 W_i H_i + W_3 H_3' + 4\pi k dT/du = W_B H_B^S$$

where  $H_1$  is the enthalpy per mole of gaseous species 1,  $H_3'$  is the enthalpy per mole of condensed  $B_2O_3$ ,  $k$  is the composite thermal conductivity of the gaseous medium and  $H_B^S$  is the enthalpy of the boron fuel at the surface temperature  $S$ . Here it is implicitly assumed that the whole of the boron particle, including any surface oxide film, is at the surface temperature. Substituting for the particle fluxes and considering  $T$  as the independent variable,

$$du/dT = 4\pi k / [W_B (H_B^S + 3/4 H_2 - 1/2 H_3) + 4\pi L f \rho_3 \tau^3/3] \quad (A-4)$$

where  $L$  is the heat of vaporization of  $B_2O_3$ . Based on a numerical study of data from the JANAF Thermochemical tables,  $Q = H_B^S + 3/4 H_2 - 1/2 H_3$  can be expressed to an accuracy of better than 0.5 kcal per mole by

$$Q = 98175 + 6.64S - 4.88T \text{ for } 800 \leq S \leq 2300 \text{ \& } 400 \leq T \leq 1400 \quad (A-5a)$$

$$Q = 92225 + 6.64S - 5.57T \text{ for } 800 \leq S \leq 2300 \text{ \& } 800 \leq T \leq 3300 \quad (A-5b)$$

$$Q = 102175 + 7.30S - 4.88T \text{ for } 2500 \leq S \leq 4000 \text{ \& } 400 \leq T \leq 1400 \quad (A-5c)$$

$$Q = 102865 + 7.30S - 5.57T \text{ for } 2500 \leq S \leq 4000 \text{ \& } 800 \leq T \leq 3500 \quad (A-5d)$$

or for a particular surface temperature  $S$ , by  $Q = H - cT$ .

For the two reactive gas phase species, Eq. A-1 becomes

$$\beta dx_2/du = -3/4 W_B + x_2 (1/4 W_B + 4\pi f\rho_3 \tau^3/3) \quad (A-6a)$$

$$\beta dx_3/du = 1/2 W_B - 4\pi f\rho_3 \tau^3/3 + x_3 (1/4 W_B + 4\pi f\rho_3 \tau^3/3) \quad (A-6b)$$

Considering  $T$  as the independent variable, Eq. A-6a becomes

$$dx_2/dT = \frac{-3 + x_2 (1 + 16\pi f\rho_3 \tau^3/3W_B)}{\delta[4(H - cT) + 16\pi L f\rho_3 \tau^3/3W_B]} \quad (A-7a)$$

where  $\delta = DP/kRT$  is insensitive to changes in temperature and pressure (Ref. 48, Appendix E). Similarly

$$dx_3/dT = \frac{2 - 16\pi Lf\rho_3\tau^3/3W_B + x_3(1 + 16\pi f\rho_3\tau^3/3W_B)}{\delta[4(H-cT) + 16\pi Lf\rho_3\tau^3/3W_B]} \quad (A-7b)$$

$$dt/dT = \frac{-16\pi k\gamma(P_T - P_{x_3})(16\pi P/\rho_3RT)^{3/2}}{W_B^2[1 + 16\pi f\rho_3\tau^3/3][4(H-cT) + 16\pi Lf\rho_3\tau^3/3W_B]u^4} \quad (A-7c)$$

In principle, Eq. A-4 and A-7a, b, c and d describe the steady-state combustion of boron within the limitations of the various approximations that have been introduced. Both Ref. 8 and 48 have used the approximation that  $k$  (the thermal conductivity) was some constant mean value. This is certainly reasonable where only conditions at the endpoints of the integrator are of interest. Since intermediate distances were of particular interest in this investigation, the conventional approximation  $k = cT^\lambda$  has been employed.

The large number of parameters can be conveniently combined for parametric variation by defining

$$z = \frac{u W_B}{16\pi\alpha} \quad (A-8a)$$

as the measure of reciprocal distance,

$$\omega = \tau \left(\frac{\rho_3 R\alpha}{\gamma}\right)^3 \left(\frac{16\pi}{PW_B}\right)^2 \quad (A-8b)$$

as the measure of fog particle radius, and

$$-Y = \frac{16\pi f}{3W_B\rho_3} \left(\frac{\gamma}{R\alpha}\right)^3 \left(\frac{PW_B}{16\pi}\right)^6 \quad (A-8c)$$

as the measure of fog particle flux. With these definitions, Eq. A-4 becomes

$$\frac{dz}{dt} = \frac{T^\lambda}{[4(H-cT) - LY\omega^3]} \quad (A-9a)$$

and Eq. A-7a, b and c become

$$\frac{dx_2}{dT} = \frac{x_2(1-Y\omega^3) - 3}{\delta[4(H-cT) - LY\omega^3]} \quad (\text{A-9b})$$

$$\frac{dx_3}{dT} = \frac{x_3(1-Y\omega^3) + 2 - \omega^3}{\delta[4(H-cT) - LY\omega^3]} \quad (\text{A-9c})$$

$$\frac{d\omega}{dT} = \frac{(x_3 - K)T^{\lambda-3/2}}{[1-Y\omega^3][4(H-cT) - LY\omega^3] z^4} \quad (\text{A-9d})$$

where  $K = P_T/P$  is the ratio of the  $B_2O_3$  vapor pressure to the ambient pressure. Thus, as far as the numerical solution of these equations is concerned there are three parameters,  $\delta$ ,  $\lambda$  and  $Y$ , for which accurate values are not readily available.

In the absence of a condensed phase,  $Y = 0$ , Eq. A-9a-d are analytically soluble. These solutions are  $x_2 = C_2/(H-cT) \frac{1}{4\delta c} + 3$ ,  $x_3 = C_3/(H-cT) \frac{1}{4\delta c} - 2$  and  $z = C_z + (T^\lambda/4c) Z(\frac{cT}{H}, \lambda)$ , where  $C_2$ ,  $C_3$  and  $C_z$  are constants related to the boundary conditions and

$$Z(y, \lambda) = \frac{y}{\lambda+1} + \frac{y^2}{\lambda+2} + \frac{y^3}{\lambda+3} + \dots$$

for  $y < 1$ . For the problem at hand  $cT/H$  is considerably less than 1 and the power series for  $Z$  is rapidly convergent.

Where there is a  $B_2O_3$  fog present, Eq. A-9a-d have been integrated numerically using a straightforward trapezoidal integration. Where  $Y$  is sufficiently small for the steady-state solution to be meaningful, this integration technique has been accepted as accurate.

The boundary conditions at  $z = 0$ , ( $r = \infty$ ) are  $x_2$  equal to the ambient mole fraction of oxygen,  $T$  equal to the ambient temperature, and  $x_3 = 0$ . For the numerical integration  $\omega$  can be set at an arbitrary value at some predetermined temperature  $T_c$  where the numerical integration is started. From ambient temperature to  $T_c$  the analytical solutions are used. Two surface boundary conditions have been explored: clean surface, where the surface is characterized by the vanishing of  $x_2$ ; and, secondly, a surface film of oxide where the surface is characterized by a net Langmuir evaporation rate of oxide given by  $W_3$ , again ignoring the effect of particle radius on the evaporation rate. It is only with the latter boundary condition that the particle radius enters explicitly into the solution.

If  $z_0$  is that value of  $z$  corresponding to the particle radius, the boundary condition is

$$z_0^2 = \frac{\gamma W_B P (K - X_3)}{16\pi\alpha^2 T^{3/2} (2 + Y\omega^3)}$$

Defining  $R^* = \alpha/\gamma Pr_0$  where  $r_0$  is the particle radius, and

$$R^* = (K - X_3)/z_0 T^{3/2} (2 + Y\omega^3) \quad (\text{A-10})$$

measures that value of reciprocal radius for which the evaporation rate would just equal the production rate of surface oxide. It should be noted that  $z_0$  appearing in Eq. A-10 is the measure of the burning rate which from Eq. A-8a is  $W_B = 16\pi\alpha z_0 r_0$ . It is implicit in the use of this boundary condition that there be a surface film of oxide which limits the burning rate to this value.

## REFERENCES

1. U. S. Naval Ordnance Test Station. Aluminum Particle Combustion Progress Report, 1 April 1964-30 June 1965, by the Metal Combustion Study Group. China Lake, Calif., NOTS, April 1966. (Technical Progress Report 415, NOTS TP 3916.)
2. Nelson, L. S., and N. L. Richardson. "The Use of Flash Heating to Study the Combustion of Liquid Metal Droplets," J PHYS CHEM, Vol. 68 (1964), pp. 1268-70.
3. Nelson, L. S., and J. L. Lundberg. "Heterogeneous Flash Initiation of Thermal Reactions," J PHYS CHEM, Vol. 63 (1959), pp. 433-36.
4. Sandia Corporation. The Combustion and Explosion of Zirconium Droplets Ignited by Flash Heating, by L. S. Nelson. Albuquerque, N. M., SANDIA, January 1966. (Report No. SC-RR-65-569.)
5. Kuebler, N. A., and L. S. Nelson. "Radiant Energies and Irradiances of Capacitor Discharge Lamps," OPT SOC AMER, J, Vol. 51 (1961), pp. 1411-16.
6. Wendlandt, W. W. Thermal Methods of Analysis. New York, Interscience, 1964. Chapter V, pp. 132-270.
7. Crump, J. E. "Aluminum Combustion in Composite Propellants," in 2nd Combustion Conference, Interagency Chemical Rocket Propulsion Group, comp. and ed. by Chemical Propulsion Information Agency. Silver Spring, Md., CPIA, May 1966. CPIA Publ. No. 105, Vol. 1, pp. 321-29.
8. (a) Brzustowski, T. A. "Vapor-Phase Diffusion Flames in the Combustion of Magnesium and Aluminum" (Ph.D. dissertation, Princeton University, 1962).  
(b) Brzustowski, T. A., and I. Glassman. "Vapor-Phase Diffusion Flames in the Combustion of Magnesium and Aluminum: I. Analytical Developments," in Heterogeneous Combustion, Progress in Astronautics and Aeronautics, ed. by H. G. Wolfhard, I. Glassman, and L. Green, Jr., New York, Academic Press, 1964. Vol. 15, pp. 75-158.
9. Markstein, G. H. "Combustion of Metals (A Survey)," AMER INST AERONAUT ASTRONAUT J, Vol. 1 (1963), pp. 550-62.

10. Princeton University. Heterogeneous Ignition of Metals: Model and Experiment, by A. M. Mellor. Princeton, N. J., 1967. (Aerospace and Mechanical Sciences Report #816.)
11. Talley, C. P. "The combustion of Elemental Boron," in Progress in Astronautics and Rocketry: Solid Propellant Rocket Research, ed. by M. Summerfield. New York, Academic Press, 1960. Vol. 1, pp. 279-85.
12. Prentice, J. L. "On the Combustion of Single Aluminum Particles," COMBUST AND FLAME, Vol. 9 (1965), pp. 208-10.
13. Prentice, J. L., C. M. Drew, and H. C. Christensen. "Preliminary Studies of High-Speed Photography of Aluminum Particle Combustion in Flames," PYRODYNAMICS, Vol. 3, Nos. 1-2 (1965), pp. 81-90.
14. Marshall, R. L., G. L. Pellett, and A. R. Saunders. "An Experimental Study of the Drag Coefficient of Burning Aluminum Droplets," in 3rd Combustion Conference, Interagency Chemical Rocket Propulsion Group, comp. and ed. by Chemical Propulsion Information Agency. Silver Spring, Md., CPIA, February 1967. CPIA Publ. No. 138, Vol. 1, pp. 125-30.
15. Smith, S. R., and A. S. Gordon. "Reactions in Hydrocarbon Diffusion Flames: The Paraffin-Candle Flame," J CHEM PHYS, Vol. 22 (1954), pp. 1150-51.
16. Smithells, C. J. Metals Reference Book, 3rd ed. Washington, D. C., Butterworths, 1962. Vol. 2, p. 577.
17. Kirk, R. E. and D. F. Othmer, eds. Encyclopedia of Chemical Technology. New York, Interscience Encyclopedia, 1962. p. 346.
18. Wählbeck, G. P. and P. W. Gilles. "Dissociation Energy of TiO(g) and the High-Temperature Vaporization and Thermodynamics of the Titanium Oxides. II. Trititanium Pentoxide," J CHEM PHYS, Vol. 46 (1967), pp. 2465-73.
19. Nelson, L. S. "Combustion of Metal Droplets Ignited by Flash Heating," in Eleventh Symposium (International) on Combustion. Pittsburgh, Pa., Combustion Institute, 1967. Pp. 409-16.
20. Fassell, W. M., C. A. Paetz, D. L. Hildenbrand, and R. P. Sernka. "The Experimental Nature of the Combustion of Metallic Powders," in Progress in Astronautics and Rocketry: Solid Propellant Research, ed. by M. Summerfield. New York, Academic Press, 1960. Vol. 1, pp. 259-69.
21. Drew, C. M., "Some Further Comments on the Paper 'Estimating Aluminum Particle Combustion Kinetics,'" COMBUST AND FLAME, Vol. 9 (1965), pp. 205-8.

22. Brzustowski, T. A. "Comments on the Paper 'Estimating Aluminum Particle Combustion Kinetics,'" COMBUST AND FLAME, Vol. 8 (1964), pp. 339-40.
23. Friedman, R., and A. Maček. "Combustion Studies of Single Aluminum Particles," in Ninth Symposium (International) on Combustion. New York, Academic Press, 1963. Pp. 703-12.
24. Gordon, D. A. "Combustion Characteristics of Metal Particles," Progress in Aeronautics and Astronautics: Solid Propellant Rocket Research, ed. by M. Summerfield. New York, Academic Press, 1960. Vol. 1, pp. 271-78.
25. Christensen, H. C., R. H. Knipe, and A. S. Gordon. "Survey of Aluminum Particle Combustion," PYRODYNAMICS, Vol. 3 (1965), p. 91.
26. Kuchl, D. K. "Ignition and Combustion of Aluminum and Beryllium," AMER INST AERONAUT ASTRONAUT J, Vol. 3 (1965), pp. 2239-47.
27. Beal, J. L., W. R. Brown, and F. A. Vassallo. "Oxidation and Explosion of Drops of Molten Zirconium Metal," PYRODYNAMICS, Vol. 3 (1965), pp. 135-60.
28. Nelson, L. S. "Combustion of Zirconium Droplets Ignited by Flash Heating," PYRODYNAMICS, Vol. 3 (1965), pp. 121-34.
29. Long, G., and L. M. Foster. "Aluminum Nitride, a Refractory for Aluminum to 2000°C," AMER CERAM SOC, J, Vol. 42 (1959), p. 53.
30. Chu, T. L., D. W. Ing, and A. J. Noreika. "Aluminum Nitride Films by Chemical Transport," ELECTROCHEM-TECHNOL, Vol. 6 (1968), pp. 56-59.
31. Long, G., and L. M. Foster. "Crystal Phases in the System  $Al_2O_3$ -AlN," AMER CERAM SOC, J, Vol. 44 (1961), pp. 255-58.
32. Le Jus, Anne-Marie. "Principal Properties and Preparation of Aluminum Oxynitrides by Reaction in the Solid-State," SOC CHIM FRANCE, BULL (1962), pp. 2123-26.
33. Leprince-Ringuet, F., Anne-Marie LeJus, and R. Collongues. "Mineral Chemistry--Preparation and Melting of Refractory Carbides, Nitrides and Oxynitrides Using a Plasma Oven," COMPT REND, Vol. 258 (1964), pp. 221-23.
34. Michel, D., M. Perez y Yorba, and R. Collongues. "Oxynitride Formation During Alumina Fusion in Air in the Presence of Aluminum," COMPT REND, Vol. C263 (1966), pp. 1366-68.

35. Stringer, J. "The Effect of Nitrogen on the Oxidation of Tantalum at High Temperatures," ELECTROCHEM SOC, J, Vol. 112 (1965), pp. 1083-91.
36. Pelton, J. F. "Flame-Plating by Detonations," U. S. Patent 2,972,550, 21 February 1961.
37. Meyer, H. "Fusion of Powders in a Plasma Jet," DEUT KERAM GES, BER, Vol. 41 (1964), pp. 112-19.
38. Koch, H., and J. Adams. "Effect of Working Conditions on the Properties of Sprayed Steel Coatings," SCHWEISSEN UND SCHNEIDEN, Vol. 5 (1953), pp. 131-2.
39. Tschorn, G. Spark Atlas of Steels. New York, McMillan, 1963.
40. Hunger, L., and O. Werner. "Influence of the Structure on Photographs of the Grinding Sparks of Unalloyed and Alloyed Steels," ARCH EISENHUTTENW, Vol. 23 (1952), pp. 277-86.
41. Stroup, P. T. "Carbothermic Smelting of Aluminum," AIME, TRANS, Vol. 230 (1964), pp. 356-72.
42. Baker, R. "Oxidation Studies of Molten Iron Alloy Droplets," IRON STEEL INST (London), Vol. 205(6) (1967), pp. 637-41.
43. Baker, L. A., and R. G. Ward. "Reaction of an Iron-Carbon Droplet During Free Fall Through Oxygen," IRON STEEL INST (London), Vol. 205 (1967), pp. 714-17.
44. Baker, L. A., N. A. Warner, and A. E. Jenkins. "Decarburization of a Levitated Iron Droplet in Oxygen," AIME, TRANS, Vol. 239 (1967), pp. 857-64.
45. Fuwa, T., and J. Chipman. "The Carbon-Oxygen Equilibria in Liquid Iron," AIME, TRANS, Vol. 218 (1960), pp. 887-91.
46. Diamond, J. J., and A. L. Dragoo. "The Solubility of Water Vapor in Molten Alumina, in Conference on Thermal Imaging Techniques, ed. by P. E. Glaser and R. F. Walker. New York, Plenum, 1964. Pp. 225-28.
47. Wartenburg, H. von. "Water Absorption by Melting Oxides," Z ANORG ALLGEM CHEM, Vol. 264 (1951), p. 226.
48. Lewis Flight Propulsion Laboratory. A General System for Calculating Burning Rates of Particles and Drops and Comparison of Calculated Rates for Carbon, Boron, Magnesium and Isooctane, by K. P. Coffin and R. S. Brokaw. Cleveland, Ohio, LFPL, 1957. (NACA TN 3929).

UNCLASSIFIED  
Security Classification

DOCUMENT CONTROL DATA - R&D		
<i>(Security classification of title, body of abstract and indexing annotation must be entered when the overall report is classified)</i>		
1. ORIGINATING ACTIVITY (Corporate author) Naval Weapons Center China Lake, California 93355		2a. REPORT SECURITY CLASSIFICATION <b>UNCLASSIFIED</b>
		2b. GROUP None
3. REPORT TITLE METAL PARTICLE COMBUSTION PROGRESS REPORT 1 July 1965-1 May 1967		
4. DESCRIPTIVE NOTES (Type of report and inclusive dates) Progress Report, 1 July 1965-1 May 1967		
5. AUTHOR(S) (Last name, first name, initial) Metal Combustion Study Group Edited by J. L. Prentice		
6. REPORT DATE August 1968	7a. TOTAL NO. OF PAGES 118	7b. NO. OF REFS 48
8a. CONTRACT OR GRANT NO.	9a. ORIGINATOR'S REPORT NUMBER(S) NWC TR 4435	
a. PROJECT NO. NASA Work Order No. 6032	9b. OTHER REPORT NO(S) (Any other numbers that may be assigned this report)	
10. AVAILABILITY/LIMITATION NOTICES This document is subject to special export controls and each transmittal to foreign governments or foreign nationals may be made only with prior approval of the Naval Weapons Center.		
11. SUPPLEMENTARY NOTES	12. SPONSORING MILITARY ACTIVITY Naval Ordnance Systems Command Naval Material Command Washington, D. C. 20360	
13. ABSTRACT This report includes: (1) a summary of experimental studies at this Center on the xenon flash-initiated combustion of single particles of aluminum, boron, titanium and zirconium in air, oxygen, carbon dioxide and various oxygen-argon mixtures at pressures from 1-4.5 atmospheres, and a summary of aluminum and boron particle combustion in various gas burner flames; (2) development and application of an analytical droplet burning model to describe boron particle combustion; and (3) a discussion of metal particle fragmentation mechanisms including definition of some necessary conditions for fragmentation as well as a description of the most probable mechanism. The report concludes with a brief summary section describing the status of the metal combustion problem. Significant new data on the agglomeration phenomenon and other preignition processes are presented. Extensive use of the scanning electron microscope (SEM) was made in studying both preignition phenomena and metal specimens quenched during various phases of burning. Results indicate that quasi-steady combustion behavior is directly related to the thermophysical properties of the metals and their oxides. Disposition of the combustion products in the reaction zone exerts the controlling influence on the mode of termination of combustion. Droplet burning models treating the case of spherical symmetry (hydrocarbon droplet analogy) are shown to be deficient, particularly for aluminum combustion, where early large scale deviation from such symmetry occurs.		

DD FORM 1473 0101-807-6000  
1 JAN 64

UNCLASSIFIED  
Security Classification

14. KEY WORDS	LINK A		LINK B		LINK C	
	ROLE	WT	ROLE	WT	ROLE	WT
Combustion Metals Aluminum Boron Titanium Zirconium Fragmentation Agglomeration						

**INSTRUCTIONS**

1. **ORIGINATING ACTIVITY:** Enter the name and address of the contractor, subcontractor, grantee, Department of Defense activity or other organization (corporate author) issuing the report.
- 2a. **REPORT SECURITY CLASSIFICATION:** Enter the overall security classification of the report. Indicate whether "Restricted Data" is included. Marking is to be in accordance with appropriate security regulations.
- 2b. **GROUP:** Automatic downgrading is specified in DoD Directive 5200.10 and Armed Forces Industrial Manual. Enter the group number. Also, when applicable, show that optional markings have been used for Group 3 and Group 4 as authorized.
3. **REPORT TITLE:** Enter the complete report title in all capital letters. Titles in all cases should be unclassified. If a meaningful title cannot be selected without classification, show title classification in all capitals in parentheses immediately following the title.
4. **DESCRIPTIVE NOTES:** If appropriate, enter the type of report, e.g., interim, progress, summary, annual, or final. Give the inclusive dates when a specific reporting period is covered.
5. **AUTHOR(S):** Enter the name(s) of author(s) as shown on or in the report. Enter last name, first name, middle initial. If military, show rank and branch of service. The name of the principal author is an absolute minimum requirement.
6. **REPORT DATE:** Enter the date of the report as day, month, year, or month, year. If more than one date appears on the report, use date of publication.
- 7a. **TOTAL NUMBER OF PAGES:** The total page count should follow normal pagination procedure, i.e., enter the number of pages containing information.
- 7b. **NUMBER OF REFERENCES:** Enter the total number of references cited in the report.
- 8a. **CONTRACT OR GRANT NUMBER:** If appropriate, enter the applicable number of the contract or grant under which the report was written.
- 8b, 8c, & 8d. **PROJECT NUMBER:** Enter the appropriate military department identification, such as project number, subproject number, system number, task number, etc.
- 9a. **ORIGINATOR'S REPORT NUMBER(S):** Enter the official report number by which the document will be identified & controlled by the originating activity. This number must be unique to this report.
- 9b. **OTHER REPORT NUMBER(S):** If the report has been assigned any other report numbers (either by the originator or by the sponsor), also enter this number(s).
10. **AVAILABILITY/LIMITATION NOTICES:** Enter any limitations on further dissemination of the report, other than those

imposed by security classification, using standard statements such as:

- (1) "Qualified requesters may obtain copies of this report from DDC."
- (2) "Foreign announcement and dissemination of this report by DDC is not authorized."
- (3) "U. S. Government agencies may obtain copies of this report directly from DDC. Other qualified ODC users shall request through \_\_\_\_\_."
- (4) "U. S. military agencies may obtain copies of this report directly from OOC. Other qualified users shall request through \_\_\_\_\_."
- (5) "All distribution of this report is controlled. Qualified ODC users shall request through \_\_\_\_\_."

If the report has been furnished to the Office of Technical Services, Department of Commerce, for sale to the public, indicate this fact and enter the price, if known.

11. **SUPPLEMENTARY NOTES:** Use for additional explanatory notes.

12. **SPONSORING MILITARY ACTIVITY:** Enter the name of the departmental project office or laboratory sponsoring (paying for) the research and development. Include address.

13. **ABSTRACT:** Enter an abstract giving a brief and factual summary of the document indicative of the report, even though it may also appear elsewhere in the body of the technical report. If additional space is required, a continuation sheet shall be attached.

It is highly desirable that the abstract of classified reports be unclassified. Each paragraph of the abstract shall end with an indication of the military security classification of the information in the paragraph, represented as (TS), (S), (C), or (U).

There is no limitation on the length of the abstract. However, the suggested length is from 150 to 225 words.

14. **KEY WORDS:** Key words are technically meaningful terms or short phrases that characterize a report and may be used as index entries for cataloging the report. Key words must be selected so that no security classification is required. Identifiers, such as equipment model designation, trade name, military project code name, geographic location, may be used as key words but will be followed by an indication of technical context. The assignment of links, roles, and weights is optional.